MUTAGENESIS STUDIES OF THE DctA C_4 DICARBOXYLATE PERMEASE OF *SINORHIZOBIUM MELILOTI*

By

MARIA ANNE ZIEGLER

A thesis submitted in partial fulfillment of
the requirements for the degree of

Master of Science in Biochemistry

WASHINGTON STATE UNIVERSITY
School of Molecular Biosciences

December 2004

To the faculty of Washington State University:

The members of the Committee appointed to examine the thesis of Maria Anne Ziegler find it satisfactory and recommend that it be accepted.

Chair

Acknowledgements

First to my advisor Dr. Michael Kahn for the help and support he has provided over the past two years. Also to my committee for their guidance and understanding through what have been not altogether easy times. I wish to extend a big thank you also to the laboratory of Dr. Michael Varnum who helped me immensely with all of the RNA work. Although it only constitutes a small portion of the final thesis, this work probably was the most time-consuming. I would also like to thank Isaac Forquer for his help with the French press, Dr. Michael Konkel for his help and advice with trouble-shooting western blots, Dr Scott Clark for doing all of my electroporations (I'm still petrified of the electroporator!), Scott Maloney for PCR assistance, and Dr. Svetlana Yurgel for all of her help, guidance and support in the lab over the past two years.

MUTAGENESIS STUDIES OF THE DctA C_4 DICARBOXYLATE PERMEASE OF *SINORHIZOBIUM MELILOTI*

Abstract

By Maria Anne Ziegler

Washington State University

December 2004

Dicarboxylic acids constitute the main bacterial catabolite used in the nitrogen-fixing symbiosis between *Sinorhizobium meliloti* and the host plant alfalfa. The dicarboxylic acids enter the bacteria through the DctA dicarboxylic acid transporter. DctA is a part of the glutamate transporter family, members of which are significant in amino acid neurotransmitter localization in higher organisms. Although the involvement of DctA in the symbiotic process has been known for many years, its precise structure and mechanism remain elusive.

The role of the highly conserved residue G114 located in transmembrane helix three, was investigated by site-directed mutagenesis. Four point mutations were made; G114A, G114D, G114F, and G114P. Analysis of the phenotypes of the-mutants revealed that this residue plays an important role in the structure and function of DctA.

dctA is expressed from a σ^{54}-dependent promoter located upstream of one of two potential start-codons. A third, in-frame methionine codon is located within the spacer region of the RpoN (σ^{54}) binding site. Point mutations were made in each of these methionines to investigate which

one is the most important one for free-living growth on dicarboxylic acids. It was shown that the third methionine (farthest from the RpoN binding site) is the main start codon used under free-living conditions, but the second methionine can play a role in translation initiation in its absence. The first methionine, located within the RpoN binding site, was not important under free-living conditions.

Table of Contents

List of Tables

List of Figures and Illustrations

List of Symbols, Abbreviations and Nomenclature

ΔG:	Change in free energy of the system
ADP:	Adenosine diphosphate
Anti-DctA:	Antibody raised against DctA protein
Anti-FLAG:	Antibodies rasied against FLAG tag
Anti-His:	Antibodies raised against hexa-histidine sequence
Ap:	Ampicillin
APS:	Ammonium Persulfate
ATP:	Adenosine triphosphate
BNF:	Biological nitrogen fixation
bp	Base pair(s)
C4:	Molecule with a four-carbon backbone
Conc.:	Concentration
CPM:	Counts per minute
DCA:	Dicarboxylic acid
dH2O:	Deionized water
EDTA:	Ethylenediaminetetraacetic acid
EtOH:	Ethanol
FOA:	Fluoroorotic acid
g:	Gram
ha:	Hectare
hr:	Hour
HCl:	Hydrochloric acid
$kcal.mol^{-1}$:	Kilocalories per mole
kDa:	Kilodalton
Kn:	Kanamycin
LB:	Luria broth
LECA:	Lightweight Expanded Clay Aggregate
M:	Molar

mA:	Milliamp
MCS:	Multiple cloning site
mg:	Milligram
min:	Minute
$MinNH_4$:	Minimal medium with ammonia
ml:	Milliliter
mM:	Millimolar
$MMNH_4$:	Minimal mannitol medium with ammonia
NaOH:	Sodium hydroxide
ng:	Nanograms
nl:	Nanoliters
Nm:	Neomycin
nM:	Nanomolar
Nmol:	Nanomoles
PAGE:	Polyacrylimide gel electrophoresis
r:	Resistant to antibiotic
rpm:	Revolutions per minute
s:	Sensitive to antibiotic
SDS:	Sodium dodecyl sulphate
Sm:	Streptomycin
TBE:	Tris-borate EDTA electrophoresis buffer
Tc:	Tetracycline
TE:	Tris-Hcl EDTA buffer
TEMED:	Tetramethylethylenediamine
Tg yr^{-1}:	Teragrams per year (1 Million metric tons per year)
Tris:	Tris buffer; Trisamine
U:	Units
v:	Volts
v/v :	Volume per volume
W:	Watts

w/v :	Weight per volume
µl:	Microliter
µg:	Microgram

Chapter One Introduction

1.1 Biological Nitrogen Fixation

Nitrogen is typically the limiting soil nutrient required in the growth of crop plants. It thus plays a key role in establishing sustainable agricultural systems, where sustainable agriculture is defined broadly as agriculture that maintains a stable ecological environment (9, 140), often focusing on increasing efficiency and crop yields through local inputs. Nitrogen compounds in the soil are in a continual state of flux as illustrated in Figures 1 and 2. Many of these processes, including microbial denitrification, soil erosion, leaching, and chemical volatilization (43, 83, 101) produce biologically unavailable dinitrogen. Therefore, modern agriculture has become increasingly dependent on the application of external nitrogen sources in order to preserve sufficient soil nitrogen to support high crop yields. As a result, the use of synthetically produced nitrogen fertilizers in farming has increased from 3 million to 80 million tons over the last 40 years (33), and worldwide annual expenditure on fertilizers now exceeds $20 billion. This phenomenon is shown graphically in Figure 3. In the United States, statistics obtained from the International Fertilizer Industry Association (4) show a four-fold increase in fertilizer consumption between 1961 to 1999, whilst nitrogen input from biological nitrogen fixation (BNF) has remained fairly constant (43, 115), this is shown graphically in Figure 4.

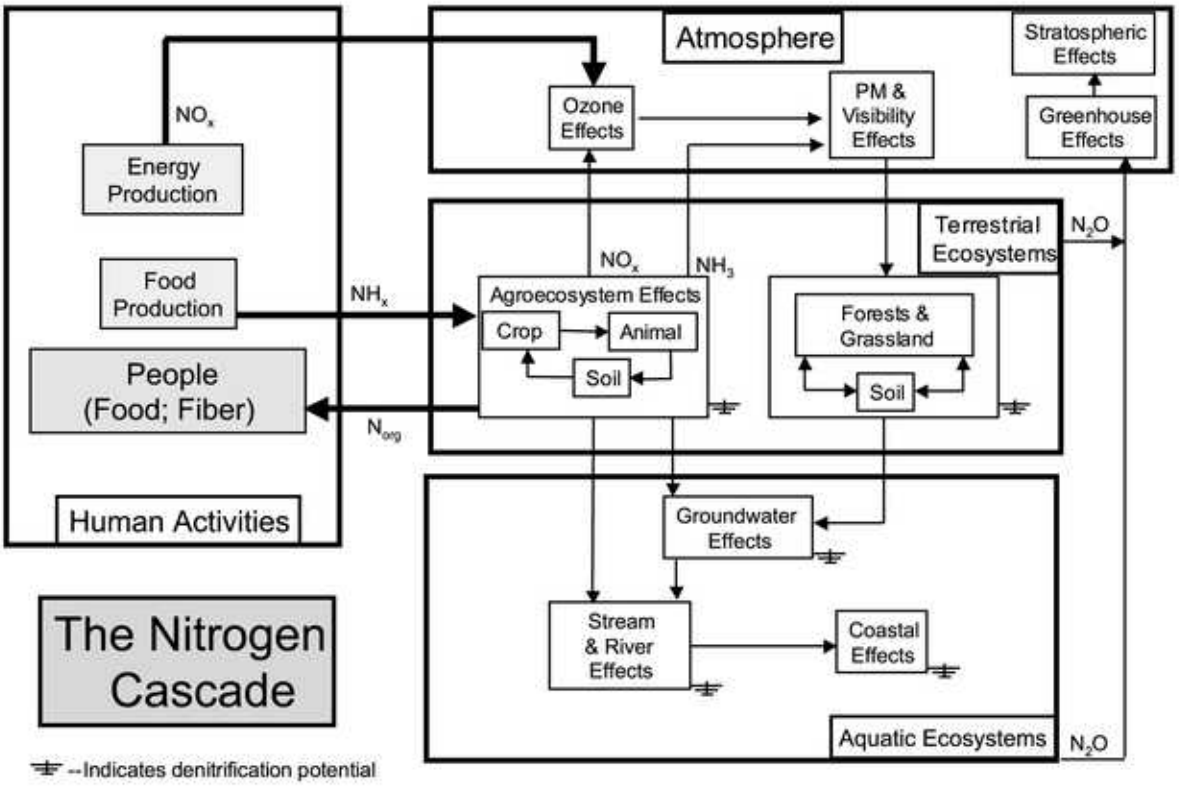

Figure 1. The nitrogen cascade

The nitrogen cascade illustrates the movement of human-produced reactive nitrogen (Nr) as it cycles through various environmental reservoirs in the atmosphere, terrestrial ecosystems, and aquatic ecosystems of the Earth (43)

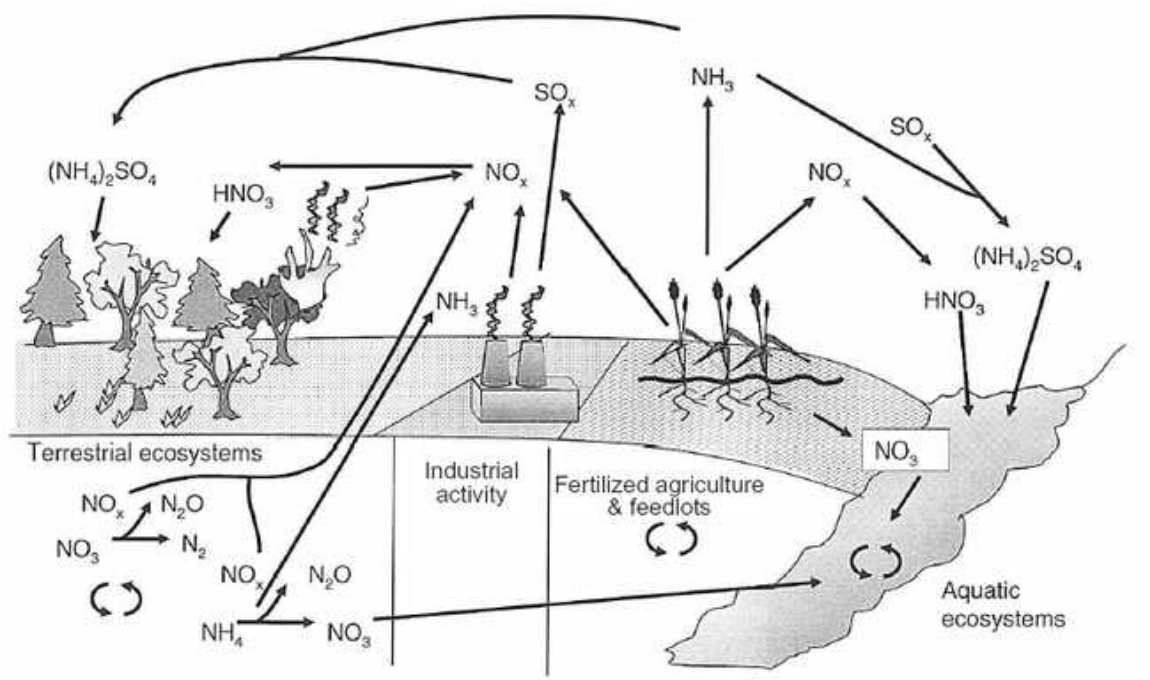

Figure 2. The nitrogen cycle

Rapid transport and transformation of nitrogen from industrial and agricultural activities to natural terrestrial and aquatic systems. Biomass burning, fossil-fuel combustion, and soil microbial activity are the primary sources of NO_2 emissions, whilst agricultural activities, including fertilized agriculture and livestock, are the primary sources of NH_3 emissions to the atmosphere. Closed, circular black arrows represent soil and aquatic nitrogen transformations, including N mineralization, immobilization, nitrification, and denitrification (83)

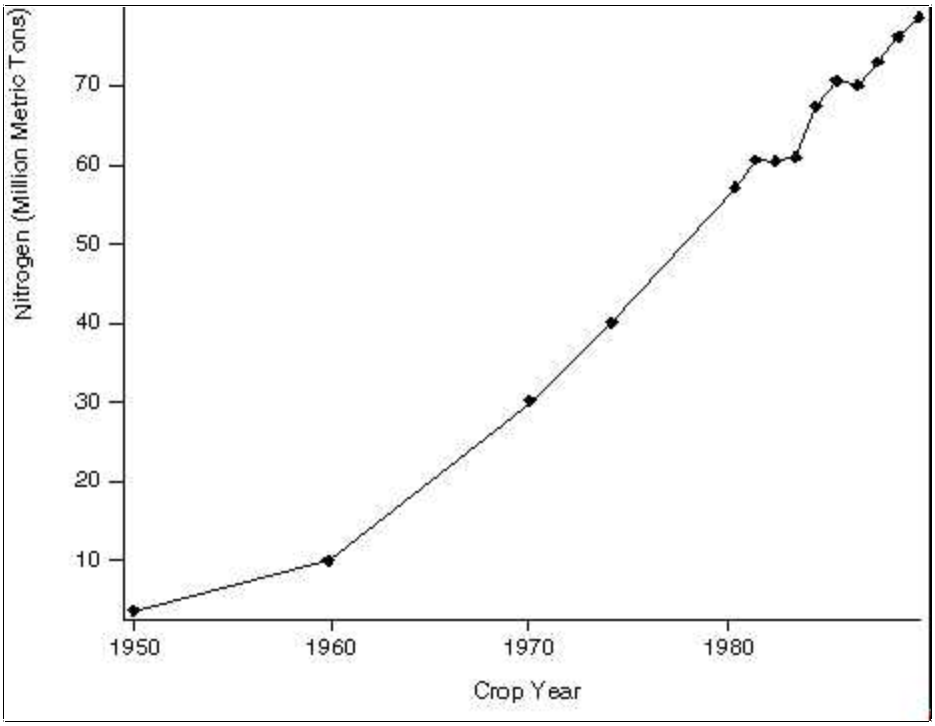

Figure3. World Fertilizer Consumption of Nitrogen Totals, 1950-1989 (55)

(Based on Fertilizer Facts and Figures. 1990. The Fertilizer Institute, Washington, D.C.)

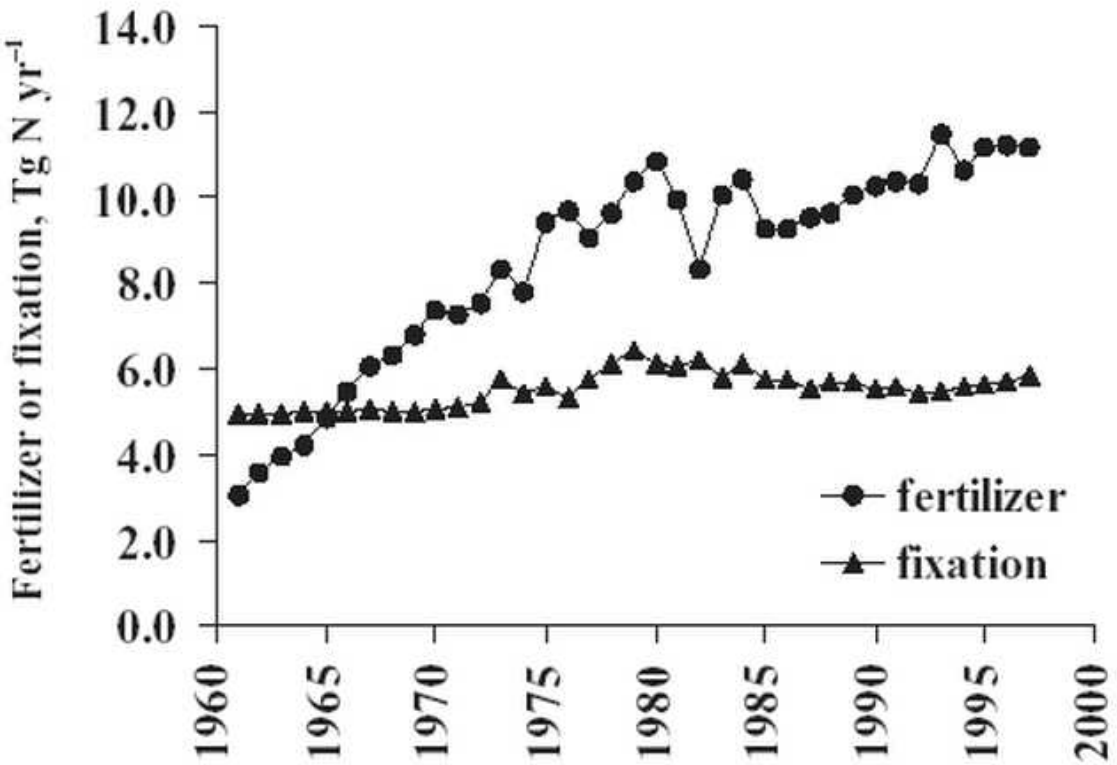

Figure 4. Nitrogen inputs in the USA from 1961 to 1999 (4, 43, 115)

Application of synthetic nitrogen fertilizers, whilst beneficial in terms of increasing crop yields, can be environmentally devastating. Application of industrially-produced nitrogen fertilizer affects the balance of the global nitrogen cycle, pollutes groundwater, increases the risk of chemical spills, and increases atmospheric nitrous oxide (N_2O), a potent "greenhouse" gas that has an energy reflectivity per mole 180-fold higher than that of carbon dioxide (33). In contrast to BNF in which all the ammonia produced is immediately assimilated into the legume, industrially-produced ammonia is used very inefficiently by crop plants, with over 50% remaining in the organic matter of the soil. Whilst some of this is available to subsequent crops, much is either converted back to atmospheric nitrogen through denitrification, volatized as ammonia, or leached from the soil as nitrate (NO_3) (43, 83). This phenomenon is shown graphically in Figure 5.

Biological nitrogen fixation currently makes available approximately 100-175 million metric tons of nitrogen annually (18, 43), a value which has probably remained fairly constant over the past century. Given the projected doubling of the world's population over the next fifty years (139), we can expect a concurrent doubling in the demand for fixed nitrogen in crop production. If this nitrogen is supplied by industrial sources, synthetic nitrogen use will exceed 160 million tons per year, equaling that produced biologically (33). To produce this amount of fertilizer will require annual use of over 270 million tons of coal or an equivalent fuel, which itself presents a major environmental risk (33). However, if biological nitrogen fixation were exploited to meet the agricultural demands of a larger population, the need for industrial fertilizer production could be dramatically reduced. Table 1 highlights the relative contributions made by the three main genera of nitrogen-fixing microorganisms and the agricultural systems that they affect (95).

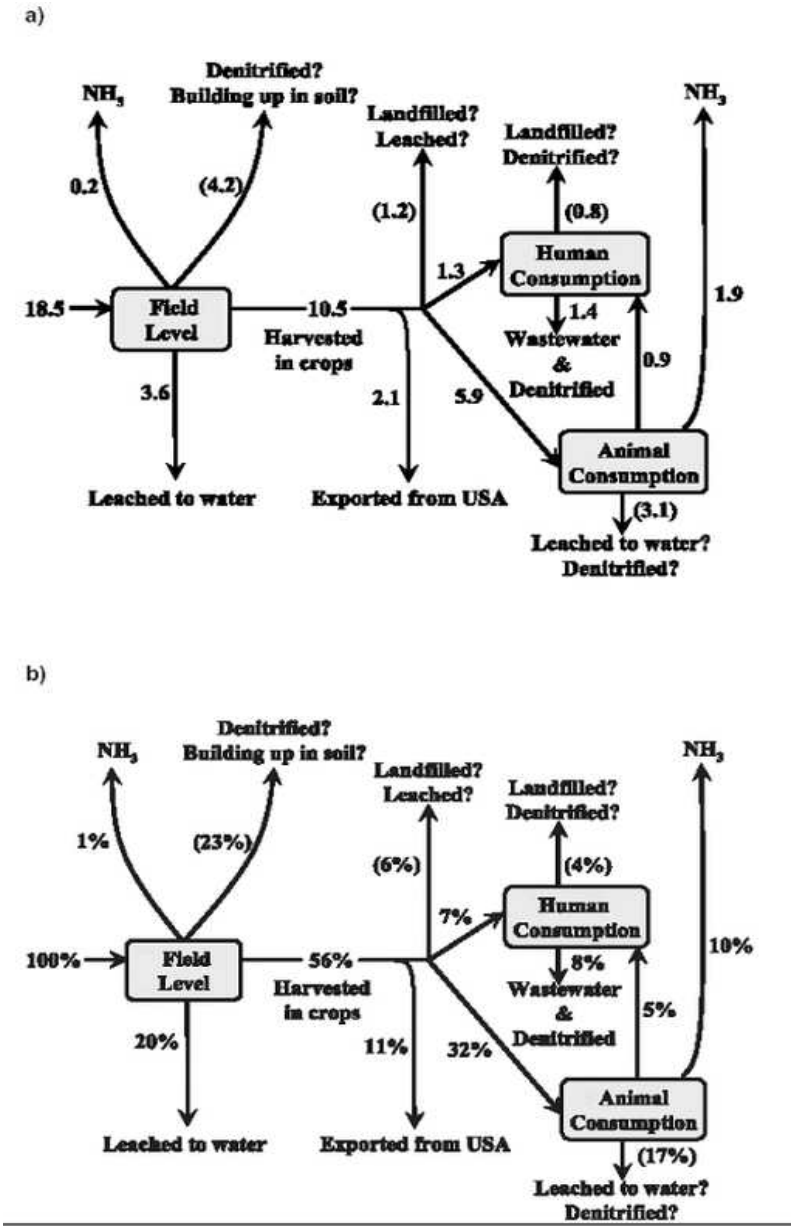

Figure 5. Average fate of Nitrogen inputs to agricultural fields in the USA as of the late 1990s

Top a) shows total flux for the country (Tg yr^{-1}); while bottom b) shows fates as percentages of the total new input of nitrogen to agricultural fields (43).

Table 1. Estimates of annual N2 fixation amounts in different agricultural systems (95)

N2-Fixing organism	System	Range measured (kg shoot N/ha)	Commonly observed (kg shoot N/ha)
Free-living	Crops	0-80	0-15
Associative	Tropical grasses	10-45	10-20
	Crops	0-240	25-65
Symbiotic	Mazola	10-150	10-50
	Actinorrhizal trees	10-440	30-75
	Green manure legumes	5-325	50-150
	Forage legumes	5-680	50-250
	Crop legumes	0-450	30-200
	Tree legumes	5-470	50-300

Adapted from Ledgard and Giller (1995) with additional information from Peoples and Craswell (1992); Peoples *et al* (1996); Unkovich, Pate (2000), Maskey *et al* (2001) and Peoples *et al* (2001) (82, 94-96, 138).

Figure 6 shows that over a range of environments, legumes are capable of fixing 20-25kg of shoot N per ton of shoot dry matter. These data demonstrate how significant the contribution made by the legume-*rhizobia* symbiosis is in terms of the amount of N that is fixed annually, and made available to other plants in the surrounding soil.

Biological nitrogen fixation is thus considered to be one of the most significant means by which the ever-increasing demands for crop-fertilizer production can be met (47), and it represents a potential solution to the economical and environmental threats posed by the application of synthetic nitrogen fertilizers. A renewable source of fixed nitrogen, BNF directly benefits agriculture by the indirect addition of fixed nitrogen to the soil where it can be utilized by non-leguminous crop plants (95).

1.2 The *Rhizobiaceae*

The use of legumes in crop rotations has a long history, dating back to the time of the Romans. However, it was not until the advent of detailed N balance studies that legumes were shown to accumulate N from sources other than simply soil and fertilizer. In 1886 it was shown that the ability of legumes to convert N_2 from the atmosphere into compounds which could be used by the plant was due to the presence of swellings or nodules on the legume root, and more specifically was due to the presence of particular bacteria within these nodules (48). The first rhizobia were isolated from nodules in 188, and were shown to possess the ability to reinfect their legume hosts, and to fix N_2 in symbiosis (7).

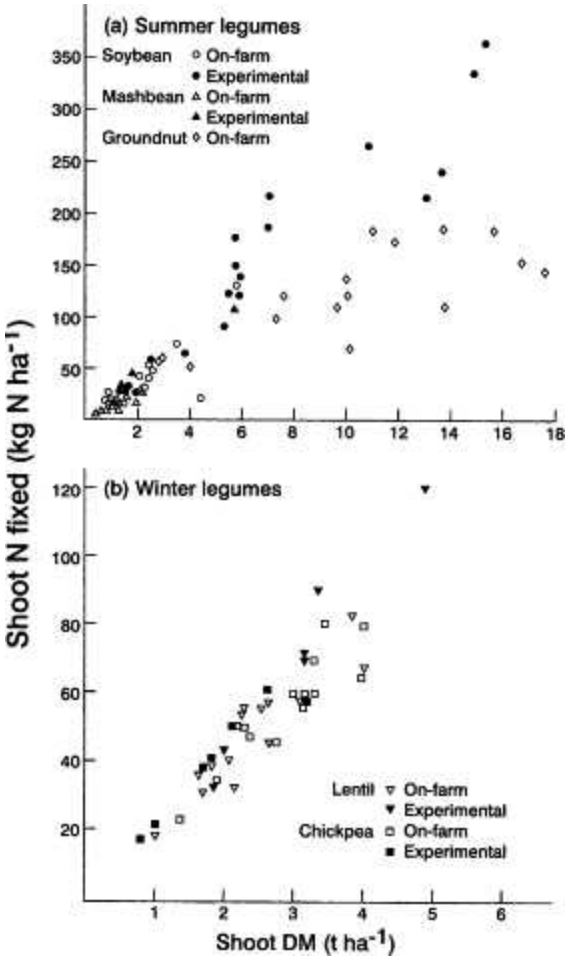

Figure 6. The relationship between shoot dry matter (DM) and shoot N fixed

for: (a) summer legumes and (b) winter legumes in Nepal. Legume species include soybean (◙), mashbean (△), groundnut (◇), lentil (▽) and chickpea (❑). Open symbols represent data collected from farmers' fields, closed symbols indicate experimental crops (82).

Several genera of soil bacteria can enter into nitrogen-fixing symbioses with leguminous plants. These genera commonly referred to as the "rhizobia", include *Sinorhizobium, Rhizobium, Bradyrhizobium,* and *Azorhizobium.* The bacteria elicit formation of specialized, microaerophilic nodules on the roots of the host plant in which, following infection and colonization of the nodule, the bacteria undergo differentiation into a mature state known as a bacteroid, which can reduce atmospheric dinitrogen to ammonia. The bacteroids are enclosed in a plant-derived, peribacteroid membrane, through which all nutrients bound for the bacteroid must pass (137, 141). The process of symbiosis is outlined in Figure 7.

Symbiosis is the result of an elaborate exchange of signals between the host and the symbiont. The rhizobia respond to the presence of plant-secreted flavonoids into the rhizosphere, the soil zone immediately surrounding the root system of the plant, by producing lipochitooligosaccharides known as Nod factors (32) which in turn, activate a transduction pathway that ultimately leads to nodule formation (21). Nod factors play a major role during early nodule development, and are known to be responsible for, among other things, determining host-symbiont specificity as a result of host-specific recognition of substitutions on the lipochitooligosaccharide backbone (24, 80, 114). During differentiation into the mature bacteroid state, the bacteria undergo significant biochemical and morphological changes in response to environmental stimuli within the nodule; these stimuli presumably include chemical signals, low oxygen concentration, pH changes, and other plant-determined conditions that are needed for the reduction of atmospheric dinitrogen to ammonia (57, 67, 100, 154).

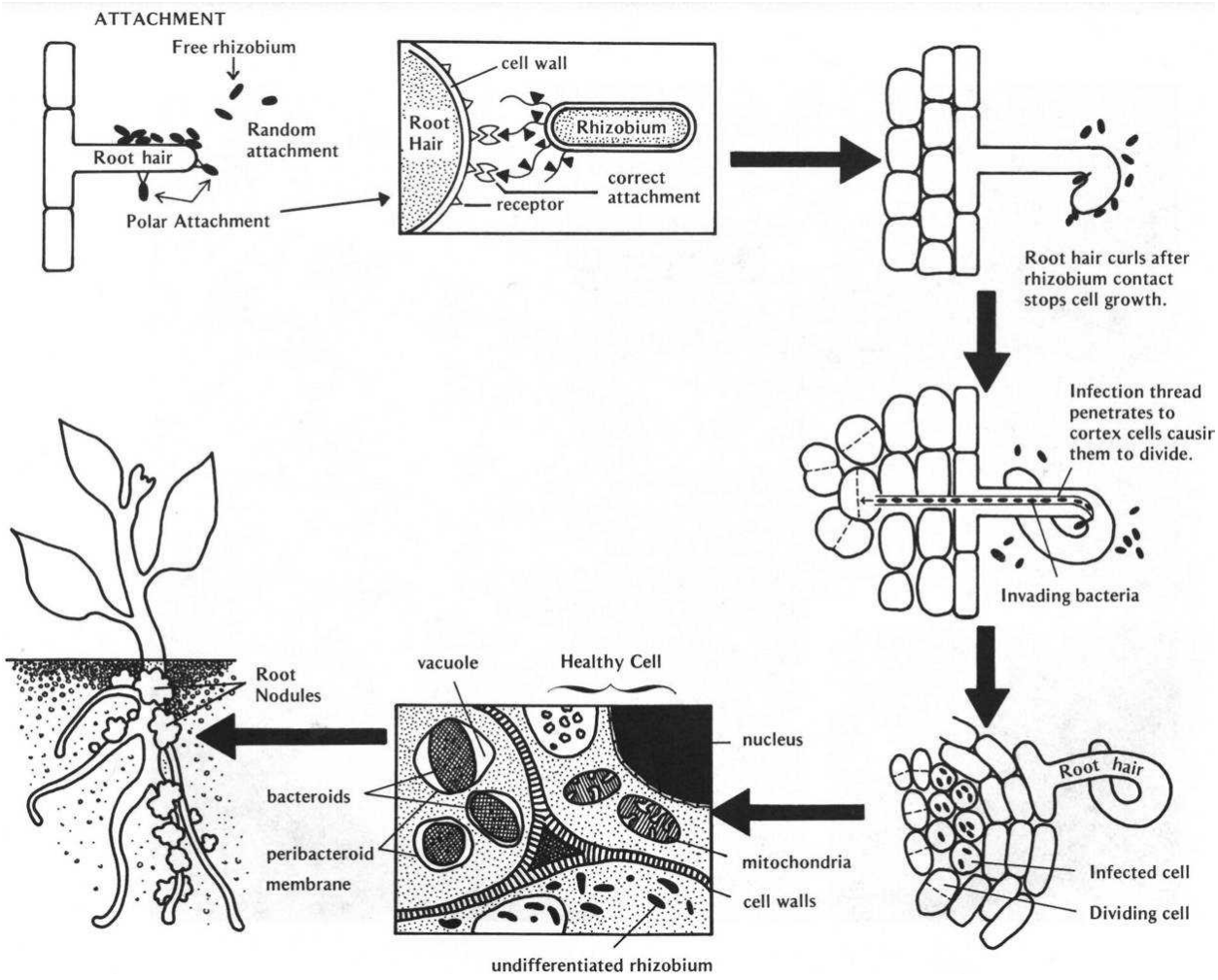

Figure 7. Schematic diagram of the nodulation process

From http://cropandsoil.oregonstate.edu/classes/css455/notes/Nitrogen_Cycle.ppt.

The infection process typically associated with the rhizobia is reminiscent of that seen in eukaryotic pathogens (49). This has generated an increased interest in the elucidation of the processes by which the bacteria are able to infect and invade the plant cells. Recently, a homologue of the *Sinorhizobium meliloti bacA* gene was identified in *Brucella* where it is required for macrophage invasion (74). In addition to the *bacA* homologue, genes homologous to those of an invasion-associated locus of *Bartonella bacilliformis* were also identified in the *S. meliloti* genome (89), potentially allowing comparisons between infection processes between a pathogen and a non-pathogenic model system.

The rhizobial species used in this work is *S. meliloti* . *S. meliloti* is a gram negative α-proteobacterium. Primarily a soil-dwelling bacterium, *S. meliloti* can enter into effective symbioses with several genera of forage legumes, including *Medicago, Melilotus* and *Trigonella.* The genome sequence of *S. meliloti* , completed in 2001 (42) contains three replicons that contain genes required for symbiosis, a 3.65-Mb chromosome and two megaplasmids, pSymA (1.35 Mb) and pSymB (1.68 Mb), all three of which contain genes required for symbiosis. The genome is estimated to encode 6204 proteins, approximately 60% of which have had functions ascribed on the basis of homology to proteins of known function.

1.3 Energy Requirements of Symbiotic Nitrogen Fixation

Nitrogen reduction is catalyzed by the two-component enzyme complex, nitrogenase. Nitrogenase contains two metalloproteins, the molybdenum-iron (MoFe), or NifKD protein and

the iron (Fe) or dinitrogenase reductase, or NifH protein (103, 106). NifH is a homodimer whose subunits symmetrically coordinate a single [4Fe:4S] cluster, and is responsible for the transfer of a low-potential electron to NifKD with the concurrent hydrolysis of ATP. NifKD is an $\alpha_2\beta_2$ heterotetramer that contains the substrate reducing site and is responsible for the actual reduction of dinitrogen (103, 106).

Although biochemically complex, the basic nitrogen reduction reaction of the nitrogenase complex can be summarized as:

$$N_2 + 8H^+ + 16ATP \text{ ------> } 2\ NH_3 + 2H_2 + 16ADP + 16\ P_i$$

The stability of the N_2 bond is the major hurdle in nitrogen reduction. Whilst the nitrogenase reaction itself is endothermic (ΔG= -7.98 kcal.mol^{-1}) the energy of activation is very large. As a result, symbiotic nitrogen fixation is an energetically expensive metabolic process, requiring 16 molecules of ATP per molecule of molecular nitrogen reduced. The energy requirements for the process are typically met by the host plant, which supplies the symbiont with carbon compounds that are catabolized to supply the needed ATP and reductant (126). Approximately 6g of carbon are needed per g N_2 reduced, accounting for 10-20% of total plant photosynthate (97). The nitrogenase complex is among the most oxygen-labile enzymes known, necessitating the development of biochemical mechanisms by the plant cells to protect it from oxygen, thus exacerbating the problems created by the high energy requirements of nitrogen reduction (106).

1.4 C_4 -Dicarboxylate Transport in *S. meliloti*

The specificity of carbon source utilization by bacteroids to support BNF has been under investigation since the 1960s when it was shown that bacteroids of *Bradyrhizobium japonicum* preferentially oxidized the tricarboxylic acid cycle intermediates succinate, malate and fumarate, all of which are dicarboxylates, over hexose sugars (136). Since then, many studies have been conducted on a variety of rhizobia which show that BNF is highly stimulated by the presence of dicarboxylates, especially succinate. C_4-dicarboxylate uptake rates by bacteroids have been shown to be 30-50 fold faster than for sugars (60, 111).

Furthermore, there have been many studies investigating the dependence of BNF on a functional dicarboxylate transport system. Prior to the isolation of the C_4-dicarboxylate transport system of *Rhizobium leguminosarum* bv. *trifolii* (108) in 1984, researchers had shown that mutants defective in the ability to transport C_4-dicarboxylates were unable to enter into effective symbioses with their respective host legumes (41, 108). Today, many examples have been documented to confirm the dependence of BNF upon C_4-dicarboxylate transport (3, 11, 36, 38, 40, 41, 50, 52, 64, 79, 152, 157) and it is widely accepted that mutants that are unable to import dicarboxylic acids (DCAs) form ineffective, non-nitrogen fixing nodules in symbiosis (10, 36, 37, 108, 151).

Transport of dicarboxylic acids into the bacteroids is also intimately linked to the transport of amino acids, and ultimately to a complex C/N exchange process between the host plant and the symbiont. The theoretical model for this exchange is shown in Figure 8. This model describes

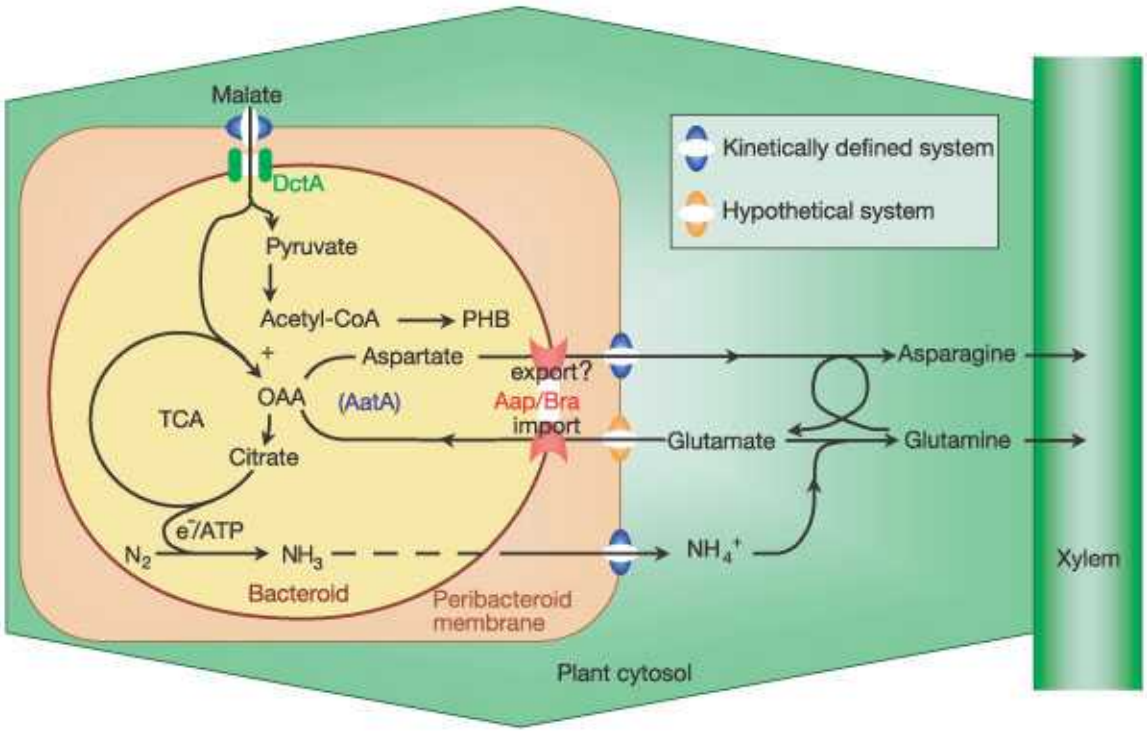

Figure 8. The role of amino-acid cycling in nitrogen fixation in pea nodules

Only reactions directly involved in amino-acid cycling in the bacteroid and plant are shown. Transport systems from the peribacteroid membrane that have been kinetically but not genetically characterized are shown in blue, while those that are hypothetical are in yellow. Although glutamate and aspartate are shown as the amino acids most likely to cycle, others (such as alanine) may be important. The reaction catalyzed by AatA also forms 2-ketoglutarate, which may be either metabolized by the bacteroid or exported back to the plant. Export via Aap/Bra is shown with a question mark to indicate that it is hypothetical. PHB, polyhydroxybutyrate; OAA, oxaloacetic acid; TCA, tricarboxylic acid cycle. (78).

how the bacteroids are believed to import glutamate from the host plant via the bacterial Aap/Bra transporters. Glutamate can then act as a transamination donor to produce aspartate. Aspartate is secreted to the plant, facilitating asparagine synthesis, and allowing the bacteria to shut down ammonia assimilation (78). This phenomenon is outlined in Figure 8. It is possible that DctA functions as the aspartate carrier allowing aspartate to be exported from the bacteria.

1.5 DctA

The dicarboxylate transport system in *S. meliloti* is encoded by three genes, *dctA, dctB and dctD* (152). *dctB* and *dctD* encode a two-component regulatory system in which the periplasmic sensor kinase, DctB, responds to the presence of C_4-dicarboxylates in the bacterial periplasm, and regulates expression of the transport protein encoded by *dctA* by means of the response regulator DctD (150, 160), which then activates transcription of *dctA* via the σ^{54}-dependent, *dctA* promoter (63, 68). The regulation of *dctA* expression is discussed in more detail in section 1.6. DctB and DctD have been well studied both structurally and functionally and both show homology to two-component regulatory systems from many other bacteria.

Less is known about the structure and mechanism DctA. DctA is approximately 46.5kDa, and is a member of an important family of secondary transporter proteins. Secondary transporter proteins use the free energy stored in transmembrane ion and/or solute gradients to drive transport (158). The glutamate transporter family, of which DctA is a member (117), includes transporters found in mammalian neuronal, glial, and retinal cells, as well as bacterial nutrient

uptake proteins. The bacterial transporters catalyze the electrogenic symport of glutamate with at least two cations (133-135), whilst the eukaryotic proteins require the symport of two or three sodium ions and one proton

and antiport of one potassium ion (1, 5, 59, 162). The precise ion requirements of DctA in *S. meliloti* remain to be determined.

Structural characterization of any glutamate transporter family members has, to date, yet to be undertaken. Membrane proteins are notoriously difficult to purify and characterize structurally using standard techniques and as a result, indirect means of structural analysis are often employed. The membrane topology of DctA has been studied by Tn*phoA* fusion analysis (57) and by analysis of its amino acid composition and hydropathy profile (Figure 9).

Hydropathy profiles of multiple glutamate transporter family members including DctA suggest a remarkable level of structural preservation. The average profile depicts six N-terminal, hydrophobic membrane-spanning domains, separated by hydrophilic regions that extend into the cytoplasm/periplasm, and a large hydrophobic region in the C-terminus (46). Analysis of the hydropathy profiles has suggested that the glutamate transporters possess a global structure that is unique amongst secondary transporters (117). The six hydrophobic regions in the N-terminus are predicted to be transmembrane α-helices (58, 98, 125, 144). The predicted structural features were confirmed by monitoring of the glycosylation status of C-terminally truncated

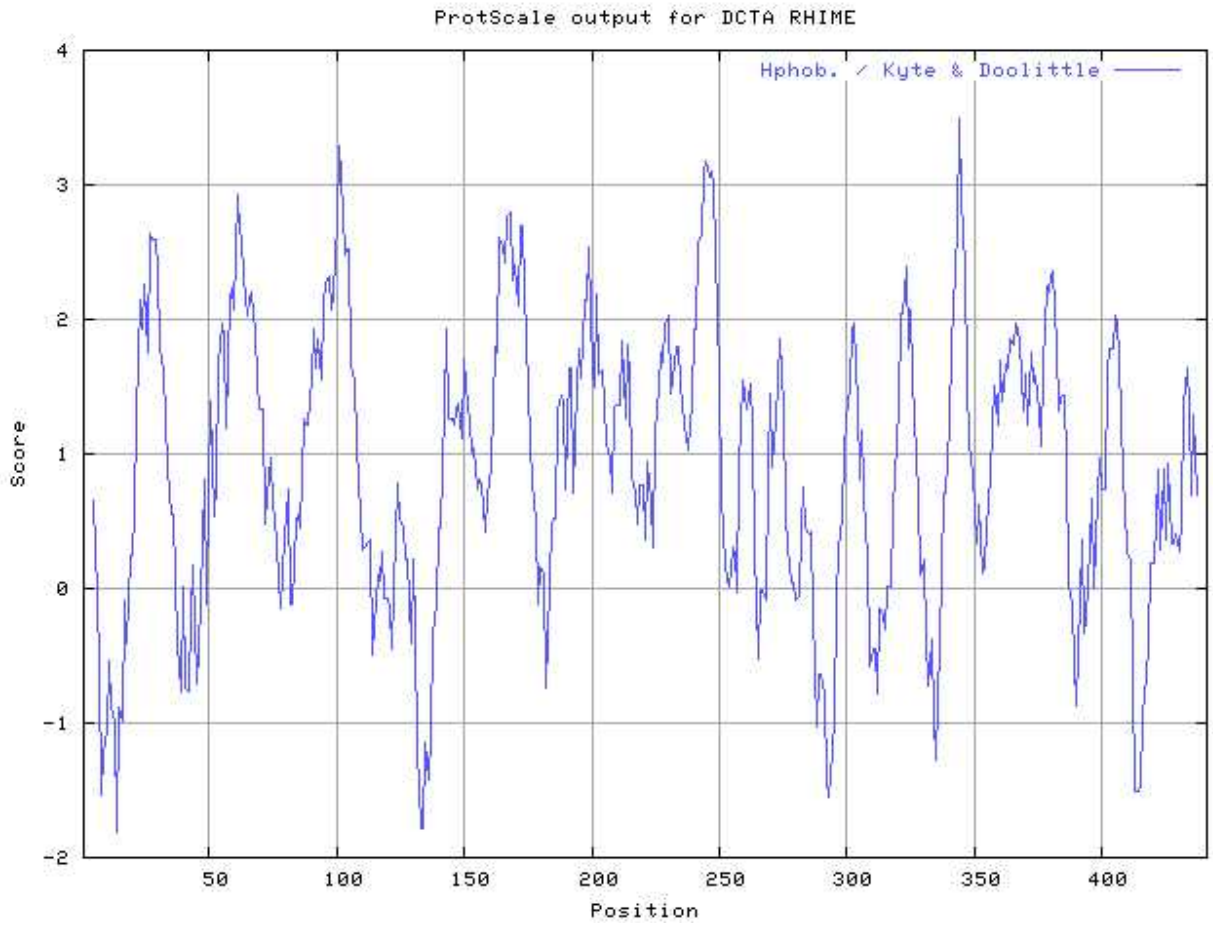

Figure 9. Kyte and Doolittle (62) Hydrophobicity plot of dctA

transporters fused to a reporter peptide containing glycosylation sites (144), and also by cysteine scanning mutagenesis (58). The current model, depicts eight α-helical trans-membrane domains (TMDs), six of which are in the N-terminal half, and two pore-loop regions, one on each face of the membrane (118). This model is shown in Figure 10.

Homology between family members is most evident in a stretch of approximately 150 residues from the C-terminal domain. This region contains four sequence motifs (A through D), that show a high level of conservation between species. All of these motifs have been suggested to play a role in the translocation pore or substrate binding site (117). Phylogenetic sequence analyses of these motifs have facilitated the subdivision of the glutamate transporter family into five subfamilies as follows: (i) eukaryotic glutamate transporters, (ii) bacterial glutamate transporters, (iii) eukaryotic neutral amino acid transporters, (iv) bacteria C4-dicarboxylate transporters (of which DctA is a member), (v) bacterial serine transporters (117). The precise function of these conserved motifs remains elusive. It has been speculated that motif A, by virtue of its serine-and-threonine rich nature may be a ligand binding site. Motif C is believed to be involved in binding the carboxylate group of substrates, as it is conserved only in the glutamate, neutral amino acid and C4-dicarboxylate carriers. Mutagenesis studies have demonstrated that motif B is involved in cation binding (117). Motif D is located within the amphipathic membrane-spanning helix 8, and, by virtue of the substrate-specific differences in sequence, is believed to be a part of the translocation pore (84, 119).

The substrate specificity of several DctA homologues has been investigated (6, 13, 15, 20), and is known to include aspartate, fumarate, malate, oxaloacetate (OAA), and succinate. D-Lactate,

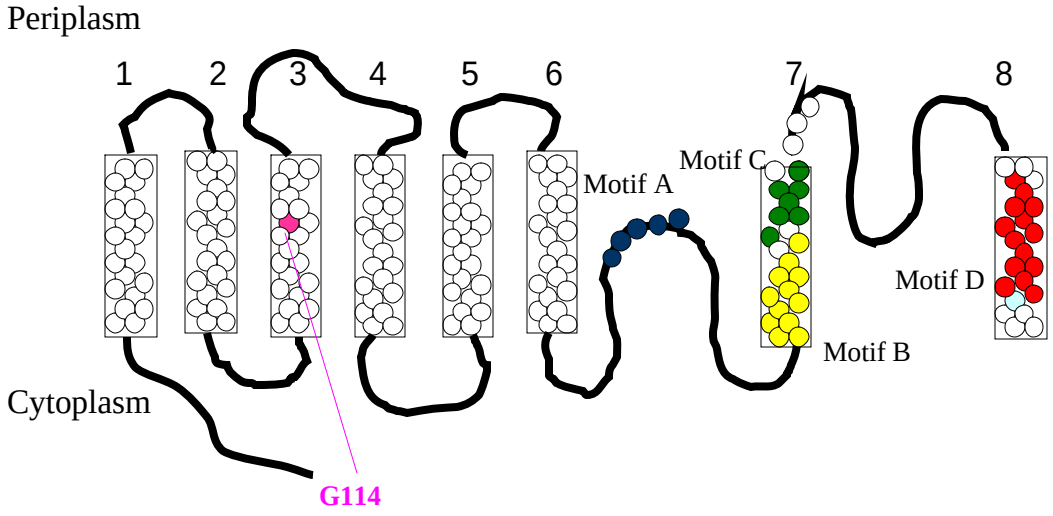

Figure 10. Model for membrane topology of DctA

Transmembrane helices labeled 1-8

Conserved C-terminal motifs shown as follows:

Motif A: Blue

Motif B: Yellow

Motif C: Green

Motif D: Red

Modified from Slotboom *et al* (119)

2-methylsuccinate, 2,2 or 2,3-dimethylsuccinate, acetoacetate, ß-hydroxybutyrate, mercaptosuccinate, α-ketoglutarate, and itaconate are also potential substrates for this system. Recent work in our laboratory (160) has demonstrated that not all substrates recognized by DctA are inducers of DctA, and not all inducers of DctA-mediated transport act as competitive inhibitors (and probably substrates) of DctA-mediated transport. This study also demonstrated the capacity of DctA to transport orotic acid and the analogue fluoroorotic acid (FOA) which, in strains possessing a functional *dctA* transport system, is toxic to cell,. and defined the roles of 17 different compounds as either inhibitors or inducers of DctA activity *in vivo*. Furthermore, it showed that DctA has a much lower affinity for orotate than either malate or succinate (160). These results imply that DctA is able to distinguish between very similar substrates based upon the relative positions of their carboxyl groups, suggesting that substrate specificity may be defined by very specific structural constraints.

The purpose of this study was to investigate specific, highly-conserved amino acid residues within DctA and its promoter region, using site-directed *in vitro* mutagenesis to determine what effects (if any) they had on *S. meliloti* growth phenotype and more specifically, upon DctA function.

1.6 Regulation of *dctA* expression

dctA is located within the *dct* cluster (Figure 11), which also contains the regulatory genes *dctB* and *dctD (38)*. In *S. meliloti*, *dctBD* encode a two-component regulatory system that, together

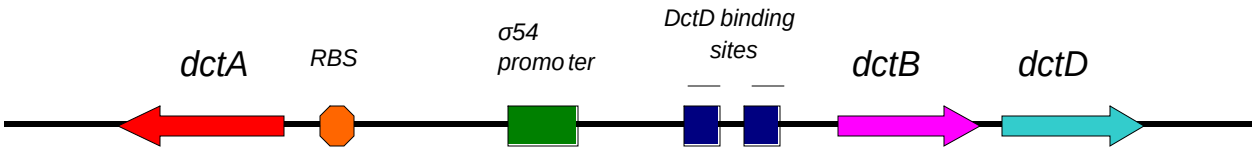

Figure 11. Organization of the *dct* cluster

RBS, ribosome binding site; UAS upstream activating sequence. Not to scale.

with the RpoN protein, activate transcription of *dctA* in the free-living state (38, 63, 68-70, 102, 107, 109, 150).

Activation of *dctA* is outlined in Figures 12 and 13. DctB and DctD are constitutively expressed at low levels (109). The *dctB* gene product is located in the cytoplasmic membrane and acts as a membrane-bound sensor that responds to the presence of C_4-dicarboxylates and transduces the signal across the membrane to activate its cytoplasmically located C-terminus. This results in autophosphorylation and phosphotransfer to DctD (44, 104). Phosphorylated DctD is able to bind to two recognition sequences upstream of the *dctA* promoter at -110 and -143 bp (44, 69) and interact with the alternative sigma factor RpoN (σ^{54}) to activate transcription of *dctA* (Figure 13) (38, 63, 68-70, 102, 107, 109, 150).

RpoN is associated with a wide variety of metabolic functions, including nitrogen and carbon metabolism amongst the proteobacteria (16). Standard phenotypes of RpoN mutants in *Rhizobium* include the inability to transport dicarboxylic acids, and form effective symbioses with host plants (23, 86, 109, 124).

Promoters activated by RpoN do not contain canonical -35 and -10 sequences, rather they possess the consensus -26 CT**GG**CACPu-N_4-TT**GC**A -12 (invariant nucleotides shown in bold) (34, 53). RpoN-dependent transcription is modulated by activator proteins, which allow σ^{54} to activate the core RNA polymerase under different physiological conditions including the availability of dicarboxylates outside of the cell (85, 93).

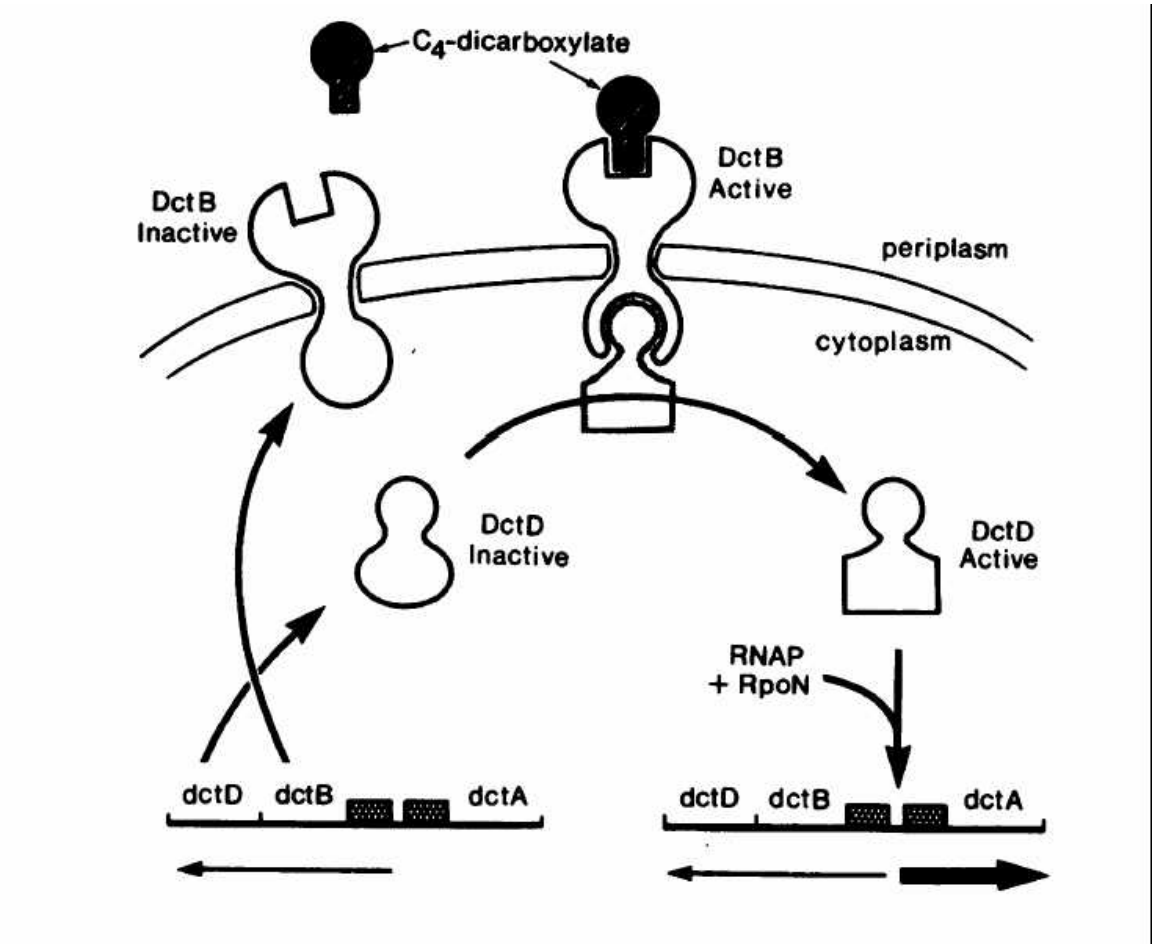

Figure 12. Model for *dctA* activation (107)

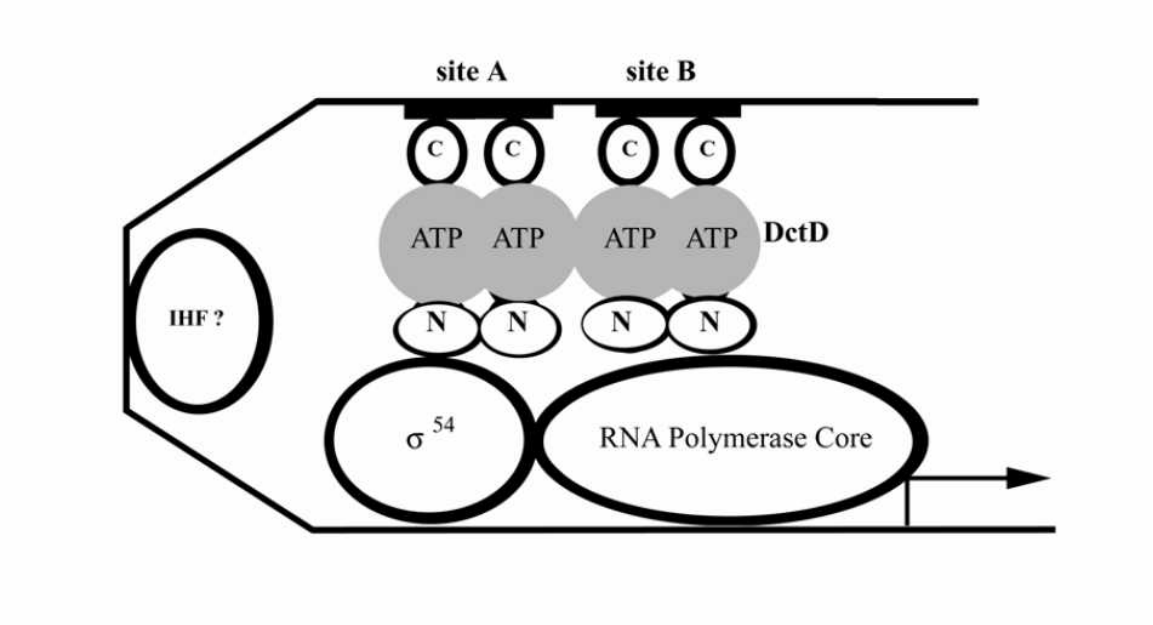

Figure 13. Transcriptional activation of *dctA*

DctD dimers bind to upstream activating sequences at -110 and -143. Each subunit has three domains, an amino terminus (N), an ATP binding site (ATP), and a carboxy terminus (C). These proteins interact with RpoN (σ^{54}). Depending upon the bacterial species, integration host factor (IHF) may be involved (93).

1.7 Role of Glycine in Transmembrane Helices

The role of glycine in the transmembrane domain of an α-helix differs from that played in a soluble protein (56). In soluble proteins, Gly is typically considered to be a "helix-breaker" (75) and ranks along with proline in most measurements of helical propensity (91). However, it is has been known for some time that glycine is commonly found within the transmembrane helices of many membrane proteins (65). Folding of soluble proteins is believed to be driven by the hydrophobic effect, with an increase in entropy resulting from the burying of hydrophobic residues within the protein core (35). The interiors of soluble proteins are thus tightly packed with densities commonly approaching those seen in crystals of small organic molecules (35, 105). In comparison, upon insertion into the membrane bilayer, polytopic membrane proteins typically form well-packed membrane-spanning α-helices (35). This spontaneous assumption of secondary structure occurs as a result of the negative free energy associated with hydrogen bonding of the polar backbone carbonyl and amide groups, combined with favorable van der Waals forces and electrostatic interactions (35).

Glycine is known to play a significant structural role in single-pass membrane proteins by promoting protein dimerization as a result of facilitating the formation of favorable van der Waals surfaces for hydrophobic packing, or by permitting closer dipole interactions of the polar backbone (17, 26, 31, 71-73, 81, 120, 122, 123). Studies now suggest that similar interactions are found in polytopic membrane proteins (31, 56). High resolution crystal structures for polytopic membrane proteins are few and far between, but with the structures for cytochrome c oxidase,

bacteriorhodopsin, the photosynthetic reaction center of *Rhodobacter sphaeroides* , and the potassium channel of *Streptomyces lividans* now available, it is apparent that glycine residues are tolerated within transmembrane helices (56). Soluble proteins have an average glycine content of approximately 9% (90), which is almost identical to the 8.7% seen in the aforementioned membrane proteins. Studies have shown that glycine is favored within the transmembrane domains of polytopic membrane proteins (31, 56). This is probably attributable to its propensity for promoting close polypeptide interactions as discussed above, providing further evidence that it plays a similar structural role in polytopic membrane proteins to single-pass membrane proteins.

In a recent study of cytochrome c oxidase (56), 25 of the 28 transmembrane helices were shown to contain glycine (56 total). Interestingly, 14 of the helices also contained proline (21 total), and 13 of these also contained a glycine residue (56). These data suggest that neither glycine nor proline are playing their "traditional" roles as helix breakers. In soluble proteins, proline is traditionally associated with the insertion of "kinks" in helical secondary structure (14, 31, 99) and thus is associated with a low packing value. In the helical regions of membrane proteins however, proline has a high packing value, leading to the theory that it is in fact the localized environment surrounding the proline residue that determines its structural propensity, and that under certain circumstances the presence of proline may even serve to stabilize helical structures (76, 127, 142). Figure 14 provides evidence to suggest that in fact, in cytochrome c oxidase, glycine and proline can adopt Ψ and Φ dihedral angles that allow them to fall within the standard α-helical region of a Ramachandran plot (56).

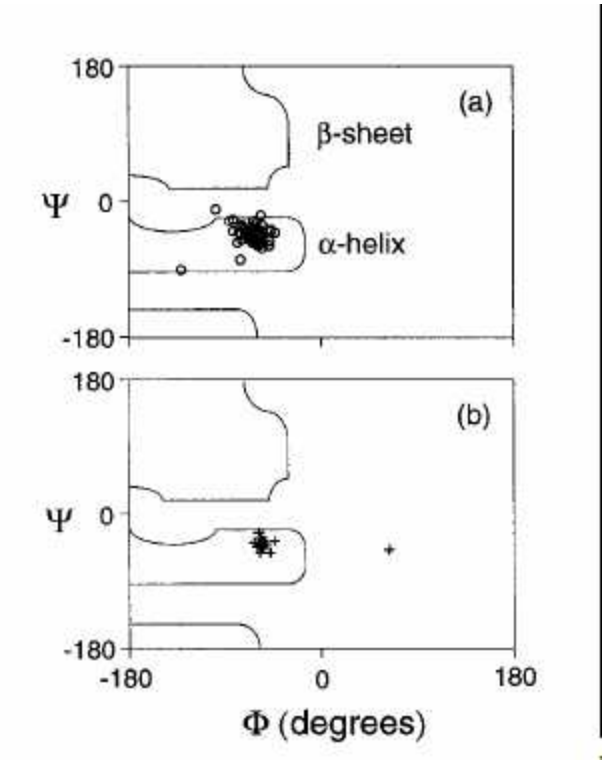

Figure 14. Dihedral Ψ and Φ angles for glycine (a) and proline (b) in the 28 transmembrane helices of cytochrome c oxidase (56).

Interestingly, membrane proteins appear to have at least twice the amount of buried glycine residues than their soluble counterparts (35). Contrary to previous assumptions that membrane proteins fold with their polar and conserved residues facing the interior of the helical bundle in order to generate the active site of the protein, it is now believed that orientation of the smaller residues into the interior of the membrane acts to guide and stabilize the tight associations of transmembrane helices (145). Glycine-glycine packing can facilitate some of the closest helical packing interactions, and can form helical "notches" into which neighboring helices can fit to facilitate orientation of the final structure upon completion of folding (56). The notches created by glycine residues within the transmembrane regions may also serve to accommodate side chains of the larger and bulkier amino acids such as phenylalanine and tyrosine (56). In single-pass membrane proteins, these associations can facilitate dimerization, whilst in polytopic membrane proteins they probably act to create an internal structure of tightly-packed helical bundles, and more loosely packed interhelical spaces (35).

DctA has a glycine content of approximately 9%, of which 34% are located in transmembrane regions; each transmembrane domain in DctA has at least one glycine residue. The proline content of DctA is approx. 4%, of which 17% are located within transmembrane regions. Further analysis of the specific roles played by glycine residues in the structure of DctA however will remain elusive in the absence of a completed structural analysis of DctA or one of its homologues by either NMR or X-ray crystallography.

1.8 *Xenopus laevis* oocytes and electrophysiology

Xenopus oocytes are highly specialized in the synthesis and storage of components required during embryogenesis (28, 66). By virtue of their large size and high metabolic activity, the oocytes can be easily injected with mRNA, used to translate membrane proteins, and subsequently clamped for electrophysiological analysis (45, 66, 131, 132). Furthermore, multiple substrates can be studied in a single experiment using a single oocyte, allowing for the generation and collection of data more easily and rapidly (153). Oocytes possess accumulated stores of cellular enzymes, organelles and proteins, all of which are required during early embryogenesis following fertilization. Microinjection of the oocyte using foreign mRNA results in a hijacking of the cell's protein synthesis apparatus, reprogramming the oocytes to produce large quantities of the corresponding foreign protein (87). Approximately 98% of oocytes have been shown to express the heterologous proteins (92).

I proposed using two-electrode voltage clamping in order to characterize DctA expressed in the *Xenopus* oocytes. Figure 15 shows a schematic representation of a two-electrode voltage clamp. In this technique, two electrodes are inserted into the oocytes to measure voltage and current.

One electrode measures membrane potential (Vm) at amplifier A, and the other is used to deliver current to maintain a predetermined voltage (Vc) at amplifier B. A computer generates a pulsed protocol in order to determine the standard current-voltage (I-V) relationship. The oocyte membrane is clamped at the specific holding voltage, Vc, and subsequently pulsed to a range of predetermined voltages, usually returning to the holding voltage between pulses. Typically, the

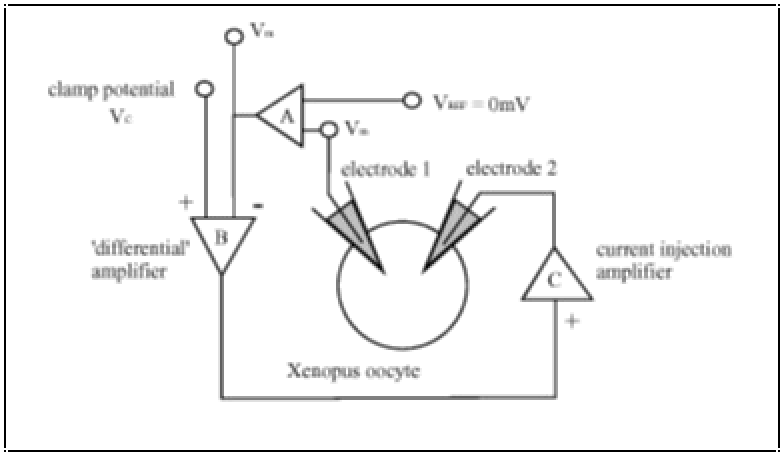

Figure 15. Schematic representation of two-electrode voltage-clamping

oocytes are voltage clamped from +20 to -150mV. If Vm and Vc differ, the output of amplifier B will cause voltage to be passed through the second electrode via the current injection amplifier C to maintain the membrane voltage during the pulses. The transporter substrate is then added to the external bathing medium, and the oocyte is again pulse-clamped through the full range of voltages, returning to the holding voltage between pulses, and the required current through amplifier C to the second electrode is measured and recorded (87). Substrate-dependent currents are calculated by subtracting the standard (before) values from those obtained after the addition of substrate and an I-V profile can be obtained by plotting the substrate-elicited currents from the standard membrane voltages (87). These currents can be fitted to Michaelis-Menton kinetics, facilitating the calculation of K_m and V_{max} (92).

Development of an assay that could utilize electrophysiological technology would allow us to more accurately analyze DctA transport activity under a multitude of different conditions. The current assay is laborious and time-consuming, thus limiting the number of experiments that can be conducted in a single day, necessitates the use of radio-labeled-substrate isotopes, and can only measure gross changes in transport activity. The *X. laevis* system is potentially much less time-consuming, does not require use of radio-labeled compounds and is extremely sensitive (87, 129). Furthermore, the current assay does not allow investigation of the coupling of cations to substrate transport, *Xenopus* oocytes have been used extensively to study this phenomenon in other glutamate transporter systems (27).

Chapter Two Materials and Methods

2.1 Bacterial strains and plasmids

A comprehensive list of bacterial strains and plasmids used in this work are listed in Table 2.

2.2 Bacterial growth and storage conditions

All growth medium recipes are listed in Appendix 6.1.1. *Escherichia coli* strains were routinely grown using Luria-Bertani (LB) media (112) or M9 minimal salts medium (112) with 0.2% glycerol, malate, fumarate, succinate, or aspartate as the carbon source, supplemented with carbamoyl aspartate (100 µg/ml) and thiamine (2 µg/ml).

Sinorhizobium meliloti were routinely grown at 30°C using either minimal mannitol medium containing NH_4 (MM NH_4) (121), minimal medium containing NH_4 and supplemented with 0.2% glycerol, malate, fumarate, succinate, or aspartate as the carbon source, or M9 medium (156) modified by replacing Na_2HPO_4 with 8.7 g of K_2HPO_4 per liter . The M9 medium was supplemented with either 20 mM mannitol or 0.2% aspartate and 5 ml of 1% yeast extract (Difco) per liter.

Table 2. List of strains and plasmids used in this study

Strain	Relevant Characteristics	Reference/Source
	Escherichia coli	
DH5α	*endA hsdR17 supE44 thi -1 recA1 gyrA96 relA1 Δ(argF-lacZYA)U169 ΦdlacZΔM15*	Invitrogen Inc.
S17-1	Integrated RP4 *tra* region, Sp^r; mobilizer strain pro hsdR recA [RP4-2(Tc::Mu) (Km::Tn7)]	Simon *et al* 1983
Kur1349	K12 *araD139 ΔlacU169 rpsL thi ΔpyrB usp -4*	Baker *et al* 1996
Kur1351	Kur1349 *out-2*	Baker *et al* 1996
XL-1 Blue	*recA1 endA1 gyrA96 thi -1 hsdR17 suoE44 RelA1 lac[F' proAB lacI ^qZΔm15 Tn10* Tc]	Stratgene, La Jolla, Ca
	Sinorhizobium meliloti	
Sm1021	Sm^r	Meade *et al* 1982
Sm1021-I	Sm^r Δ*dctA* from 2nd Met	Yurgel (unpublished)
Sm1021-II	Sm^r Δ*dctA* from 3rd Met	Yurgel (unpublished)
WSUb20611-II xDCTA_MET1	Sm^r Δ*dctA* from 3rd Met pDCTA_MET1 chromosomal integrant Nmr	This Work
WSUb20611-II xDCTA_MET2	Sm^r Δ*dctA* from 3rd Met pDCTA_MET2 chromosomal integrant Nmr	This Work
WSUb20611-II xDCTA_MET3	Sm^r Δ*dctA* from 3rd Met pDCTA_MET3 chromosomal integrant Nmr	This Work
WSUb20611-II xDCTA_MET1-2	Sm^r Δ*dctA* from 3rd Met pDCTA_MET1-2 chromosomal integrant Nmr	This Work
WSUb20611-II xDCTA_MET1-3	Sm^r Δ*dctA* from 3rd Met pDCTA_MET1-3 chromosomal integrant Nmr	This Work
WSUb20611-II xDCTA_MET2-3	Sm^r Δ*dctA* from 3rd Met pDCTA_MET2-3 chromosomal integrant Nmr	This Work
	Plasmids	
pK19*mob*	Km^r *lacZα* OriT	Schafer *et al* 1994
pCPP30	IncP LacZ; Tc^r	Huang *et al* 1992
pUC18	Amp^r	Yanisch-Perron *et al* 1985
pWhitescript™	Amp^r	Stratgene, La Jolla, Ca
pTH32	2.2-kb *Eco*RI *dctA* subclone from pTH24 into pRK7813-1	Yarosh *et al* 1989

pSM100	1.5-kb *Bam*HI *dctA* subclone from pTH32 into pCPP33	Yurgel *et al* 2000
pSM105	1.8kb *Bam*HI *Eco*RI *dctA*-FLAG Subclone from pTH32 into pCPP30	This Work
pSM100-32	1.5-kb BamHI dctA subclone from pTH32 into pCPP33 containing a randomly generated G114D mutation	Yurgel and Kahn, 2004
pK19*mob*-105	1.8kb *Bam*HI *Eco*RI *dctA*-FLAG Subclone from pTH32 into pK19*mob*	This Work
pK19*mob*-105-G114A	pK19*mob*-105 with G114A substitution	This Work
pK19*mob*-105-G114D	pK19mob-105 with G114D substitution	This Work
pK19*mob*-105-G114F	pK19mob-105 with G114F substitution	This Work
pK19*mob*-105-G114P	pK19mob-105 with G114P substitution	This Work
pSM105-G114A	pSM105 with G114A substitution	This Work
pSM105-G114D	pSM105 with G114D substitution	This Work
pSM105-G114F	pSM105 with G114F substitution	This Work
pSM105-G114P	pSM105 with G114P substitution	This Work
pGEM-HE	Amp^r	Liman *et al* 1992
pGEM-HE *dctA*-His	pGEM-HE with *dctA*-His	This Work
pKDCTA_MET1	pK19mob dctA with Met1 substitution	This Work
pKDCTA_MET2	pK19mob dctA with Met2 substitution	This Work
pKDCTA_MET3	pK19mob dctA with Met3 substitution	This Work
pKDCTA_MET1-2	pK19mob dctA with Met1-2 substitution	This Work
pKDCTA_MET1-3	pK19mob dctA with Met1-3 substitution	This Work
pKDCTA_MET2-3	pK19mob dctA with Met2-3 substitution	This Work

Antibiotics were used in the growth media when appropriate. All antibiotics used, and their respective concentrations are listed in Appendix 6.1.2.

All bacterial cultures were stored at -80ºC in cryotubes containing liquid growth medium and either 12.5% v/v DMSO or 20% v/v glycerol.

2.3 Molecular Biology Techniques

2.3.1 Small-scale preparation of plasmid DNA

Plasmid DNA was routinely isolated using a modified version of the standard alkaline lysis protocol (112), as developed by Qiagen (Qiagen, Alameda, CA) as per manufacturers directions. Plasmid DNA was typically stored at -20ºC.

2.3.2 Medium-Scale preparation of pDNA

Low-copy number plasmids and larger amounts of other plasmids were prepared using the Qiagen Midi-Prep kit (Qiagen, Alameda, CA) as per manufacturers directions.

2.3.3 Small scale preparation of total genomic DNA from *S. meliloti*

Genomic DNA was isolated from *S. meliloti* using the Qiagen DNeasy Tissue kit (Qiagen, Alameda, CA) as per manufacturer instructions. All genomic DNA was stored at -20°C.

2.3.4 DNA Manipulations

2.3.4.1 Restriction analyses, gel electrophoresis, and cloning of DNA

Standard protocols were used to manipulate DNA (112). Restriction digests were typically performed using enzymes purchased from Promega (Promega US, Madison WI). Reaction mixes were incubated at 37ºC for 30 min to 3 hr depending upon the reaction volume and its intended use. The restriction products were typically analyzed by gel electrophoresis using 1% agarose TBE. Samples were mixed with an appropriate volume of 6X loading buffer (see Appendix 6.2.1) and run at 80-120V for 30 min to 2 hr depending upon size of gel and desired resolution of restriction products. When specific restriction fragments were needed in subsequent experiments, the band of interest was cut from the gel and the DNA fragment isolated using the Zymoclean Gel DNA Recovery Kit™ as per manufacturers instructions.

2.3.4.2 Transformation of plasmid DNA

Plasmid DNA of the desired concentration was transformed into the appropriate *E. coli* strain which had previously been made either chemically competent by calcium chloride, or electrocompetent with 10% glycerol and stored at -80ºC. For electroporation, 100 µl electrocompetent cells were mixed with 1-5 µl of plasmid DNA depending on concentration, and shocked with 1.50 kV. The cells were recovered for at least 1 hr at 37ºC in 1 ml LB before plating onto solid media containing the appropriate antibiotics. Chemically competent cells were mixed with 1-5 µl DNA and incubated on ice for at least 30 min before being heat shocked for 90 sec at 42ºC, returned to ice for 2 min and recovered for at least 1 hr at 37ºC in 1 ml LB before plating onto selective media.

2.3.4.3 Conjugation of plasmid DNA into *S. meliloti*

Conjugation was performed in a biparental mating between an *E. coli* donor and an *S. meliloti* recipient. Matings were performed by combining 500 µl saturated broth culture of each strain, pelleting by centrifugation, washing in 0.85% NaCl to remove antibiotics, and resuspending in 100 µl for spotting onto a non-selective LB plate. The matings were incubated from 6 hr to overnight at 30ºC before the spot was resuspended in 0.85% NaCl.

2.3.5 DNA Sequencing

All DNA sequencing was performed at the WSU LBB1 Sequencing Center. Primers used in the sequencing reactions include Dct3 and Dct4 which are internal to the *dctA* gene for sequencing putative mutant *dctA*, and MZdctF1 and 1XFLAGRev which are external to the *dctA* gene for sequencing the entire fragment cloned from genomic DNA into pK19*mob*.

2.3.6 PCR

PCR was performed using either an MJ Research PTC Peltier Thermal Cycler or Minicycler (MJ Research Inc. Reno, NV). A typical PCR reaction to clone from genomic DNA is shown in Appendix 6.2.2, and utilized reagents from Invitrogen Life Technologies (Invitrogen Life Technologies, Carlsbad, Ca). A typical PCR reaction used in the generation of amino acid point mutations is shown in Appendix 6.2.3, and utilized reagents from Stratagene (Stratgene, La Jolla, Ca). Primers were obtained from Invitrogen Life Technologies. A comprehensive list of primers used in this study is shown in Table 3.

2.3.7 Site-Directed mutagenesis

In vitro site-directed mutagenesis was performed using the Stratagene Quik-Change® Site-Directed Mutagenesis Kit (Stratgene, La Jolla, Ca) as per manufacturers directions. Primers

Table 3. Primers used in this study

Primer Name	Tm °C	Use	Sequence
DctAHis		Addition of Hexa-His tag to Cterm	CATGGGATCCTTAGTGATGGTGATGGTGATGTTCGG CGGGCTGGACGACC
Dct7		N-term of *dctA*-his	GCATGGATCCCGGAAGGCATAGTCGTTGCC
1XFLAG Rev Primer	80	Addition of FLAG tag to C-term	CCTGAATTCTTATTTGTCATCGTCATCCTTGTAT TCGGCGGGCTGGACGACCGC
MZdctF1	69	N-term of *dctA*-FLAG	CCTGGATCCCGACTGCTCGAAGAAGCGAGG
MZG114PF	79.6	G114P Forward	CGCGCTTGTCGTCCCCCTCGTCGTCGCAA
MZG114PR	79.6	G114P Reverse	TTGCGACGACGAGGGGGACGACAAGCGCG
MZG114FF	79.8	G114F Forward	TCGCGCTTGTCGTCTTCCTCGTCGTCGCAAAC
MZG114FR	79.8	G114F Reverse	GTTTGCGACGACGAGGAAGACGACAAGCGCGA
MZG114DF	78.4	G114D Forward	CGCTTGTCGTCGACCTCGTCGTCGC
MZG114DR	78.4	G114D Reverse	GCGACGACGAGGTCGACGACAAGCG
G114AF	81	G114A Forward	CGCTTGTCGTCGCCCTCGTCGTCGC
G114AR	81	G114A Reverse	GCGACGACGAGGGCGACGACAAGCG
MET-I-DCT-S	101	Delete 1st Met	GCAAACTGGCACGCATATTGCTGACAAGCTCCA
MET-I-DCT-A	101	Delete 1st Met	TGGAGCTTGTCAGCAATATGCGTGCCAGTTTGC
MET-II-DCT-S	100	Delete 2nd Met	GAGGCCCGGCAATTGCCGGACTGG
MET-II-DCT-A	100	Delete 2nd Met	CCAGTCCGGCAATATGCCGGGCCTC
MET-III-DCT-S	100	Delete 3rd Met	CCACGTGGAGGATATCCTGATCATCGAACATTCCG
MET-III-DCT-A	100	Delete 3rd Met	CGGAATGTTCGATGATCAGGATATCCTCCACGTGG

were designed using the Stratagene Quik-Change® Site-Directed Mutagenesis primer design program available through their homepage at http://labtools.stratagene.com. All primers used are listed in Table 3. Primers were purchased from Invitrogen (Invitrogen Life Technologies, Carlsbad, Ca). PCR was performed using an MJ Research PTC Peltier Thermal Cycler (MJ Research Inc. Reno, NV), a typical mutagenesis PCR reaction is shown in Appendix 6.2.4.

2.4 Protein Analysis

2.4.1 Anti-DctA antibody design and generation

The sequence VATYAEKAHEQSIT, which corresponds to the periplasmic region between transmembrane helices 3 and 4, was chosen as the sequence against which antibodies were to be generated. Analysis by Pacific Immunology Corporation (San Diego, Ca) indicated that this was a good choice due to its hydrophilic character and minimal homology with other proteins in *S. meliloti*. A cysteine residue was added to the C-terminal end of this polypeptide to facilitate conjugation to a KLH-carrier protein. The C-terminal end was chosen as the attachment point to maximize presentation of the N-terminus as this is the region in which the peptide sequence is found in DctA.

The polypeptide was synthesized by Pacific Immunology Corporation (San Diego, Ca) and conjugated to the carrier protein KLH. The peptide conjugate was used to immunize two rabbit four times each. Pre-immune sera were collected from each rabbit, and anti-sera were collected

four times over thirteen weeks. The anti-sera used in this study were collected seven weeks post-inoculation and was unpurified. Following completion of this study we are expecting to receive affinity-purified anti-sera.

2.4.2 Western Blot Analysis

2.4.2.1 Polyacrylamide Gel Electrophoresis

All buffer and gel recipes are listed in Appendix 6.3. Strains of *E. coli* and *S. meliloti* were grown to mid exponential phase in an appropriate liquid medium prior to harvest. A 200 µl sample was then pelleted and the supernatant decanted. *S. meliloti* cells were then washed twice in 200 µl 0.85% NaCl to remove their exopolysaccharide layer (155). The pellet was resuspended in 50 µl SDS Loading Buffer and incubated at 100°C for approximately 5 min. Typically 25 µl of sample was loaded onto a 12% SDS-PAGE EDTA gel in a continuous buffer system and the gel was run at 80-100V for approximately 2-3 hr.

2.4.2.2 Coomassie Brilliant Blue Staining

The gel was incubated in a volume of coomassie brilliant blue stain solution sufficient to submerge it completely, for approximately 1hr on a slowly rocking platform. The gel was then typically destained for 6 hr to overnight at room temperature on a slowly rocking platform (112).

Occasionally the destained gel might have been used in a subsequent electrophoretic transfer to a PVDF membrane. More typically the destained gel would be scanned and the image saved as a .gif file.

2.4.2.3 Western blot transfer and hybridization

Proteins were transferred from the SDS-PAGE gel to a Millipore Immobilon-P polyvinylidene difluoride (PVDF) membrane (Millipore, Billerica, Mass, USA) using an Invitrogen X-Cell Surelock™ mini cell (Invitrogen Life Technologies, Carlsbad, Ca) as per manufacturers instructions. Protein transfer typically took 2-5 hr at 25mA, depending upon gel size and total surface area of gels to be transferred. Transfer efficiency was monitored by analyzing the transfer of protein standards, and occasionally by subsequent staining of the PVDF membrane using a coomassie brilliant blue membrane stain. Following transfer, the membrane was blocked from 30 min to overnight in 5% dried milk blocking buffer prior to a brief wash in TTBS and subsequent incubation with the appropriate dilution of primary antibody. The membranes were typically probed with a 1:50,000 dilution of mouse monoclonal anti-FLAG primary antibody (Sigma-Aldrich Corp. St. Louis, MO) for 2 hr, although this was extended up to overnight if increased sensitivity was required. This was followed by a thorough wash in approximately 2 l TTBS on a slowly rocking platform. A 1:20,000 dilution of either alkaline phosphatase or horseradish peroxidase conjugated GAM secondary antibody (Pierce Biotechnology Inc. Rockford, Il) was used to probe for the presence of the primary antibody. The membranes were

exposed to the secondary antibody solution for approximately 1 hr before being thoroughly washed in TTBS.

This protocol was modified during the trouble-shooting of the anti-DctA antibody. Following transfer, membranes were incubated from 1 hr to overnight in blocking buffer containing 9% non-fat dried milk in PBS with 1% Tween-20. PBS was used in an attempt to decrease the stringency of epitope-antigen binding as the higher NaCl content of TBS was thought to be potentially problematical. The membranes were incubated overnight at 4°C in a 9% dried milk PBS-Tween-20 buffer containing between 1:50 to 1:5000 dilution of primary antibody, and approximately 2mg/ml of whole-cell protein from either *E. coli* or *S. meliloti* , depending upon the strain used to express the DctA protein.. The following morning the membranes were washed well with PBS-Tween-20 and then incubated for 2 hours in a 9% dried milk PBS-Tween-20 buffer containing a 1:20,000 dilution of secondary antibody, before being washed in PBS-Tween-20.

2.4.2.4 Western blot visualization

Hybridization was visualized by chemiluminescent detection using either Immun-Star-AP Chemiluminescent Kit (Bio-Rad Laboratories, Hercules, Ca) for alkaline-phosphatase conjugated secondary antibody or SuperSignal® West Pico Chemiluminescent Substrate (Pierce Biotechnology Inc. Rockford, Il) for horseradish peroxidase conjugated secondary antibody followed by exposure to X-ray film.

2.5 Phenotypic Analyses

2.5.1 Substrate utilization plate tests

Growth substrate phenotypes were analyzed by plating serial dilutions of the strains of interest onto plates containing different defined carbon sources and analyzing the ability of the strain to utilize a particular substrate. Typically 200 µl of cells grown to mid-exponential phase were washed twice and resuspended in 200 µl 0.85% saline. Serial dilutions were made to 10^{-5} in one half of a 96-well plate, and these were replica plated onto the media of interest. Plates were incubated for 48hours before being analyzed and photographed. DctA function was also assessed by analyzing growth of strains in the presence of the toxic substrate 5-Fluoroorotate (FOA). Replicates were made onto $MMNH_4$ containing 1, 2, 3, and 5µg/ml FOA. Growth in the presence of FOA is indicative of impaired DctA function.

2.5.2 Growth curve analyses

Growth assays using a 96-well microtiter plate were used to quantitatively examine the ability of each strain to transport different substrates. Single colonies of each strain were resuspended in 5 ml $MinNH_4$ liquid medium. 20 µl of the cell suspension was used to inoculate 180 µl of defined media in a Cellstar® 96-well plate (Greiner Bio-one, Longwood FL). The 96-well plate was then incubated at 30°C in a Spectramax 250 microplate spectrophotometer (Molecular Devices Corporation, Sunnyvale Ca) for 72 hr with absorbance readings taken at 600nm every 10 min.

2.5.3 Transport assays with whole cells of *S. meliloti*

To induce transport, cells were cultured overnight in M9 medium containing mannitol and then sub-cultured overnight by a 1:50 dilution into 50ml M9 medium containing mannitol and 0.1% maleate as an inducer. Maleate induces succinate transport by DctA by approximately 100-fold (160). To assess transport, the cells were chilled, washed twice in M9 salts, and resuspended in M9 medium. A 300 µl aliquot of cells was added to a vial at 30°C and warmed for 2 min. Labeled substrate was added and 100-µl aliquots were taken at 1 min intervals. The uptake was measured using various concentrations of [^{14}C]succinate (Moravek Biochemicals, Brea, Ca) containing 0.1 µCi ml^{-1}. Samples were filtered through 0.45-µm-pore-size nitrocellulose membrane filters (NitroBind), washed twice with 3 ml of M9 salts, and dried. Their radioactivity was measured in Scintisafe Econol scintillation fluid (Fisher Scientific, Pittsburgh, Pa.) using a Packard Tri-Carb 2100 TR scintillation counter. A 10-µl aliquot was spotted on a dry filter and counted to measure total radioactivity in the assay culture. Experiments were repeated at least twice.

2.6 Membrane isolation and analysis

2.6.1 *E. coli*

All solutions pertaining to membrane isolation are listed in appendix 6.3.3.1. *E. coli* membranes were isolated using a modified version of the protocol developed by Ward *et al* (110, 146-148).

Cells were grown in 50 ml LB broth to mid-logarithmic stage, and were harvested by centrifugation at 12,000 rpm, 10°C for 10 min. The pellet was resuspended in 10 ml 0.2M Tris-HCl buffer and shaken at room temperature for 25 min. At zero time, 9.7 ml sucrose buffer was added, at 1.5min 1 ml of 1.3 mg/ml lysozyme was added and at 2 min 20 ml dH_2O was added. This was shaken at room temperature for 30-60 min before sedimentation at 20,000xg, 10°C for 20 min. The supernatant from this spin contained the periplasmic fraction and was stored at 4°C. The pellet was resuspended in 30 ml dH_2O and was allowed to stand at room temperature for 30 min. This solution was centrifuged at 30,000 x g for 20 min, the supernatant contained the cytoplasmic fraction, and it was stored at 4°C. The pellet was washed three times in 15 ml membrane resuspension buffer, before being resuspended in 1 ml membrane resuspension buffer. $MgCl_2$ was added to final concentration of 1 mM, and DNase was added to 20µg/ml. This reaction was left at 37°C for 30 min before it was stopped by EDTA to a final concentration of 1 mM. This whole tube was flash frozen and stored at -80°C.

The frozen pellet was thawed on ice and the volume increased to 5ml with Tris-EDTA buffer. This solution was passed through a French pressure cell at 20,000 psi and the outflow was collected. Unbroken cells and debris were removed from the solution by centrifugation at 10,000 x g for 45 min. The supernatant was then centrifuged at 131,000 x g using a Beckman L1 Ultracentrifuge (Beckmann Coulter Inc., Fullerton, Ca) for 2 hr and the pellet, which contained the membranes, was taken up in 250 µl of 25% sucrose in tris-EDTA. This solution was then analyzed by SDS-PAGE and western blot.

2.6.2 *S. meliloti*

All solutions pertaining to membrane isolation are listed in appendix 6.3.3.2. *S. meliloti* membranes were isolated using a modified version of the protocol developed by De Maagd and Lugtenberg (30).

Cells were grown to mid-log phase in 50ml TY using a 1:100 dilution from a 5 ml seed culture. The cells were harvested by centrifugation at 6000 rpm and resuspended in 10ml Tris-HCl buffer containing 0.2mg/ml DNase and 0.2mg/ml RNase. The cells were lysed by three passages through a French pressure cell at 20-25,000 psi followed by treatment with 0.2 mg/ml of lysozyme for 30 min. Unbroken cells and debris were removed by centrifugation at 900 x g for 20 min at 4°C. To check for inclusion bodies, the supernatant from this spin was then centrifuged at 10,000 x g for 45 min. The resultant supernatant was centrifuged at 262,000 x g for 2 hr using a Beckman L1 Ultracentrifuge (Beckmann Coulter Inc., Fullerton, Ca), and the pellet was resuspended in 1ml Tris-HCl pH 8.0. This solution was analyzed by SDS-PAGE and western blot.

2.7 Plant Growth and Assay Conditions

2.7.1 Plant Growth Conditions

Alfalfa (*Medicago sativa cv.* Champ) was used for all nodulation studies. Seeds were surface sterilized using concentrated sulfuric acid, washed several times in sterile water and soaked in bleach (5% sodium hypochlorite) for 5 min. Seeds were again rinsed several times in sterile distilled water, then spread evenly on YMB agar plates and allowed to germinate at 30^{o}C. Seedlings showing no signs of contamination were moved to sterile growth boxes, consisting of two Magenta (Sigma GA-7 vessel) plant tissue boxes with the top box inverted to act as an aseptic barrier and containing a mixture of sand and LECA clay aggregate (Eco Enterprises, Shoreline, WA). Six seedlings were used per box and each strain was evaluated in at least 3 boxes. Each growth box was inoculated with the tested strains by applying 10^{8} cells suspended in sterile water. Plants were grown in a walk-in growth room at 22^{o}C. Five to six weeks after inoculation, plants were harvested and examined for root nodule formation. Shoot dry mass of the plants was measured and nitrogenase activity was assayed by using the acetylene reduction technique on whole individual nodules.

2.7.2 Acetylene Reduction Assay

Alfalfa plants were carefully removed from the boxes and the roots gently rinsed in dH_2O to loosen and remove residual sand. Nodules were removed from the roots using clean tweezers,

the nodules from plants in each box were weighed, and 10-50 mg nodules were transferred to a glass serum bottle. Each bottle was sealed with a rubber septum, and, using a 1 cc syringe and needle, 1 ml of air was removed from the bottle and replaced with 1 ml acetylene. Acetylene was generated by adding calcium carbide (Sigma C-5562, Sigma-Aldrich Corp, St. Louis MO) to water and trapping the gas formed. 50 µl samples were taken from the serum bottle after 2, 4, and 6 min following addition of acetylene and were injected into a Shimadzu GC-8A chromatograph (Shimadzu Biotech. USA, Columbia MD) containing a Poropak N column and equipped with an SP4290 Integrator (Spectra-Physics, Mountain View Ca). Ethylene was detected as a peak between 0.69 and 0.75.

2.7.2.1 Calculation of acetylene reduction rates

Acetylene reduction rates were calculated using the following equation:

$$\text{Reduction} = \frac{[(\text{Slope} \times A_E) + \text{Intercept}] \times (V/V_{INJ})}{M \times T}$$

Where:

Slope and Intercept are calculated from a linear regression with ethylene controls

A_E is the area under the experimental ethylene peak

Inj_S is the nmoles ethylene in the standard injection

V is the volume of the reaction vial (10,000µl)

V_{INJ} is the volume of experimental injection (50µl)

M is the mass of experimental nodules (in mg)

T is the time under acetylene (in minutes)

The resultant rates are expressed as nmole.mg^{-1}.min^{-1}.

2.7.3 *Xenopus laevis* Protocols

2.7.3.1 Preparation of RNase-free reagents and working conditions

RNase-free dH_2O was prepared using the Barnstead Nonpure Infinity Water Purification System (Barnstead International, Boston Ma). Bench tops were washed down with 10% bleach solution and 100% EtOH, then covered with a double layer of bench paper. All pipettes and racks were washed with the above solutions, and were kept between the sheets of bench paper when not in use. Reagents were prepared using RNase-free water, and were used exclusively for RNase-free work with RNase-free plasticware. All work was performed wearing gloves. All plasticware used was disposable and purchased RNase-free from USA Scientific (USA Scientific Inc., Ocala, FL).

2.7.3.2 *In vitro* Transcription

In vitro transcription was performed using the Ambion mMessage mMachine® High Yield Capped Transcription kits (Ambion Inc. Austin, TX) as per manufacturers instructions. Plasmid DNA was purified for transcription using the Qiagen Midi-Prep plasmid purification kit (Qiagen, Alameda, CA) to produce extremely clean DNA. The DNA was then prepared for transcription by linearization. Following transcription, the RNA product was confirmed by running 1µl on a formaldehyde gel. All RNA samples were stored at -80°C.

2.7.3.3 Formaldehyde-Agarose Gel Electrophoresis

1.5% Formaldehyde-agarose gels were made using standard techniques. RNA molecular standards were purchased from Initrogen (Invitrogen Life Technologies, Carlsbad, Ca). All solutions pertaining to this protocol are described in appendix 6.2.4

2.7.3.4 *X. laevis* oocyte isolation and injection

All solutions pertaining to this protocol are listed in appendix 6.2.4

Female *X. laevis* were kept at room temperature (16-18°C). The frogs were anaesthetized and a small abdominal incision was made to remove the ovarian lobes. The follicular cell layer was removed by digestion with collagenase (2mg/ml) in OR2 solution for 2-3 hr. The oocytes were

then transferred to ND96 solution and pressure-injected with approximately 40nl of mRNA solution. Once injected, oocytes were maintained at approximately 18-20°C in ND96 supplemented with 2.5 mM sodium pyruvate (Sigma Cat. #P5280, -Aldrich Corp, St. Louis MO) and 100 µg/ml gentamycin (Sigma Cat. # G1264, Sigma-Aldrich Corp, St. Louis MO). The incubation medium was changed daily, and the oocytes were monitored for signs of degradation, any oocytes that appeared to be degrading were removed.

2.7.3.5 *X. laevis* bulk transport assays

After incubation at approximately 18-20°C for 48 hr, the oocytes were assayed for bulk transport activity. The oocytes were incubated for 15 min at room temperature in 2 ml ND96 supplemented with either 50 µM ^{14}C-Succinate or 3 µM ^{14}C-Orotate at a specific activity of 2µCi/ml. The oocytes were washed three times with 1 ml ND96 and transferred to individual scintillation vials where they were homogenized in 100 µl 1% SDS (25). Radioactivity was measured in Scintisafe Econol scintillation fluid (Fisher Scientific, Pittsburgh, Pa.) using a Packard Tri-Carb 2100 TR scintillation counter (Global Medical Instrumentation Inc., Albertville MN).

2.7.3.6 Preparation of *X. laevis* oocytes for western blot analysis

Oocytes were transferred to an eppendorf tube containing 1ml standard tris-free buffer. The buffer was drawn off and replaced with 20 µl lysis buffer per oocyte. Oocytes were lysed

initially by pipetting the mixture up and down approximately 20 times. Lysis was completed by sonicating the oocytes on ice for 3 10sec pulses followed by pipetting up and down 10 times, for a total of three repetitions. The oocytes were incubated on ice on a rocking platform for 1 hr. Following lysis, the lysate was pelleted at 13,000rpm, 4°C for 10sec and the clear supernatant component was removed and transferred to a clean tube. This was repeated a further two times to ensure the soluble lysate was completely separated from the yolk and insoluble fractions.

Chapter Three Results and Discussion

3.1 Cloning of *dctA*

3.1.1 Generation of a *dctA*-FLAG translational fusion

dctA was amplified by PCR from pTH32, a 10 kb, broad host range plasmid, containing a 2.2 kb fragment that includes *dctA* and its promoter region (157). The primers (listed in Table 3), were designed to amplify *dctA* as a 1815 kb fragment which included 419 bp of upstream region to capture the entire *dctA* promoter. The size of the PCR product was confirmed by agarose gel electrophoresis. The primers were designed to incorporate a 21 bp FLAG epitope tag, and to attach *BamHI* and *EcoRI* sites on the 5' and 3' ends of this fragment, respectively. FLAG is an octapeptide DYKDDDDK, against which commercially available monoclonal antibodies have been raised (22, 143). FLAG was included in this construction to provide a means by which *dctA* expression could be detected and confirmed by western blot as there is no anti-DctA antibody available.

3.1.2 Cloning of *dctA*-FLAG into pK19*mob*

The *dctA*-FLAG PCR product was cloned into pK19*mob* (113) as a *BamHI/EcoRI* fragment to facilitate directional cloning, yielding plasmid pK19*dctA*-FLAG. pK19*dctA*-FLAG was then transformed into chemically competent *E. coli* strain Kur1351, and selected on LB Kan_{40}. The native promoter region was included to allow induction of DctA expression by the addition of dicarboxylates to the growth media, and also to provide sufficient homology to allow chromosomal recombination if needed. The presence of the *dctA*-FLAG construct was confirmed by sequencing of both the 5' and 3' regions of the gene,, and DctA-FLAG expression in *E. coli* was confirmed by western blot analysis.

3.1.3 Subcloning of *dctA*-FLAG into pCPP30 in *E. coli*

pK19*mob* has a narrow host-range replicon that can not replicate in *S. meliloti* . To allow transfer and subsequent expression in *S. meliloti* , *dctA*-FLAG was subcloned as a *BamHI/EcoRI* fragment into the MCS of the broad host range plasmid pCPP30, downstream of the lacZα promoter and part of the *lacZ* gene (51).This construct is called pSM105, and is shown diagrammatically in Figure 16. The presence of the insert was confirmed by restriction endonuclease digestion, and DctA-FLAG expression in *E. coli* was confirmed by western blot.

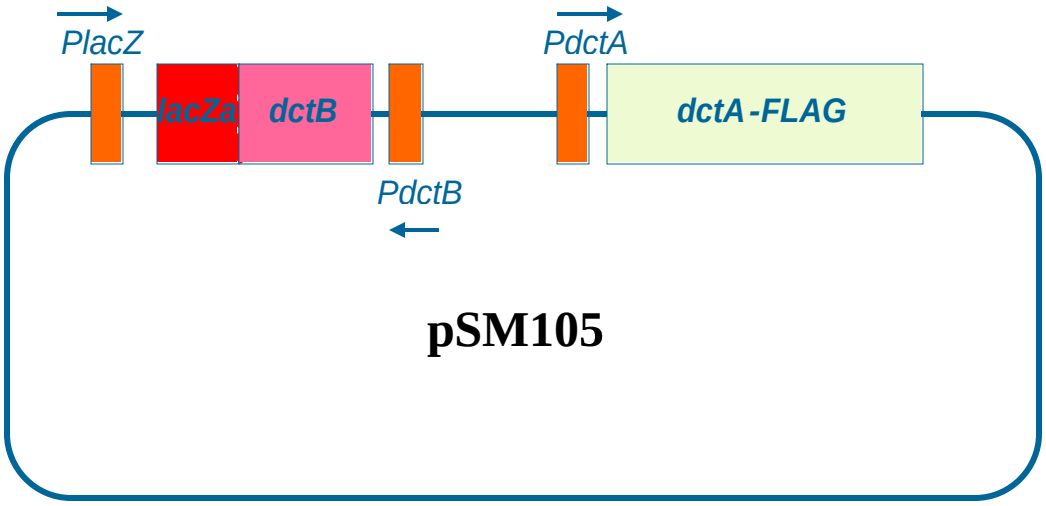

Figure 16. pSM105.

dctA-FLAG and its endogenous upstream region including the native *dctA* promoter, and the region encoding the start of dctB were cloned as a *Bam*HI/*Eco*RII fragment into pCPP30 to create pSM105.

3.1.4 Expression of DctA-FLAG in *S. meliloti*

Expression of *dctA*-FLAG and functionality of the fusion protein in *S. meliloti* was confirmed by the ability of pSM105 to rescue the *dctA* mutant RM1021-II. However, DctA-FLAG expression could not be confirmed by western blot using anti-FLAG antibodies. It was theorized that this might be due to C-terminal processing of DctA in *S. meliloti*, which would remove the FLAG epitope from the fusion peptide. The availability of a specific anti-DctA antibody is expected to allow confirmation by western blot; all blots performed on *S. meliloti* lysates using anti-FLAG were stripped and have been saved for reprobing with anti-DctA.

3.2 Anti-DctA Antibody Construction

When it became apparent that probing for DctA expression using anti-FLAG antibodies was not working, we explored different means by which expression could be studied. To date, the DctA protein has not been purified, due to the inherent difficulties associated with purifying membrane proteins, making antibody generation against the entire DctA protein impossible. However, it was possible to synthesize a peptide containing a sequence identical to a region on DctA that could be used as an antigen, against which antibodies could be raised. Such antibodies are known as anti-peptide antibodies.

Antipeptide antibodies have been used extensively to identify and quantitate proteins containing the sequence against which they were raised (88). Studies have shown that the best peptide

sequences to use are tyipcally hydrophilic, located on the surface, within a flexible region of the protein, between 6 and 25 amino acids long, and not subject to post-translational modifications (88). To ensure their immunogenicity, the peptide is attached to a larger carrier molecule. To maximize the immune response, antigens are typically mixed with adjuvants, materials used to stimulate and enhance the immune response, prior to immunization. By mixing the immunogen with the adjuvant, a sustained presentation of the antigen is maintained (54).

For this study, the peptide VATYAEKAHEQSIT, which is in the periplasmic region between transmembrane helices 3 and 4 was chosen as the sequence against which antibodies were to be raised. The polypeptide was synthesized by Pacific Immunology Corporation (San Diego, Ca) and conjugated to the carrier protein Keyhole Limpet Hemocyanin (KLH). The peptide conjugate was combined with AdjuLite® Adjuvant (Pacific Immunology Corp. San Diego, Ca) and used to immunize each of two rabbits four times each. Anti-sera were collected four times over thirteen weeks.

Initial experiments using serum from the first and second bleeds of each rabbit did not show any significant difference between *dctA* strains of either *E. coli* or *S. meliloti* or strains carrying a plasmid-borne copy of *dctA*. A representative western blot is shown in Figure17. The amount of non-specific binding of antibodies present in the blood sera is much higher for *E. coli* samples than for *S. meliloti* samples (Figure17), however, no discernable difference can be seen between *dctA*$^-$ and wild-type strains.

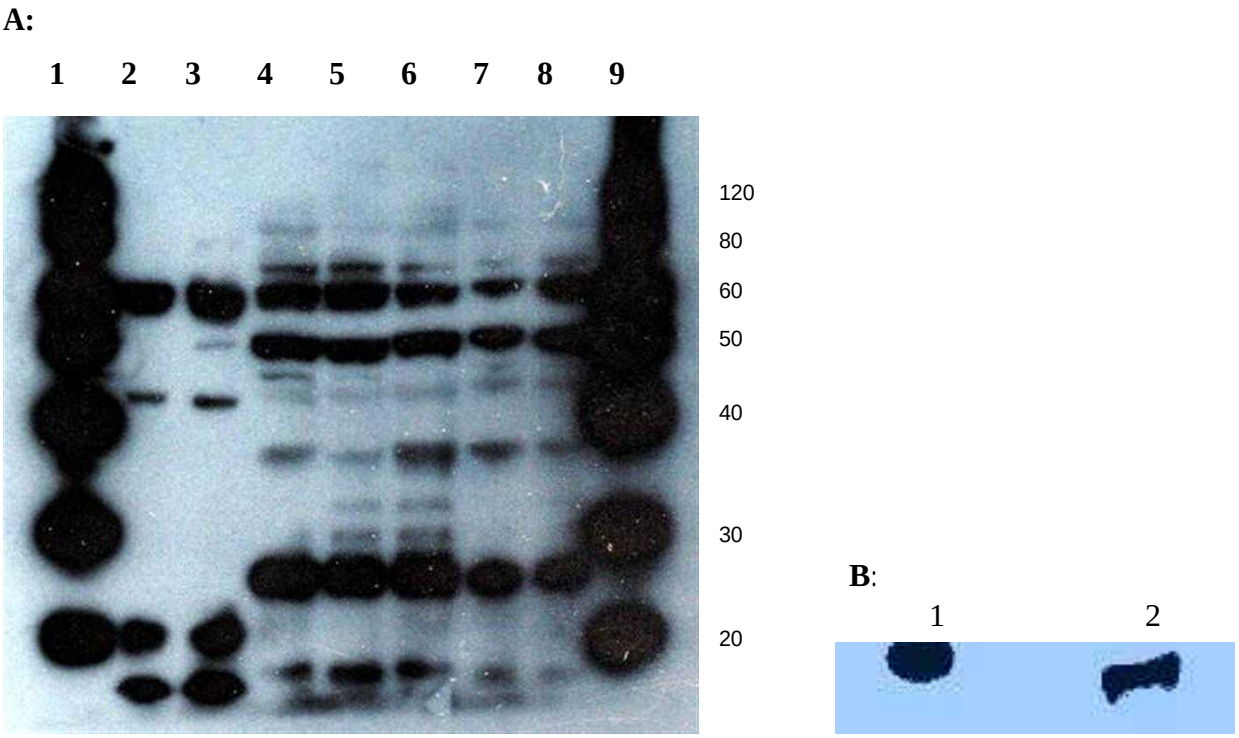

Figure 17. Western blot of *E. coli* and *S. meliloti* lysates

A: probed with anti-DctA peptide antiserum

Lane #	Sample
1	MagicMark
2	Sm1021
3	Sm1021-II
4	Kur1351
5	S17-1 pK19*dctA*-FLAG
6	Kur1349
7	Kur1351
8	S17-1 pK19*dctA*-FLAG
9	MagicMark

B: Probed with Anti-FLAG

Lane #	Sample
1	MagicMark 40kDa band
2	Kur1351 pK19*dctA*-FLAG

The standard western blot protocol was modified to try and reduce the amount of binding of endogenous rabbit antibodies to *E.coli* and *S. meliloti* proteins. This protocol is described in full in chapter two, section 2.4.2.3. The percentage of non-fat, dried milk (Western Family Foods Inc., Tigard OR) used in the blocking and antibody buffers was raised to 9%, and 2mg/ml of whole-cell protein from either *E. coli* or *S. meliloti* was added to the antibody buffer. The antibody was exposed to the whole cell protein extract for at least two hours before being exposed to the blot.To date, this technique has reduced the number of bands that appear upon developing the blot, but has not definitively revealed a band corresponding to DctA whilst controls using antibody specific to both the FLAG and HIS epitopes present on the plasmid-borne copies of *dctA* in *E. coli* demonstrated that the experiments themselves worked. As a result it has not been possible to quantitate relative levels of DctA protein between strains, nor has it been possible to confirm the presence of the inactive mutants in the membrane.

We are awaiting receipt of an affinity-purified shipment of the Anti-DctA antibody following completion of this study. It is hoped that this will yield some more interpretable results.

3.3 Site-directed mutagenesis of *dctA*-FLAG

G114 was chosen as the candidate for site-directed mutagenesis. G114 was chosen primarily because a randomly generated mutation at this locus had yielded a transport impaired, Fix^- mutant in a screen that also identified several previously known sites in regions important for Dcta function (161); furthermore, it is also highly conserved throughout the glutamate

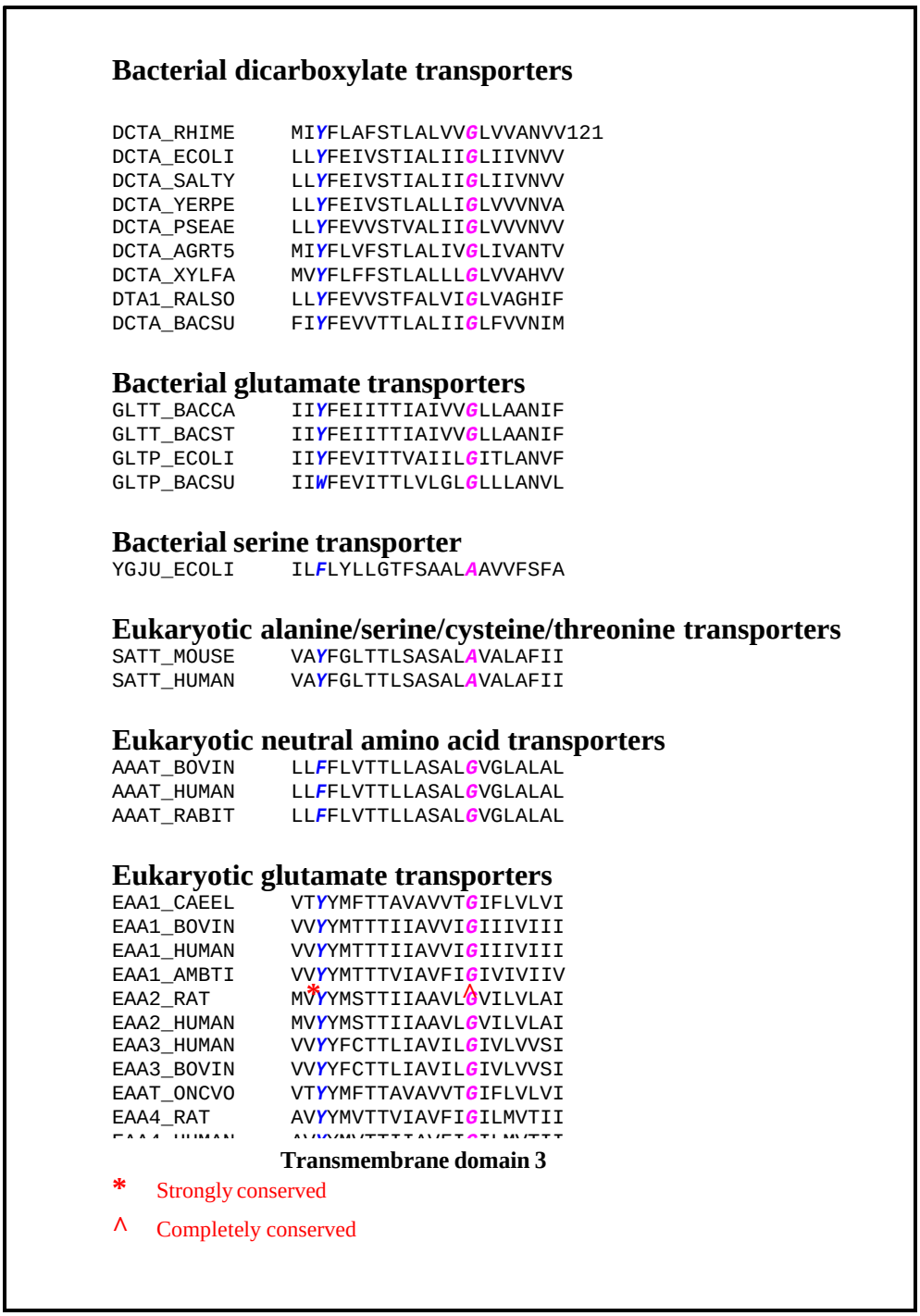

Figure 18. Alignment of third transmembrane domain of DctA homologues from 35 members of the Glutamate Transporter family

transporter family (Figure 18)

Although no structure has been solved for any member of the glutamate transporter family there is a widely accepted model (117), this is shown in Figure 10. Based upon this model, G114 is located in the third transmembrane domain (TMD).

Mutagenesis was performed using the Stratagene Quik-Change® Site-Directed Mutagenesis Kit (Stratgene, La Jolla, Ca) as per manufacturers directions. Primers for the mutagenesis were designed using the Stratagene Quik-Change® Site-Directed Mutagenesis primer design program available through their homepage, and are listed in Table 3. The mutagenesis protocol, outlined in Figure 19, takes advantage of the non-strand displacing properties of *Pfu* polymerase, and has proven to be highly efficient and effective, taking approximately 24 hr from initiation until mutant colonies can be picked from a transformation plate.

All mutations were made using *dctA*-FLAG carried on the *pK19mob* (113) backbone which, by virtue of its high copy number, makes plasmid isolation easier. Mutations were confirmed by DNA sequencing of the region containing the point mutation. The mutant *dctA*-FLAG gene was then subcloned as a *BamHI/EcoRI* fragment into the broad host range plasmid, pCPP30, to create pSM105-G114X, and transformed into *E. coli* strain S17-1 (29, 116) for transfer into *S. meliloti* by biparental conjugation.

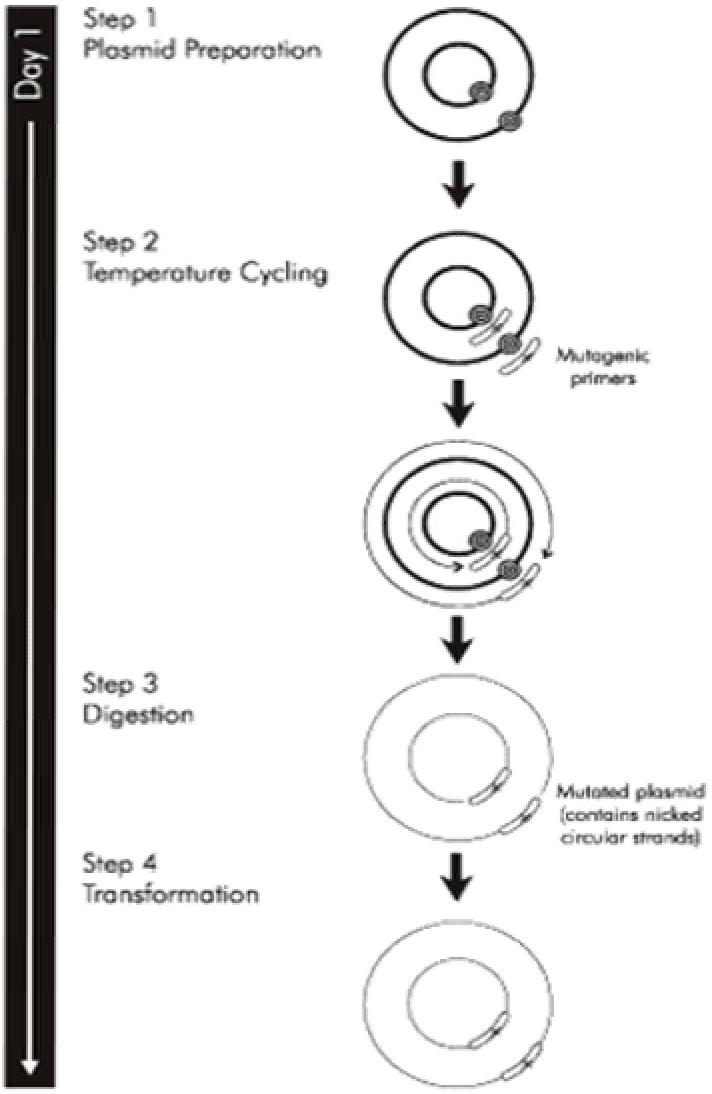

dctA-FLAG in pK19*mob*

Denature plasmid. Anneal mutagenic oligonucleotides

Use *pfu*-turbo polymerase to extend and incorporate mutagenic primers to generate nicked, circular strands

Digest methylated, non-mutated parental DNA with *Dpn*I

Transform into competent XL-1 Blue *E. coli*

After transformation, the cells repair the nicked DNA

Figure 19. Site-directed in-vitro mutagenesis protocol

3.3.1 Phenotypic analyses of mutant DctA

Biparental conjugation resulted in transfer of the pSM105 vector from *E. coli* to *S. meliloti* . The conjugations were carried out overnight at 30°C on non-selective LB plates. The mating spot was resuspended in liquid medium and spread-plated onto $MMNH_4$ Str_{200} Tc_{10} plates. S17-1 is a proline auxotroph and therefore cannot grow on $MMNH_4$. *S. meliloti* transconjugants were purified by streaking three times on selective media before phenotypic analyses were conducted.

Phenotypic analyses included looking at the ability of each point mutant to grow on a variety of different DctA substrates, to transport radio-labeled succinate, and to nodulate alfalfa.

3.3.1.1 Plate Tests

The growth phenotype of each point mutant was analyzed by replica plating onto a variety of defined media, each containing a different carbon source. DctA is the sole means by which *S. meliloti* transports dicarboxylates into the cell, so *dctA*$^-$ strains are unable to grow using dicarboxylates as the sole carbon source. Growth was also analyzed in the presence of fluroorotate (FOA), a toxic compound that is transported by DctA. Wild-type strains are unable to grow in the presence of FOA, whilst *dctA*$^-$ strains can grow normally. The growth of the point mutants on each medium tested was compared to the growth of both Sm1021-II, a *dctA*$^-$ strain of *S. meliloti* , and the wild-type strain Sm1021. The results of these plate tests are shown in Table 4 and a representative plate test is shown in Figure 20.

Table 4. Results of growth phenotype analyses

Strain	Succ	Fum	Malate	Tc	FOA1	FOA2	FOA3	FOA5	Asp	Maleate
SM 1021	3	3	3	0	0	0	0	0	1	1
SM 1021-II	1	1	1	0	3	3	3	0	1	1
SM 1021-II pSM105	3	3	3	3	0	0	0	0	0.5	1
G114A	2	2	1.5	3	2.5	2	1	1	0.5	1
G114D	1	1	1	3	3	3	3	3	0.5	0.5
G114F	1	1	1	3	3	3	3	3	0.5	0.5
G114P	2	2	2	3	2.5	2	1	1	1	1

3: Growth equivalent to wild-type *S. meliloti* growing on equivalent medium or in the case of media containing FOA, growth on media without FOA

2: Slightly less growth. Diameter of single colonies is 75% of that formed by strains designated as '3'

1: Visible but poor growth. Colonies hardly visible

0: No growth

Succ: Succinate
Fum: Fumarate
Asp: Aspartate
FOA_1: Fluoroorotate 1µg/ml
FOA_2: Fluoroorotate 2µg/ml
FOA_3: Fluoroorotate 3µg/ml
FOA_5: Fluoroorotate 5µg/ml

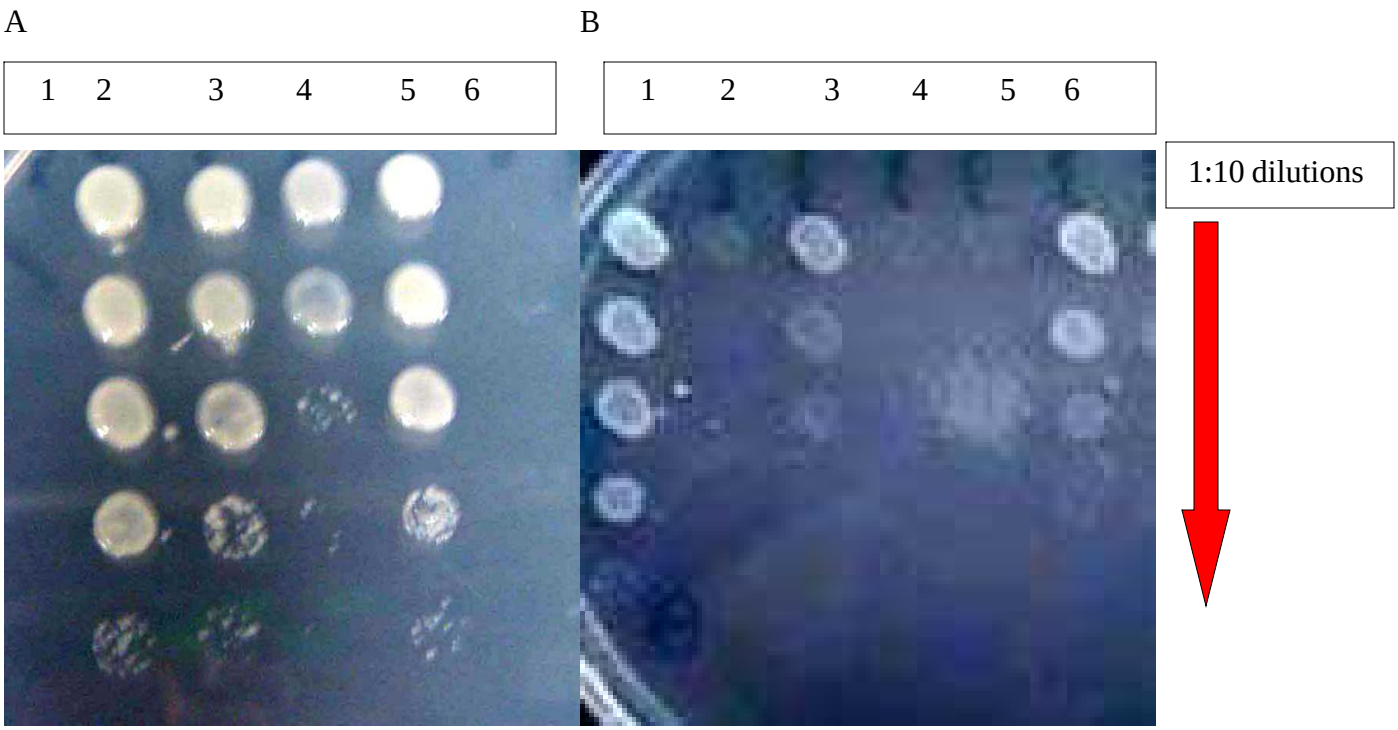

Figure 20. Plate tests of strains expressing mutant copies of DctA

Plate A: $MMNH_4$ containing 1µg/ml FOA

Plate B: $MinNH_4$ containing 0.2% Succinate

From left to right

1. Sm1021
2. Sm1021-II
3. Sm1021-II pSM105 G114A -
4. Sm1021-II pSM105 G114D
5. Sm1021-II pSM105 G114F
6. Sm1021-II pSM105 G114P

Interestingly, whilst all of the point mutants could grow in the presence of FOA, both G114A & G114P appeared to grow well using dicarboxylates as a sole carbon source, suggesting that the functionality of DctA in these cases was sufficiently impaired to allow growth in the presence of FOA, but adequate to transport enough carbon source to support growth. FOA resistance was presumably not due to loss of the pSM105 plasmid derivative, as the same results were observed with maintenance of the plasmid by the addition of Tc_{10} to the growth medium.

The point mutants were exposed to increasing concentrations of FOA ranging from 1µg/ml to 5µg/ml to determine the level of resistance conferred by each point mutation (Table 4). G114D and G114F were both resistant to the increased FOA concentrations, growing equally well at FOA_1 and FOA_5, mirroring the phenotype of the *dctA* strain RM1021-II and supporting the hypothesis that little or no transport is occurring in these strains. G114A and G114P were both marginally more sensitive to FOA_1, and more sensitive to FOA_5 than G114D and G114F. These data support the hypothesis that whilst FOA transport by G114A and G114P is reduced relative to wild-type, some level of transport is occurring, resulting in a decreased capacity to tolerate high concentrations of FOA relative to the *dctA* strain

These data infer that all four point mutants have impared functionality of DctA, but that G114A and G114P are active enough to support growth on the presence of dicarboxylates. This might be explained by a difference in the K_m values for FOA and succinate. If the K_m for succinate is lower than that for FOA it might explain how transport of succinate is sufficient to support growth, whilst transport of FOA remains low enough for FOA to not prove toxic to the cells.

An interesting phenomenon that was observed in these experiments, which has been independently confirmed in this laboratory, relates to the dependence of colony growth in the presence of FOA on the call density of colonies. Visual inspection showed that colonies consistently appeared to be more robust in the presence of FOA under conditions of lower cell density. Whether this was due to down-regulation of certain transporter elements under these conditions is unclear.

3.3.1.2 Growth Curves

In order to further examine the growth phenotypes described previously, growth curves were generated by examining growth of each strain in different substrates. OD600 readings were taken at 10 minute intervals over the course of 72 hr, giving a total of 433 data points for each strain. These data are shown graphically in Figures 21-30 which depict the ability of each strain to grow in a particular substrate. Growth curves were assessed by analyzing the slope of the curve to assess its progression into and through a logarithmic growth phase, the duration of the initial lag phase and the final optical density reached by the cultures.

Figures 21-26 show growth data for strains grown in $MMNH_4$, $MMNH_4$ supplemented with 1 and 5µg/ml FOA, and $MinNH_4$ supplemented with L -malate, succinate or fumarate. Additional data are presented in Figures 27-30 which show growth of the same strains in D-malate, β-alanine, aspartate, and maleate.

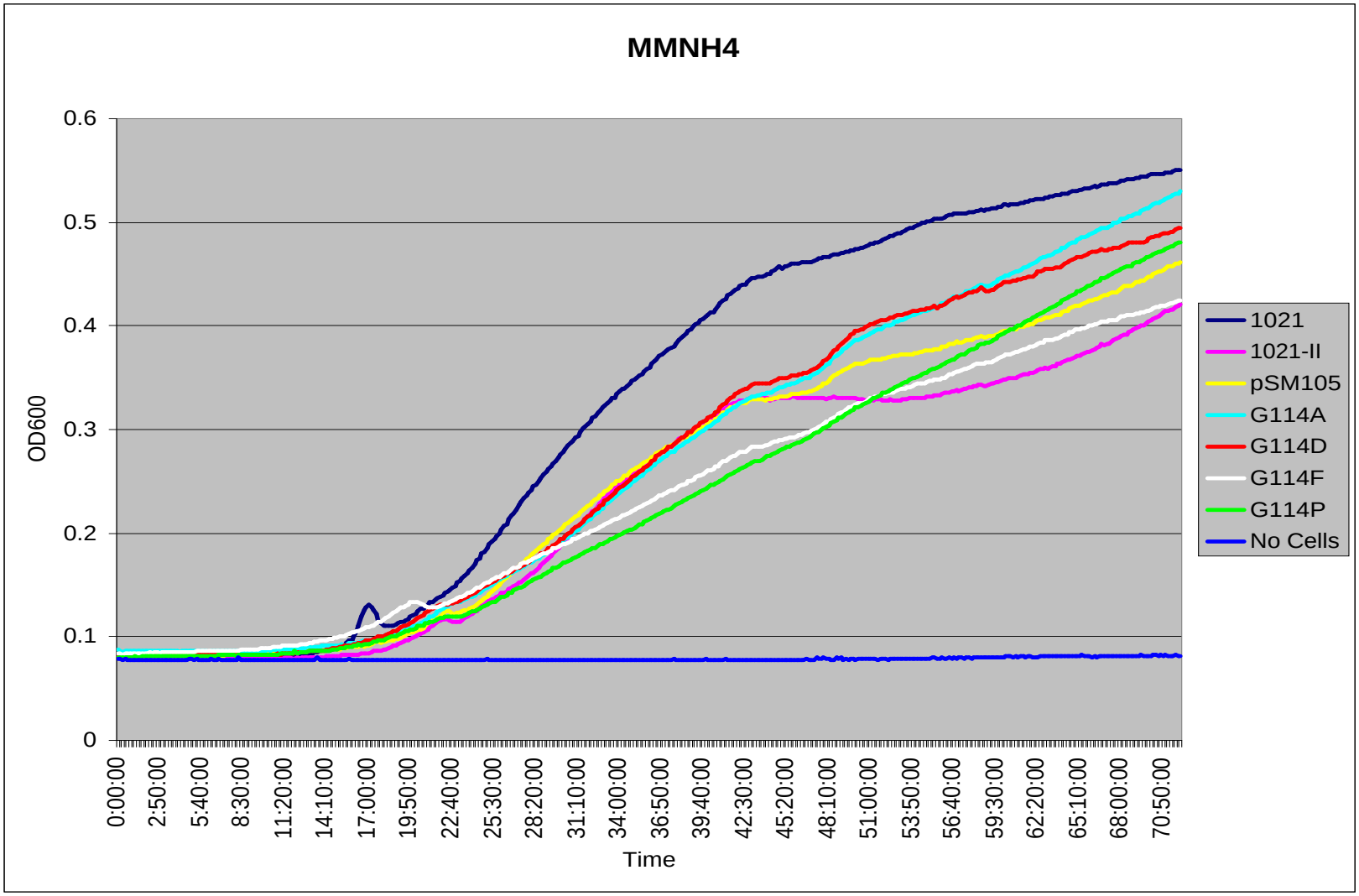

Figure 21. Growth Curve of *S. meliloti* strains in MMNH4

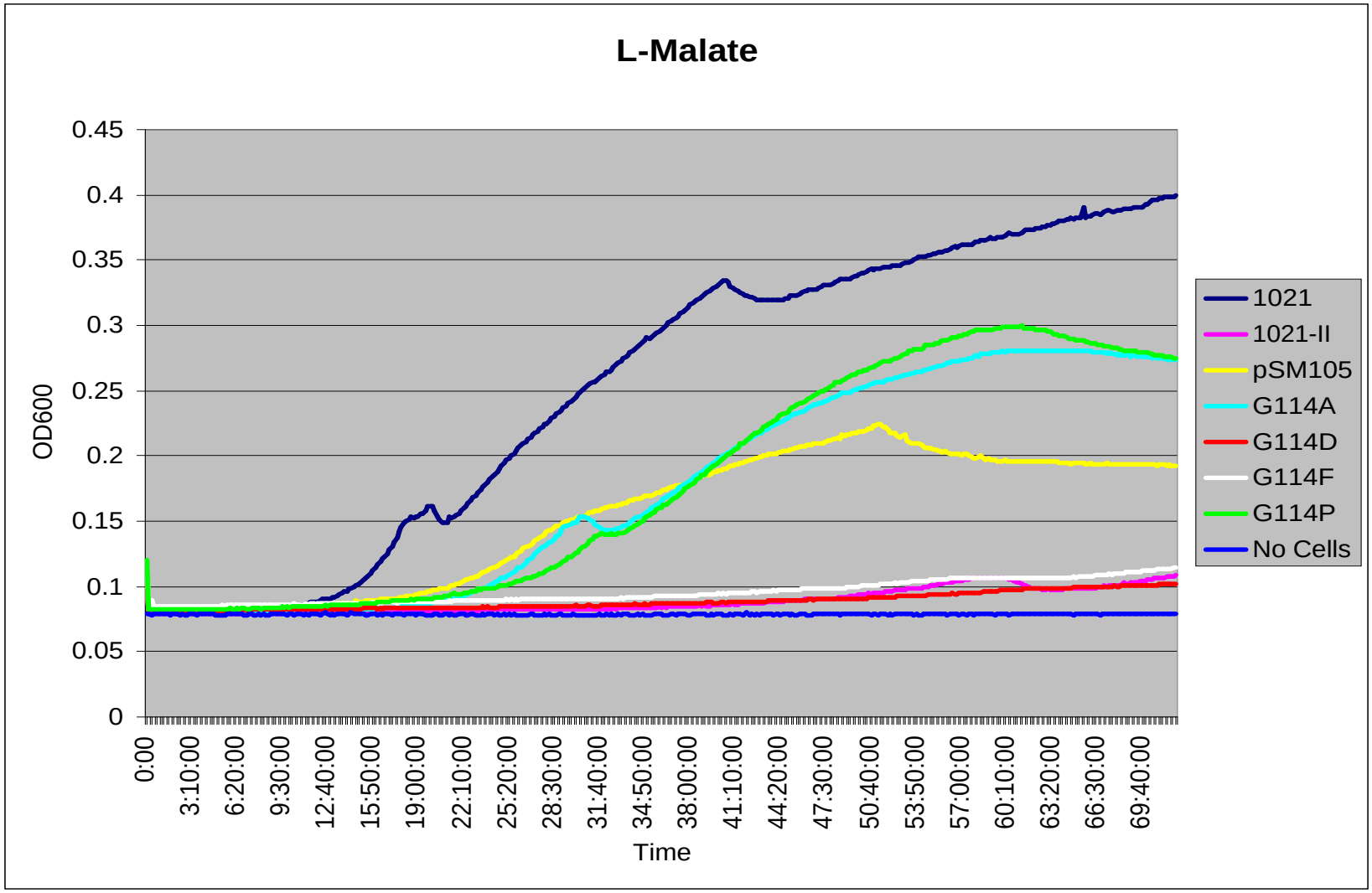

Figure 22. Growth Curve of *S. meliloti* strains in MinNH4 supplemented with 0.2% L-Malate

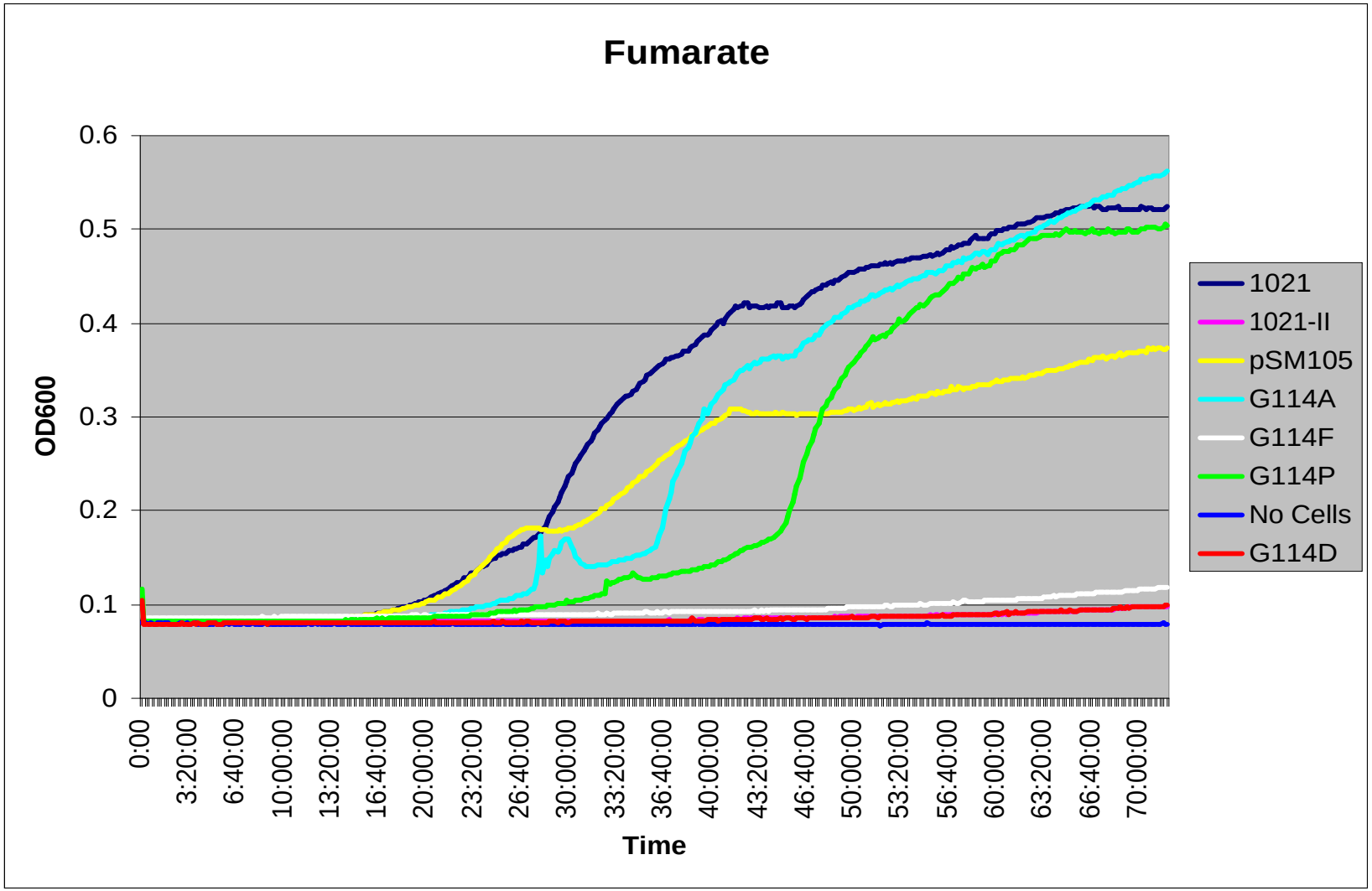

Figure 23. Growth Curve of *S. meliloti* strains in MinNH4 supplemented with 0.2% Fumarate

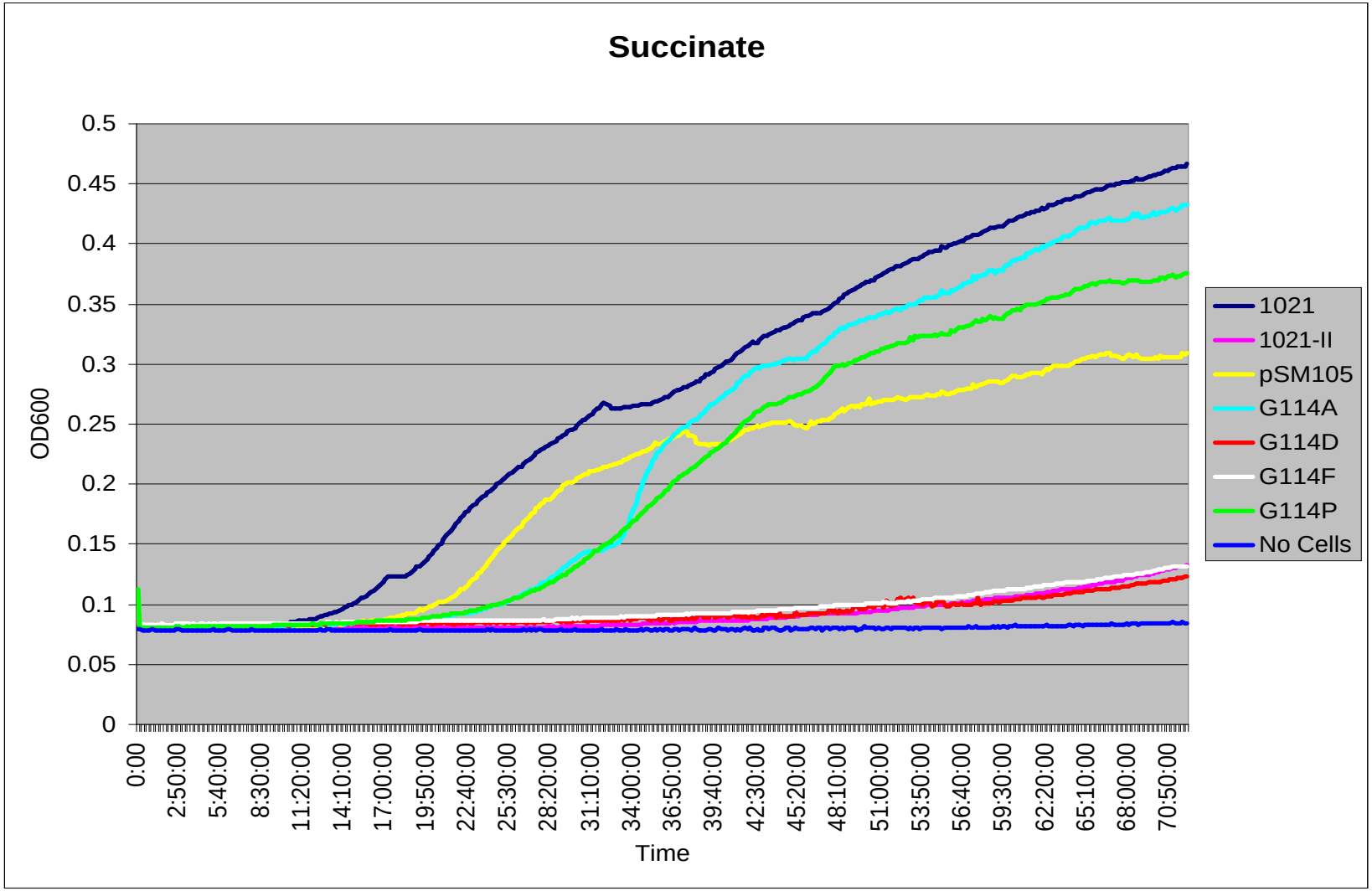

Figure 24. Growth Curve of *S. meliloti* strains in MinNH4 supplemented with 0.2% Succinate

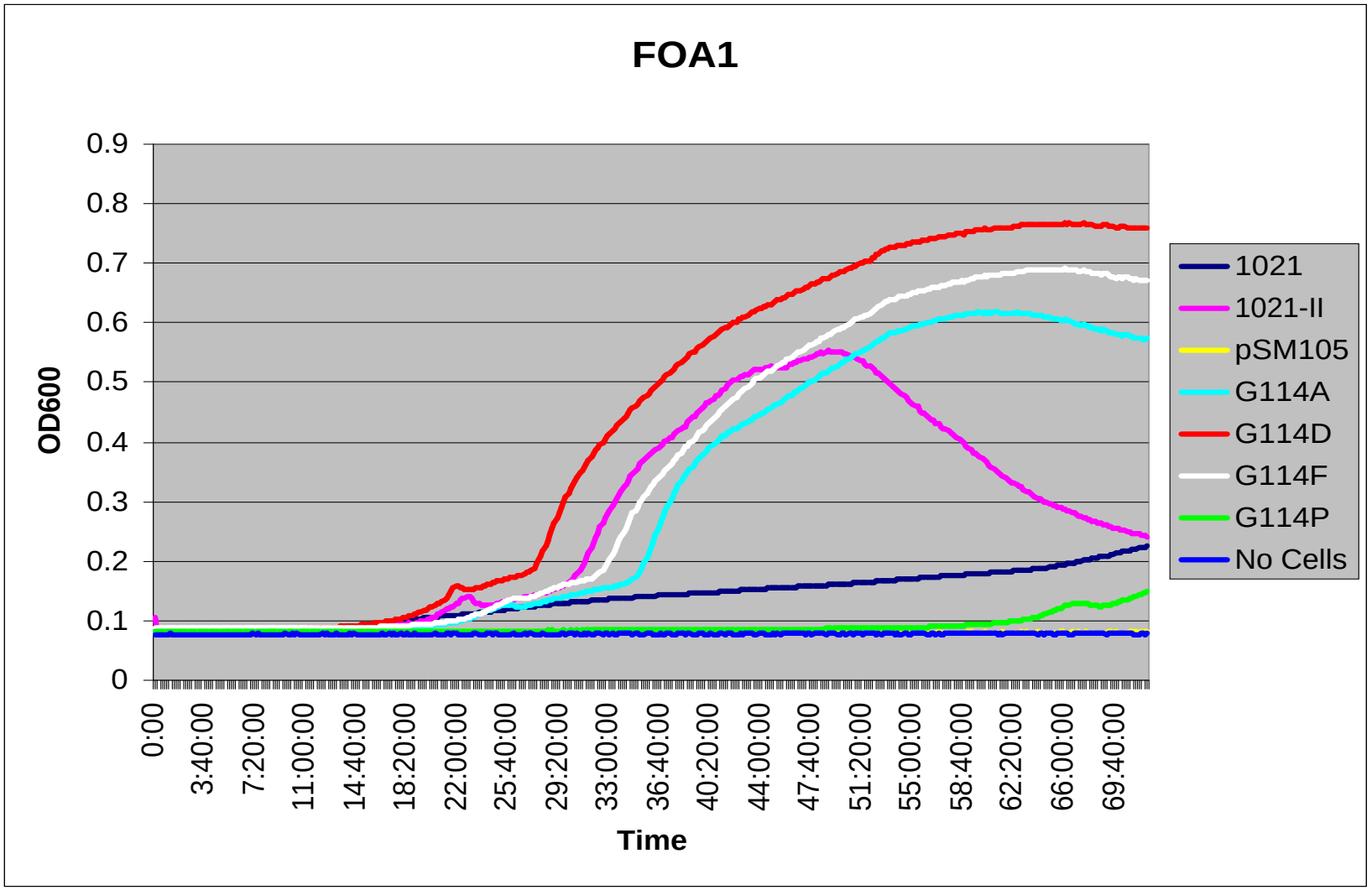

Figure 25. Growth Curve of *S. meliloti* strains in MMNH4 supplemented with 1µg/ml FOA

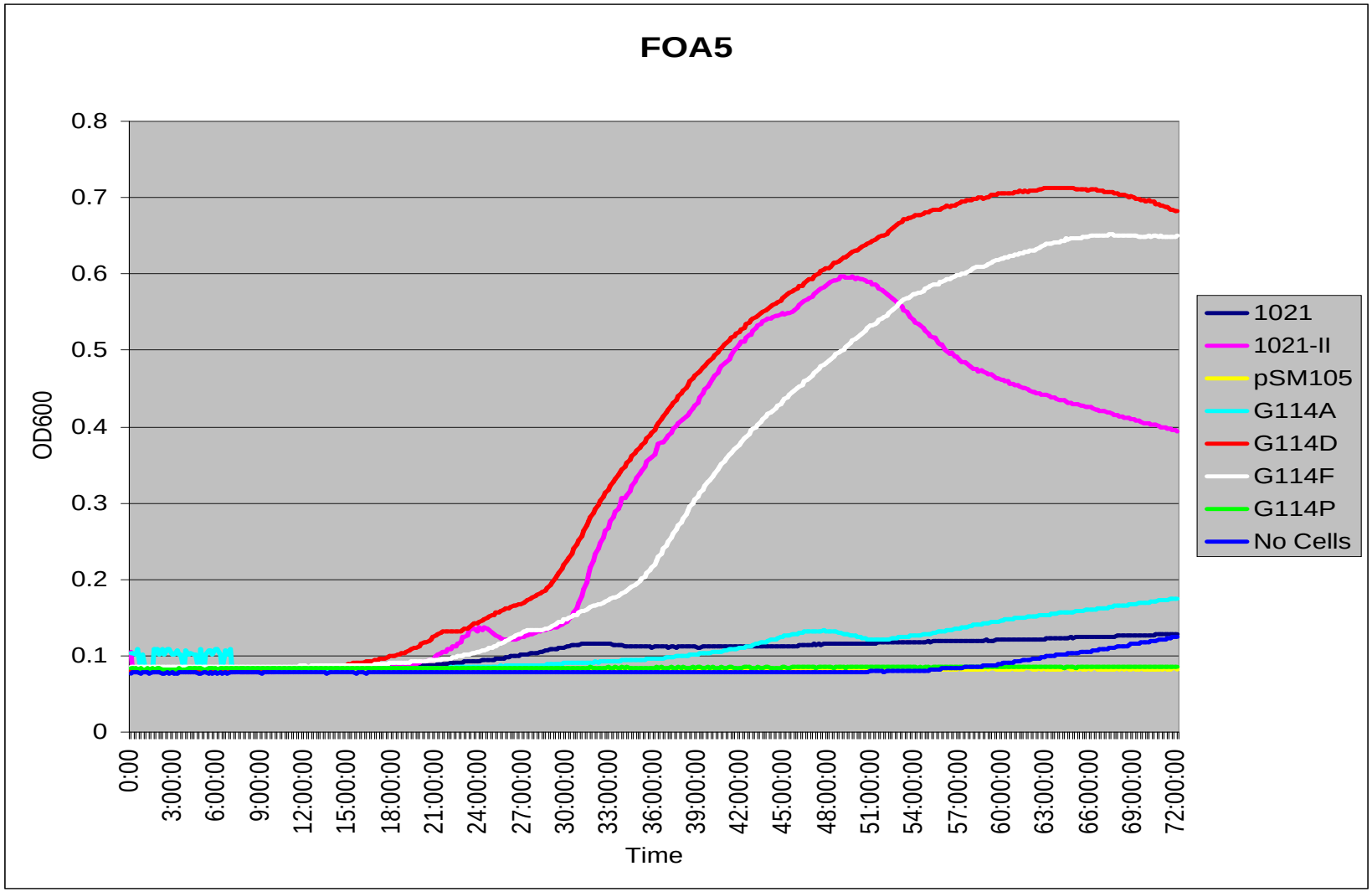

Figure 26. Growth Curve of *S. melilo ti* strains in MMNH4 supplemented with 5µg/ml FOA

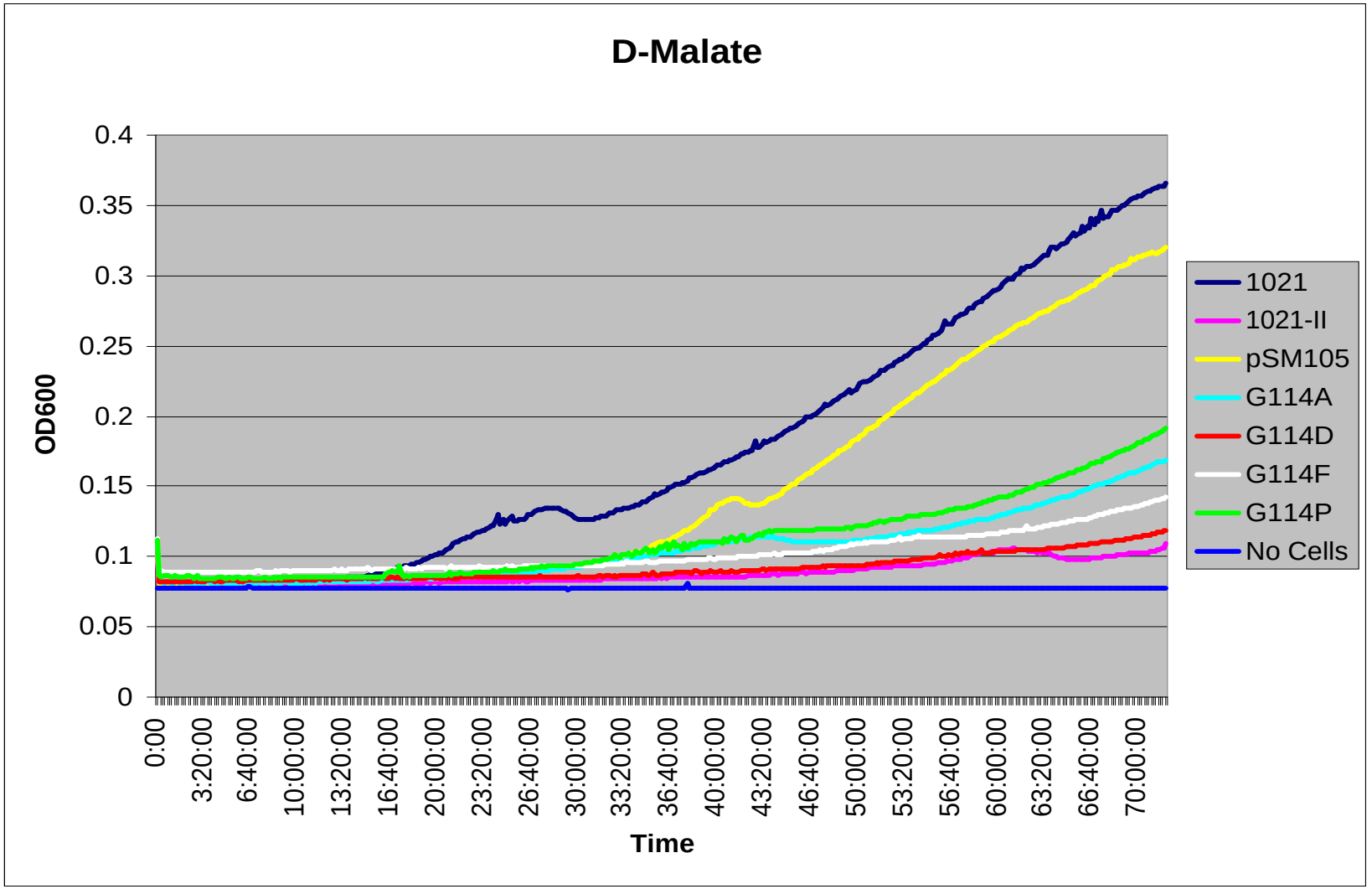

Figure 27. Growth Curve of *S. meliloti* strains in MMNH4 supplemented with 0.2% D-Malate

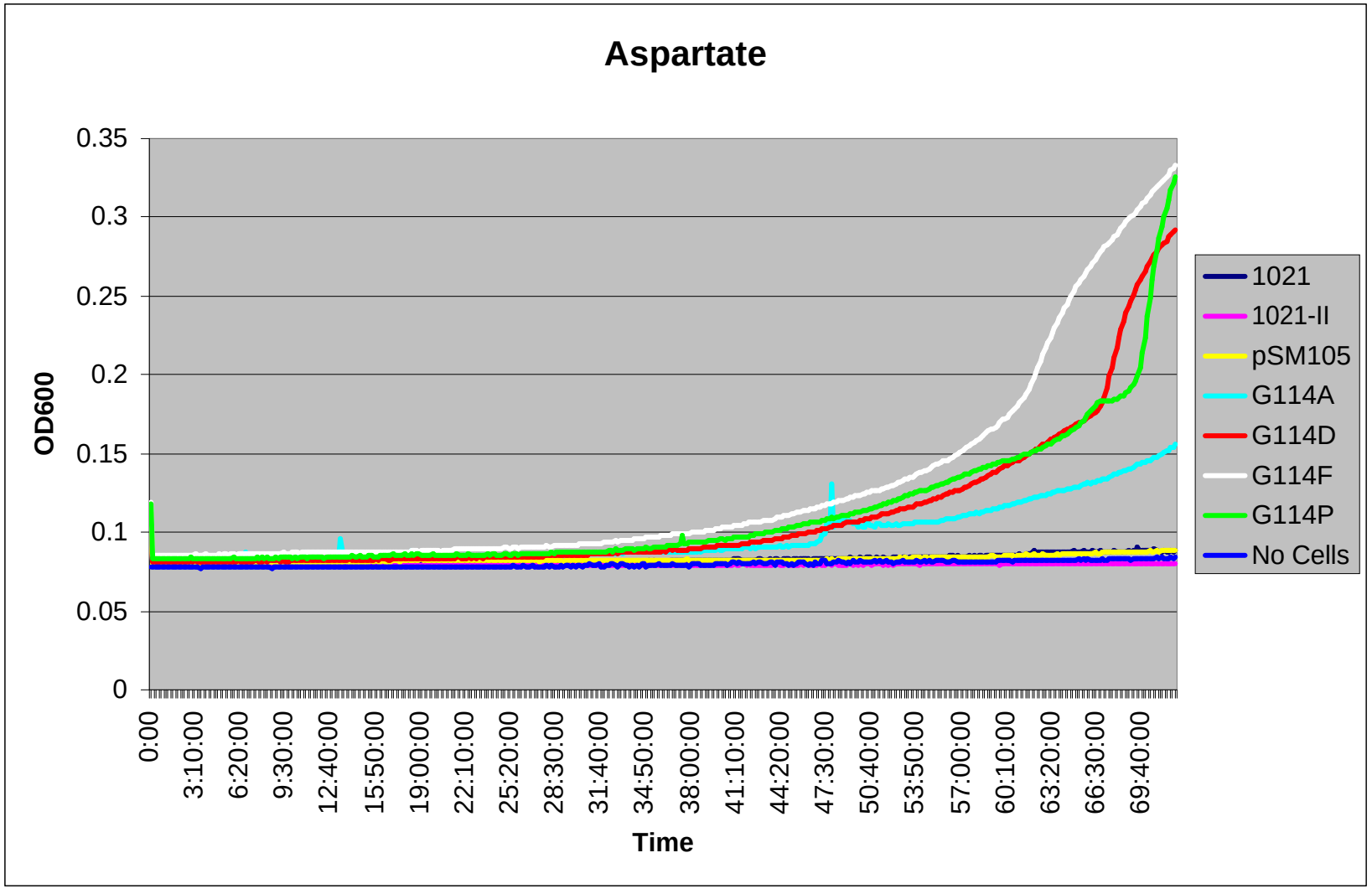

Figure 28. Growth Curve of *S. meliloti* strains in MMNH4 supplemented with 0.2% Aspartate

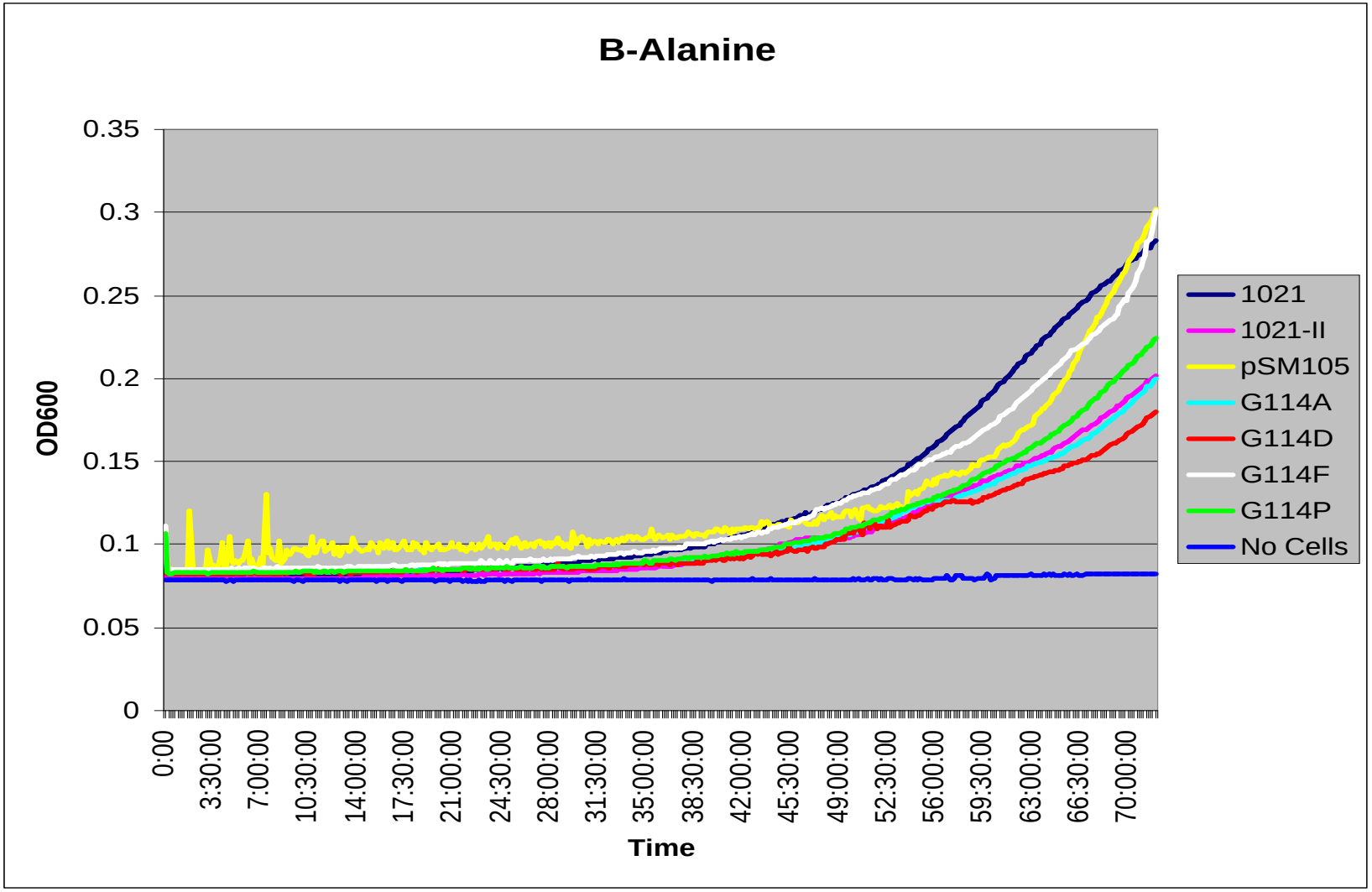

Figure 29. Growth Curve of *S. meliloti* strains in MMNH4 supplemented with 0.2% β-Alanine

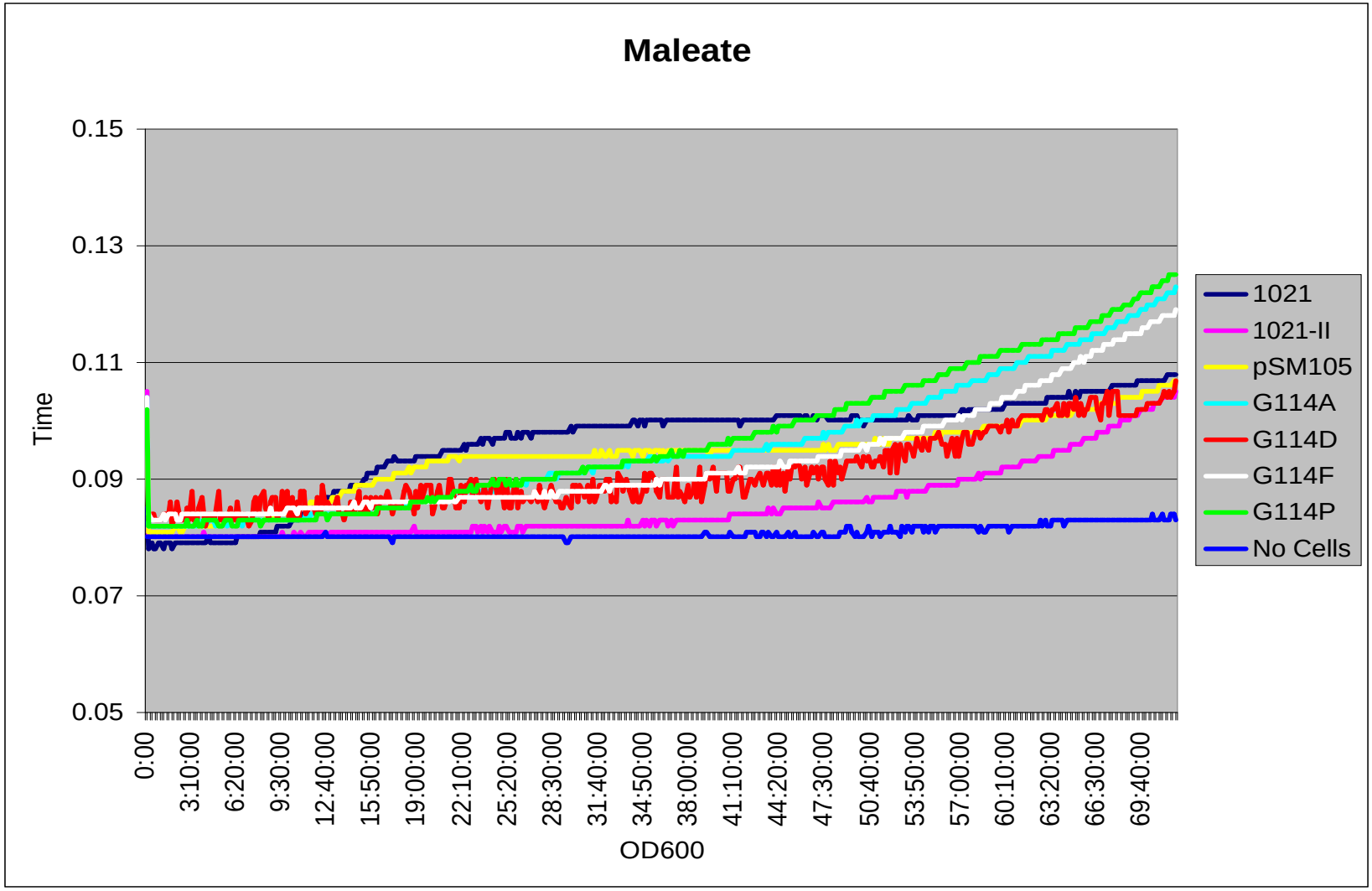

Figure 30. Growth Curve of *S. meliloti* strains in MMNH4 supplemented with 0.2% Maleate

The growth curves largely corroborate the data that were grossly demonstrated by the plate assays but they also give a more detailed insight into the growth behaviors of the individual strains. Growth in the control medium $MMNH_4$ is shown in Figure 21 (MMNH4), and as expected, all strains are able to grow well. Growth on succinate is shown in Figure 24, and interestingly, both G114A and G114P appear to be as capable of growth on succinate as pSM105. This pattern is repeated for growth on both L-malate and Fumarate, shown in Figures 22 and 23. No growth is seen for either G114D or G114F, suggesting that any DctA activity that might be present is insufficient to support growth.

Growth on FOA is restricted to the *dctA* strain 1021-II and the two mutants G114D and G114F, giving further evidence to support the theory that transport by these two mutants is minimal. These data are shown in Figures 25 and 26. A low level of growth on FOA_1 is seen in G114A, mirroring its behavior in the plate assays. This would suggest that transport by this mutant was low enough that the levels of FOA entering the cell were not completely inhibitory, but that succinate transport was sufficient to support growth.

Additional substrates that were tested are shown graphically in Figures 27-30. The active mutants G114A and G114P did not grow as well on D-malate as on the more common isomer, L-malate Figure 27. The wild-type DctA has a much higher K_m for D-malate than L-malate. The difficulty that the mutants have growing on D-malate suggests that they do not transport D-malate very well.

Changes in the ability of strains to transport aspartate might indicate alterations in the amino acid cycling pathway (78), so growth of the point-mutant strains using aspartate as a carbon source was analyzed, and is show in Figure 28. These results suggests that all four of the point-mutant strains may have an increased capacity to transport aspartate relative to wild-type and deletion strains, with G114D and F (the two inactive mutants), demonstrating the most robust growth. Growth on aspartate is slow however, with apparent logarithmic growth being achieved after approximately 65 hours (compared to approximately 24 hours for $MMNH_4$) suggesting that future experiments using aspartate should be conducted over a longer period of time than similar experiments using other substrates.

Growth curves for β-alanine and maleate are shown in Figures 29 and 30 respectively. All strains appear to be capable of growth on β-alanine, and it is believed that there are alternative transporters for β-alanine in *S. meliloti* . Conversely, no strain appears capable of growth on maleate, the *cis*-isomer of fumarate. As SM1021 lacks the isomerase needed to convert maleate to fumarate it is not surprising that there is no growth. Even if maleate were transported by the DctA, the cells would be unable to metabolize it.

3.3.1.3 Transport Assays

Transport assays were performed as described in section 2.5.3 to analyze the ability of each point-mutant to transport ^{14}C-labeled succinate. *S. meliloti* cells were grown for a total of 48 hr in minimal medium containing 0.2% mannitol as a carbon source, and 0.1% maleate as an

inducer. The cells were spun down, and washed three times in minimal media containing no carbon source. The cells were then kept on ice, and warmed up to 30°C 1 minute prior to starting each assay. The cells were exposed to different concentrations of succinate containing a total of 0.3 µCi [^{14}C-succinate (Moravek Biochemicals, Brea, Ca). Cell samples were taken at 1 and 2 min, washed three times by filtration, and lysed. Radioactivity was measured using scintillation fluid (Fisher Scientific, Pittsburgh, Pa.) and a Packard Tri-Carb 2100 TR scintillation counter. A 10-µl aliquot was spotted on a dry filter and counted to measure total radioactivity in the assay culture. Experiments were repeated in triplicate.

3.3.1.4 Analysis of succinate transport by Sm1021-II pSM105

A significant limitation to the current transport assay protocol was encountered when Sm1021-II pSM105 was assayed and, for this reason, no conclusive kinetic data is presented for this strain. The current assay protocol proscribes that samples are taken 1 and 2 min after substrate is added to the cell suspension, on the assumption that, at these time points, transport is occurring linearly. However, analysis of Sm1021-II pSM105 suggests that DctA activity may be so high that, under low substrate concentrations, a significant percentage of the substrate pool is rapidly being depleted upon exposure of the cells to the substrate. If transport is occurring linearly, we should see doubling of transported substrate between 1 and 2 min. This is not the case for Sm1021-II pSM105. Therefore, taking measurements after 1 and 2 min yields data that is not representative of transport in the range required for determination of the kinetic parameters of DctA.

The experiment was adjusted so that samples of Sm1021-II pSM105 were taken 10s and 30s after addition of substrate. This produced numbers that suggest that some transport is still occurring after 30 seconds (Table 5); however, a tripling between these two time points is not observed, suggesting transport is still not occurring linearly.

The counts per minute (CPM) signal for 10µl of cell suspension plus substrate solution was adjusted to 100µl and used to calculate a percentage reduction in signal after 10s and 30s:

$$\% \text{ Signal Depleted} = \frac{\text{CPM(time point)}}{10 \times \text{CPM(background)}}$$

This percentage value was then used to calculate the concentration of substrate remaining in the substrate pool at each time point, as per the equation:

$$\text{Conc. Succinate Remaining} = \text{Original Succinate Conc.} \times (1 - \% \text{ Signal Depleted})$$

As seen in Figure 31, these data suggest that, at lower concentrations of succinate, up to 76% of the total substrate pool is being transported in the first 10s. This results in a massive reduction in overall substrate concentration, violating the assumptions needed in order to satisfy Michaelis-Menton kinetics (128). This would suggest that samples need to be taken at shorter intervals, perhaps 5 seconds and 10 seconds; however, logistically this would be very difficult owing to the design of the experiment.

Table 5. Estimated depletion in substrate concentration by Sm1021-II pSM105

Strain	Succ Conc.	Adjusted CPM Background		CPM 10 Sec	% signal depleted after 10 sec	Estimated succ conc. after 10 sec		CPM 30 Sec	% signal depleted after 30 sec	Estimated succ conc.after 30 sec
pSM105	5uM	70506		40362.8	57.2	2.14uM		55273	78.4	1.08uM
	12.5uM	67868		34041.6	50.2	6.23uM		49434.8	72.8	3.4uM
	25uM	81714		62202	76.1	5.98uM		62955	77	5.75uM
	50uM	111008		44061.8	39.7	30.15uM		48328.8	43.5	28.25uM
	100uM	88070		31233.4	35.5	64.5uM		51976.8	59	41uM
	150uM	79454		23006.4	29	106.5uM		37589.6	47.3	79.05uM
	200uM	120842		18125.2	15	170uM		33857	28	144uM
	250uM	77448		16946.8	21.9	195.25uM		28861.6	37.3	156.75uM
	500uM	69824		7409.8	10.6	447uM		9366.2	13.4	433uM

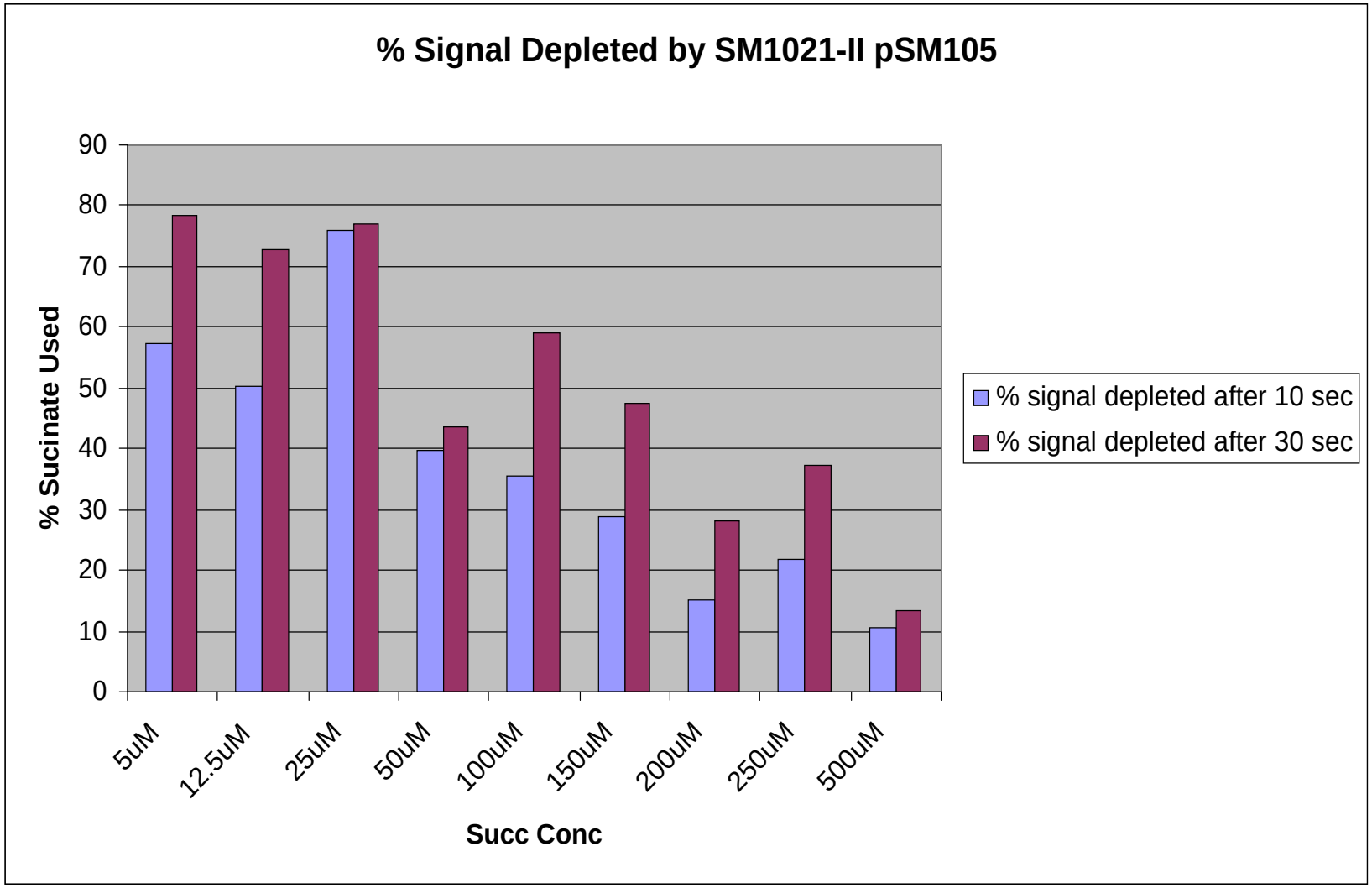

Figure 31. Percentage succinate used by Sm1021-II pSM105

The experiment was repeated using a lower cell density, which did result in a reduction in overall transport levels (data not shown) but substrate depletion was still significant. Potentially future experiments could be performed using very high dilutions of cells; however previous experiments in this laboratory have suggested that cell density affect transport activities of the cells (S.Yurgel, unpublished data).

Gross assessment of these data would suggest that the apparent V_{max} of DctA in Sm1021-II pSM105 is greater than that observed for Sm1021. The apparent V_{max} is presumably inflated due to *dctA* being expressed from a multiple-copy number plasmid; one would predict that, on a per protein basis, the V_{max} of the DctA protein itself should be consistent between the strains. While it is not possible to directly assay DctA concentration in each strain, it may be appropriate to look at mRNA transcript levels by quantitative, real-time, qPCR. Normalizing transcription levels with cell density may provide an indirect way of comparing DctA levels between these two strains.

RT-PCR is probably not an appropriate means of assessing DctA levels in any of the G114 point-mutant strains as mRNA transcript levels do not indicate whether or not a protein is capable of being correctly localized within the cell. However, for the wild-type DctA, it is reasonable to assume that the protein is being localized correctly, and therefore would provide a useful means of directly comparing the two strains.

3.3.1.4.1 Optimal assay conditions

Early assay data showed that the transport activity of DctA was highly dependent upon the age of the culture being assayed (data not shown) and this was independently confirmed by S. Yurgel. This is presumably due to alterations in expression levels of various proteins throughout the growth period of the culture, in response to a multitude of metabolic and physiological stimuli. The following growth conditions were used in all transport assays presented in this work.

A 1.5ml seed culture of each *S. meliloti* strain to be assayed was grown for 24 hr at 30°C in M9-*Rhizobium* (appendix 6.1.1.3) supplemented with 0.2% mannitol as a carbon source. The seed culture was used to inoculate 50 ml of M9-*Rhizobium* supplemented with 0.2% mannitol and 0.1% maleate as a *dctA* inducer (160), which was then grown for a further 24 hr at 30°C. Subsequent growth curve data (Figure 21) demonstrates that it might be prudent in future studies to grow the cells longer to ensure they enter mid-log phase. However, all experiements reported here utilized the aforementioned conditions to ensure internal consistency.

3.3.1.4.2 Transport activity of *dctA* point-mutants

For the reasons discussed previously, it was not possible to determine a K_m and V_{max} for DctA expressed in pSM105. The calculated K_m values for each of the point mutants can be compared to that of wild-type DctA in Sm1021, however, the V_{max} values are probably inaccurate owing to

the difference in levels of DctA expressed off of a multiple-copy number plasmid, and potentially differences in protein levels between mutant strains.

Lineweaver Burke plots shown in Figure 32 were generated from the raw transport data collected (data not shown), and the values for K_m and V_{max} shown in Table 6 were calculated. Transport data for both the *dctA*$^-$ strain Sm1021-II and wild-type Sm1021 were collected to permit a direct comparison with the data obtained from the mutant strains.

As predicted from the growth phenotypes discussed previously, G114D and G114F show little to no transport activity relative to SM1021-II. Presumably the introduction of either the negatively charged aspartate residue, or the bulky phenylalanine caused sufficient disruption of structure and microenvironment to prevent transport. Glycine is believed to facilitate the close packing of helices within the tertiary and quarternary structures of membrane helices (76, 127, 142). Introduction of bulky side chains in place of a glycine residue is likely to severely disrupt the packing of these helices, potentially disrupting the three-dimensional structure of the protein sufficiently to impare and even prevent transport.

G114A and G114P both possess dicarboxylate transport activity, but at rates significantly lower than wild type DctA in Sm1021. G114A shows a 2.5-fold increase in K_m relative to wild-type indicating that the affinity of the protein for succinate is significantly decreased. Concurrent with this is a reduction in turnover rates relative to wild type as indicated by a large decrease in V_{max}. Interestingly G114P has an approximately wild-type K_m suggesting that the affinity of DctA for its substrate is unchanged. The V_{max} of G114P is much smaller than that of Sm1021

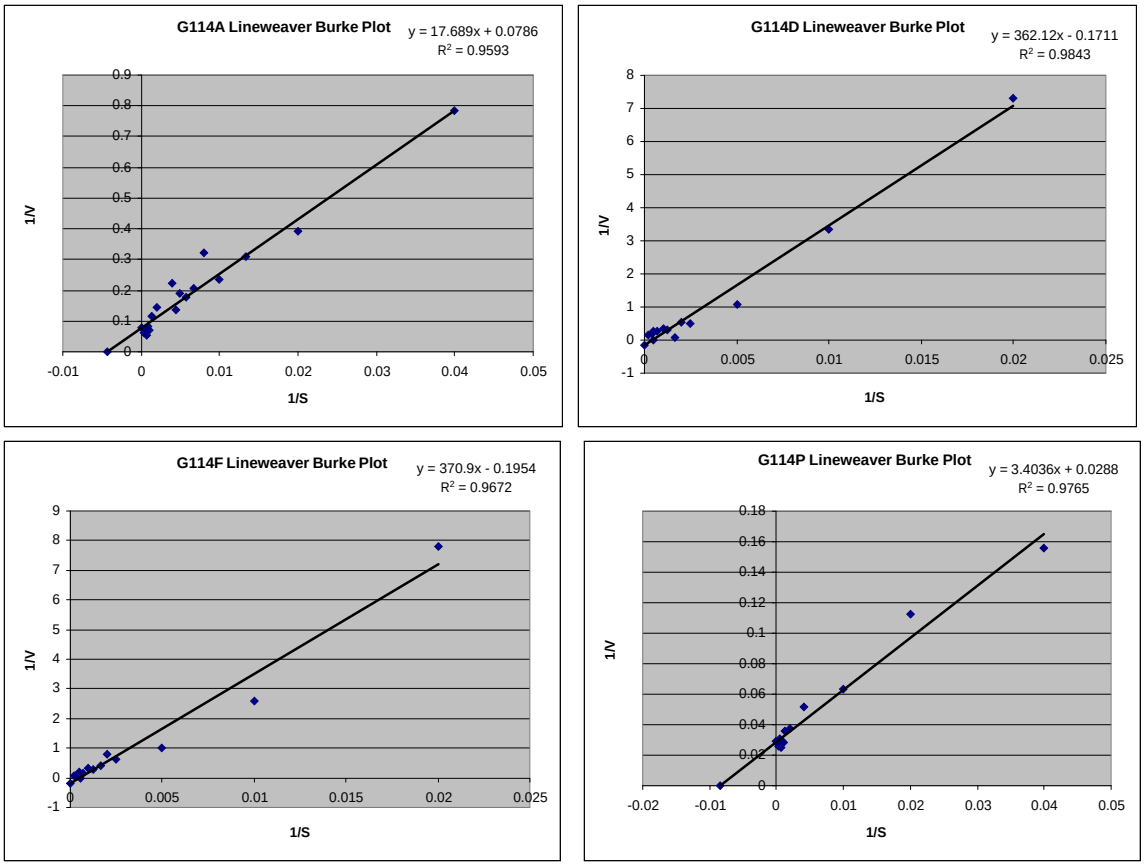

Figure 32. Lineweaver Burke plots of ^{14}C succinate transport data for individual DctA mutants

Table 6. Kinetic parameters for G114 mutants relative to wild-type and deletion strains

	Km Succinate uM	Vmax nmol/ug/min
SM1021	91	161
SM1021-II	1891.2	4.4
G114A	225.1	12.7
G114D	2116.4	5.85
G114F	1898.2	5.12
G114P	94.4	33.6

however, presumably due to a reduction in transport capacity. As mentioned previously, the V_{max} values for the G114 point-mutants are likely to be inflated due to the expression of these *dctA* from a multiple-copy-number plasmid. These data suggest therefore, that the V_{max} values for the point-mutants are severely reduced relative to wild-type. Interestingly, whilst the V_{max} values of the mutant DctAs appear to be extremely low, both G114A and G114P demonstrate approximately wild-type growth on dicarbxylates. This suggests that physiologically, DctA can operate well-below its V_{max} and still support a functional metabolic exchange.

These data corroborate the results seen in the growth curves and plate assays, which suggested that both G114A and G114P were active whilst G114D and G114F were not. The transport data also highlights differences in transport properties of G114A and G114P, a difference which could not be seen simply by looking at the growth properties of these strains because of the high substrate concentrations present in the growth media.

G114P appears to be the most active of the mutants which is initially surprising. This can be explained by considering the potential role that proline can play as a component of a trans-membrane helix. As discussed in the introduction, glycine can play a significant structural role in single-path membrane proteins by promoting protein dimerization, by facilitating the formation of favorable van der Waals surfaces for hydrophobic packing, or by permitting closer dipole interactions of the polar backbone (17, 26, 31, 71-73, 81, 120, 122, 123).

In soluble proteins, proline is typically considered to be a helix breaker because of its propensity for introducing “kinks” into the secondary structure of polypeptide chains (14, 31, 99).

However, in transmembrane helices, proline can act as a stabilizer (56) in much the same way as glycine, by facilitating packing of helices by virtue of its size and range of permissible dihedral angles (56). This kind of functional equivalence would allow a certain degree of interchangability between the two residues that is not seen between glycine and other amino acids including alanine.

3.3.1.5 Plant Tests

The ability of each point-mutant strain to nodulate alfalfa and form an effective, nitrogen-fixing symbiosis was studied by inoculating three-day old seedlings of alfalfa with each strain. Plants were grown for five weeks before being assessed. Plants were analyzed on the basis of observed characteristics that included nodulation phenotype, total dry weight, and overall vigor. The point-mutant-inoculated plants were compared to plants inoculated with wild-type SM1021, the *dctA* strain SM1021-II, and SM1021-II carrying pSM105 (wild-type *dctA*-FLAG).

3.3.1.5.1 Nodulation phenotype

Both G114A and G114P mutant strains produced nodules that resembled those of wild-type plants (data not shown) and the plants were healthy and well grown (for examples, see Figure 33), displaying a characteristic Fix^+ phenotype. This suggested that these strains are behaving the same as wild type *S. meliloti* and are capable of entering into functional symbioses.

FIGURE 33. Alfalfa plants inoculated with *dctA* mutants

Plants inoculated with Fix$^-$ strains appear nitrogen starved; smaller, yellow, and less vigorous than plants innoculated with Fix$^+$ strains.

From left to right:

Sm1021-II pSM105 G114A

Sm1021-II pSM105 G114D

Sm1021-II pSM105 G114F

Sm1021-II pSM105

Table 7. Dry mass of plants inoculated with *dctA* mutant strains

	plant mass (g) trial 1	plant mass (g) trial 2	plant mass (g) trial 3	Mean	Standard Deviation
SM1021	102.8	86.2	109.2	99.4	11.87
SM1021-II	30.6	23.5	27.2	27.1	3.55
No inoculation	21.3			21.3	
SM1021-II pSM105	53.4	61.8	41.2	52.13	10.3
G114A	61.7	54.5	30.9	49.03	16.11
G114F	32.3	20.9	34.2	29.13	7.19
G114D	33.4	22.2	25	26.87	5.83

3.3.1.5.2 Dry masses

The dry masses of plants inoculated with individual S. meliloti dctA mutant strains are presented in Table 7. These data support the phenotypic observations discussed above, with the dry masses of the Fix+ strains exceeding those for the Fix- strains.

3.3.2 Localization of mutant DctA proteins

3.3.2.1 *E. coli*

Membranes were isolated from *E. coli* cells expressing DctA-FLAG and were separated by SDS-PAGE gel electrophoresis. The proteins were then transferred to a PVDF membrane and probed with monoclonal mouse anti-FLAG antibody (Sigma-Aldrich, St. Louis, MO). DctA-FLAG was visualized using horseradish peroxidase (HRP) conjugated goat-anti-mouse secondary antibody.

Interestingly DctA-FLAG appears to run at approximately 35kDa, which is much smaller than its predicted 46kDa; however it is typical for integral membrane proteins to migrate at 65-75% of their true molecular weight (110). This is possibly due to retention of secondary structure accelerating migration, hydrophobicity or SDS binding (149). Results from these experiments were varied and not consistently reproducible. In the absence of any conclusive western blot data, it would be safe to assume that for strains G114A and G114P, at least some of the protein is localized to the membrane due to the presence of transport activity in these strains. No protein

was detected in either the cytoplasmic of periplasmic fractions suggesting that any protein that was not inserted into the membrane was degraded and did not form inclusion bodies.

3.3.2.2 *S. meliloti*

As discussed previously, development of an anti-DctA antibody has so far been unsuccessful. Attempts to visualize DctA in *S. meliloti* by western blotting have been unsuccessful. *S. meliloti* appears to have several endogenous proteins that cross-react with Anti-FLAG, one of which runs at approximately 35kDa and could potentially mask any reactivity of DctA. However, upon isolation of the membrane fraction, no signal is detected in *S. meliloti*. I think it is likely therefore that some form of C-terminal processing may be occuring that removes the FLAG epitope from DctA. It is reasonable to assume that G114A and G114P both are transported to the membrane successfully as transport activity can be detected in both of these strains. For the inactive point-mutants, G114D and G114F, it has not been possible to confirm the presence of DctA in the *S. meliloti* membrane and thus distinguish whether the proteins were localized properly but inactive, from the possibility that the inactive proteins were unable to be localized properly.

3.4 *dctA* Start codon mutagenesis

According to Engelke *et al* (38), there are two potential start codons for *dctA* in *S. meliloti*. As shown in Figure 34, these codons are separated by 33 base pairs (bp), and are each preceded by a

FIGURE 34. Upstream region of *dctA* showing three potential start codons (blue), transcriptional start site, and σ54 binding site (red)

Shine-Delgarno sequence, resulting in ORFs of 1,359 and 1,323 bp respectively. 152bp upstream of the first ATG is the sequence TGT-N_{10}-GCA, which is homologous to the NifA consensus sequence TGT-N_{10}-ACA (38) and may play a role in transcription activation under symbiotic conditions (109). 60bp upstream of the first ATG is the sequence CTGGCACG-N_4-TTGCA (38) which has strong homology to the RpoN consensus sequence CTGGCACPu-N_4-TTGCA (34, 53), and is believed to used for transcriptional activation of *dctA* under free-living conditions (38). Primer extension analysis has confirmed that, under free-living conditions, the transcriptional start site is 10 or 11bp downstream of the RpoN binding site (68).

To date, no work has been done to determine which of the two potential ATGs is the translational start codon, and to examine if any differences exist in start codon usage between the free-living and symbiotic states. The purpose of this part of my research was to examine the relative importance of each start codon under free-living conditions.

In addition to the two potential start codons already discussed, there is a third ATG within the RpoN binding site of *S. meliloti* that is in frame with the other two. It is reasonable to assume that because it is located within the spacer region of the RpoN binding site and is thus upstream of the transcriptional start site, it is not used under free-living conditions. However, if alternative promoters are used during symbiosis, this start codon could potentially be important. For this reason it was included in the experiment conducted in this section, and will be used at a later date in plant tests.

3.4.1 Generation of start codon mutants

Each of the three possible methionine start codons was changed by site-directed mutagenesis, from methionine to isoleucine (half of these mutations were made by S. Yurgel, half by M. Ziegler). Methionine mutations were made individually and in each combination of double mutant. This resulted in six mutants, three of which contained two possible start codons and three with just one start codon. Table 8 shows the genotype of each mutant.

3.4.2 Integration into the *S. meliloti* chromosome

dctA was cloned by S. Yurgel, into pK19*mob* as a 1.9kb fragment, and electroprated into *E. coli* strain S17-1. pK19mob is an *E. coli* expression vector which contains an origin of transfer that allows it to be transferred conjugally into *S. meliloti* . However, it lacks an *S. melilo ti* origin of replication and so once in *S. meliloti* it is unable to replicate. Selection of drug-resistant exconjugants yields strains in which the plasmid has integrated into the chromosome (Figure 35). Integrants were selected on $MMNH_4$ containing 200µg/ml neomycin (Nm). Integrants were purified by three successive rounds of colony isolation before being used for assays.

Table 8. Genotype of each methionine mutant

Name	Met(s) Mutated	Met Used
Met-1	1	2 or 3
Met-2	2	1 or 3
Met-3	3	1 or 2
Met 1-2	1 and 2	3
Met 1-3	1 and 3	2
Met 2-3	2 and 3	1

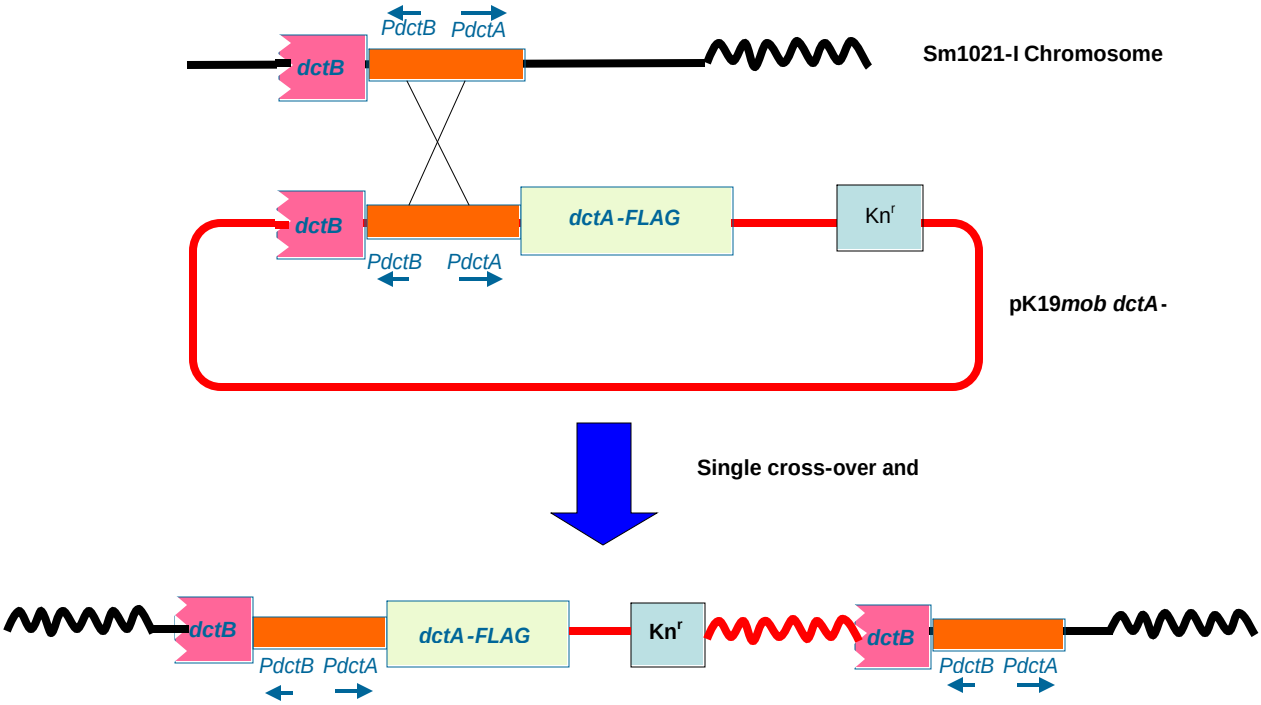

FIGURE 35. Integration of pK19*mob dctA* -FLAG into the Sm1021-I chromosome

A single cross-over event occurs in the intact *dctA* promoter region. This results in integration of the pK19*mob dctA* -FLAG vector into the Sm1021-I chromosome, producing a strain that is neomycin resistant.

Table 9. Summary of the growth properties of each methionine mutant

Name	Met(s) Mutated	Met Used	Growth on DCAs	Growth in presence of FOA
Met-1	1	2 or 3	+++	Poor
Met-2	2	1 or 3	+++	Poor
Met-3	3	1 or 2	+	Good
Met 1-2	1 and 2	3	+++	Some
Met 1-3	1 and 3	2	+	Good
Met 2-3	2 and 3	1	-	Good

3.4.3 Phenotypic Analyses

3.4.3.1 Growth Curves

Growth of the methionine mutants was assessed in liquid culture as described in the previous section. OD_{600} spectrophotometric readings were measured every 10 min for 72 hr. Growth data are summarized in Table 9, and are depicted graphically in Figures 36-42 which show growth data for strains grown in $MMNH_4$, $MMNH_4$ supplemented with FOA 1 and 5µg/ml, and $MinNH_4$ supplemented with L-malate, succinate or fumarate.

Growth on the control medium $MMNH_4$ is shown in FIGURE 32 and as anticipated, all strains grew well, although it appears that strain Met 2-3 started lysing in the final stages of the experiement. DctA is not required for the transport of mannitol (the carbon source in $MMNH_4$), so it is unlikely that this was a result of any disruption of *dctA* expression. FIGURE 37-42 shows growth of each strain on $MinNH_4$ supplemented with 0.2% succinate, fumarate, L-malate, and D-malate. These data show that the most deleterious effect upon growth ability is caused by changing the third methionine, which is consistent with the results on solid media. Interestingly, the largest effect on growth was seen in strains where both the second and third methionines were altered, suggesting that whilst the third methionine appears to be the most important, the second one is also needed for optimal expression of DctA.

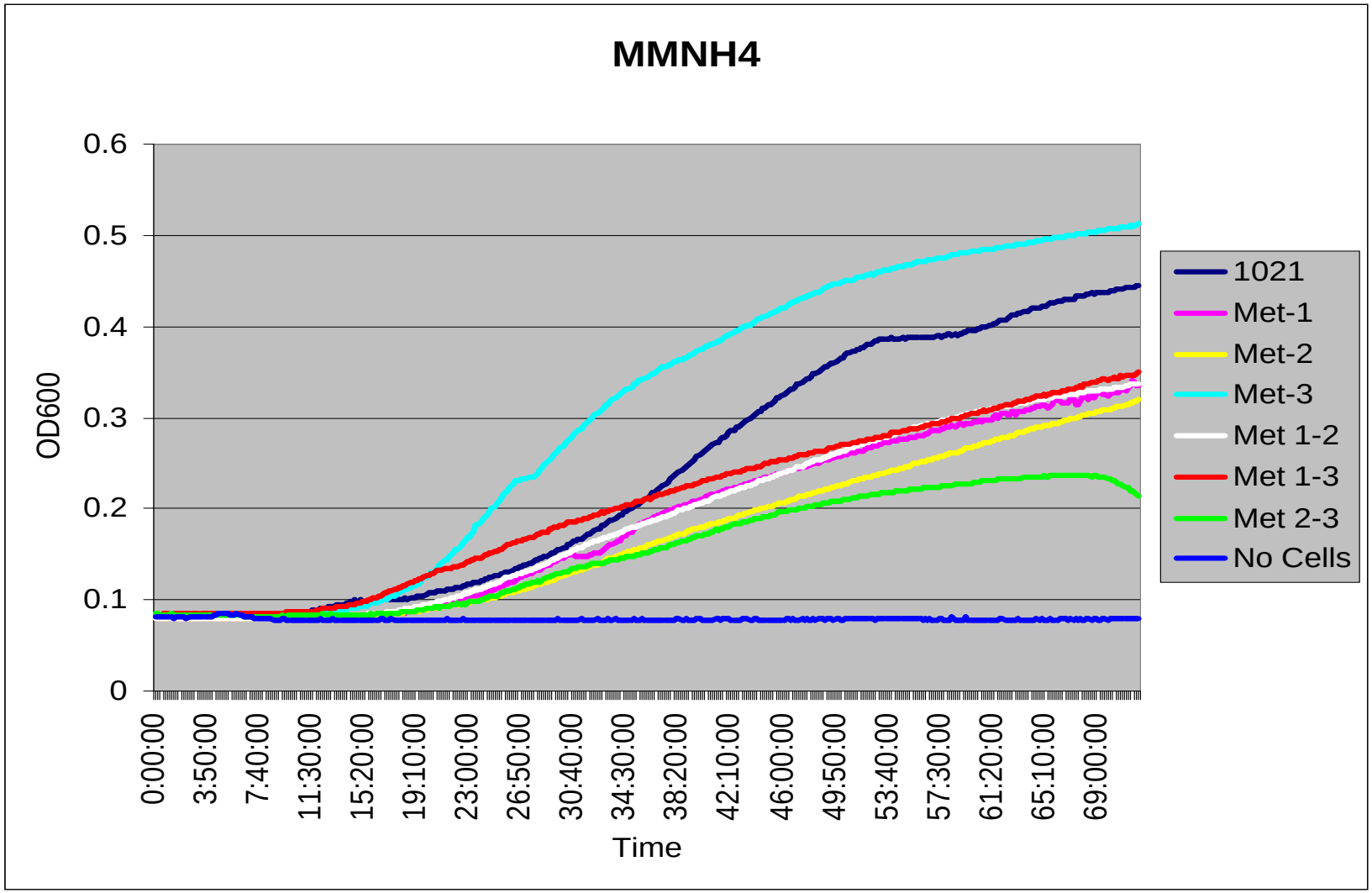

Figure 36. Growth Curve of *S. meliloti dctA* Methionine mutant strains in MMNH4

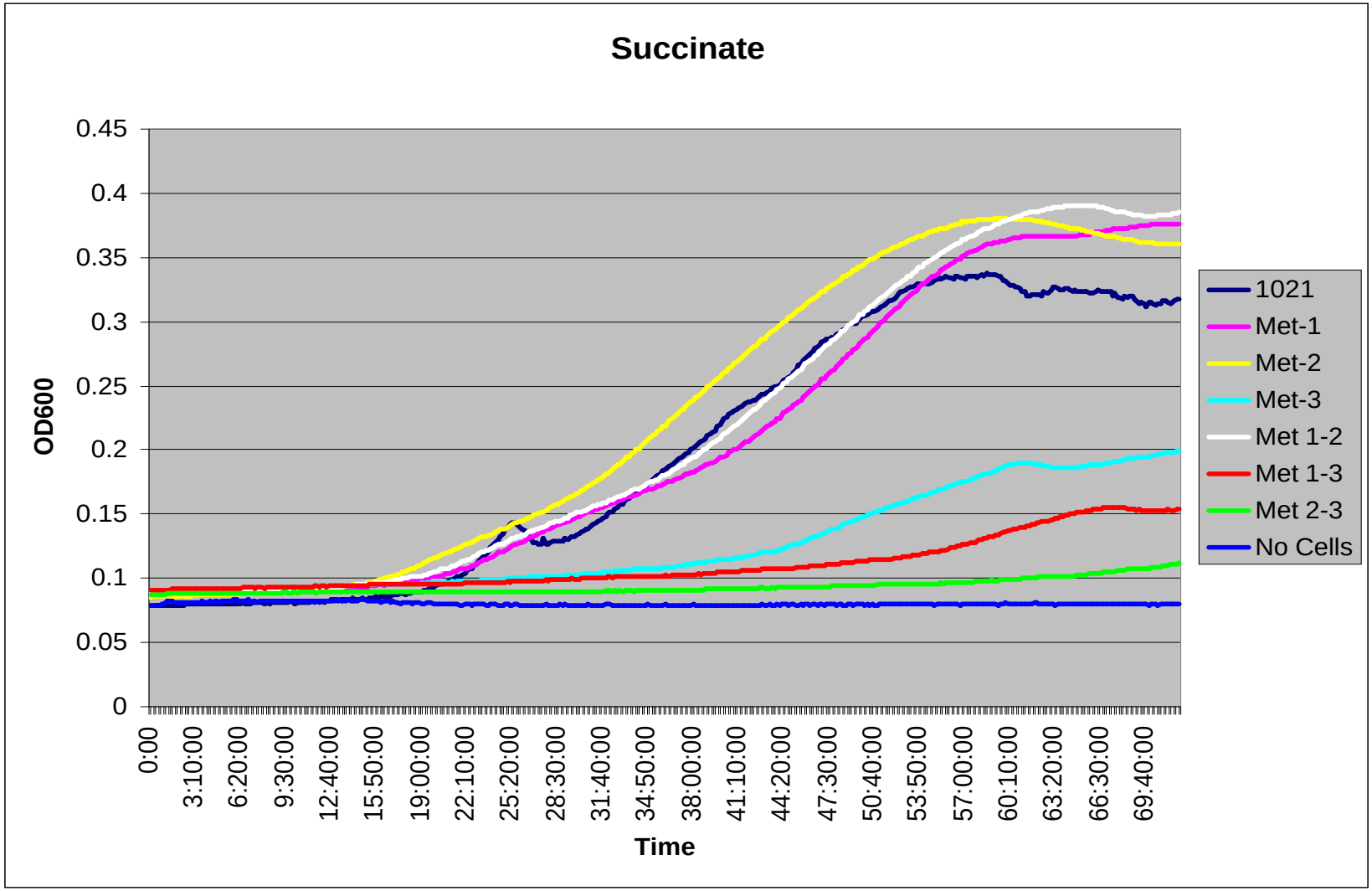

Figure 37. Growth Curve of *S. meliloti dctA* Methionine mutant strains in MinNH4 supplemented with 0.2% Succinate

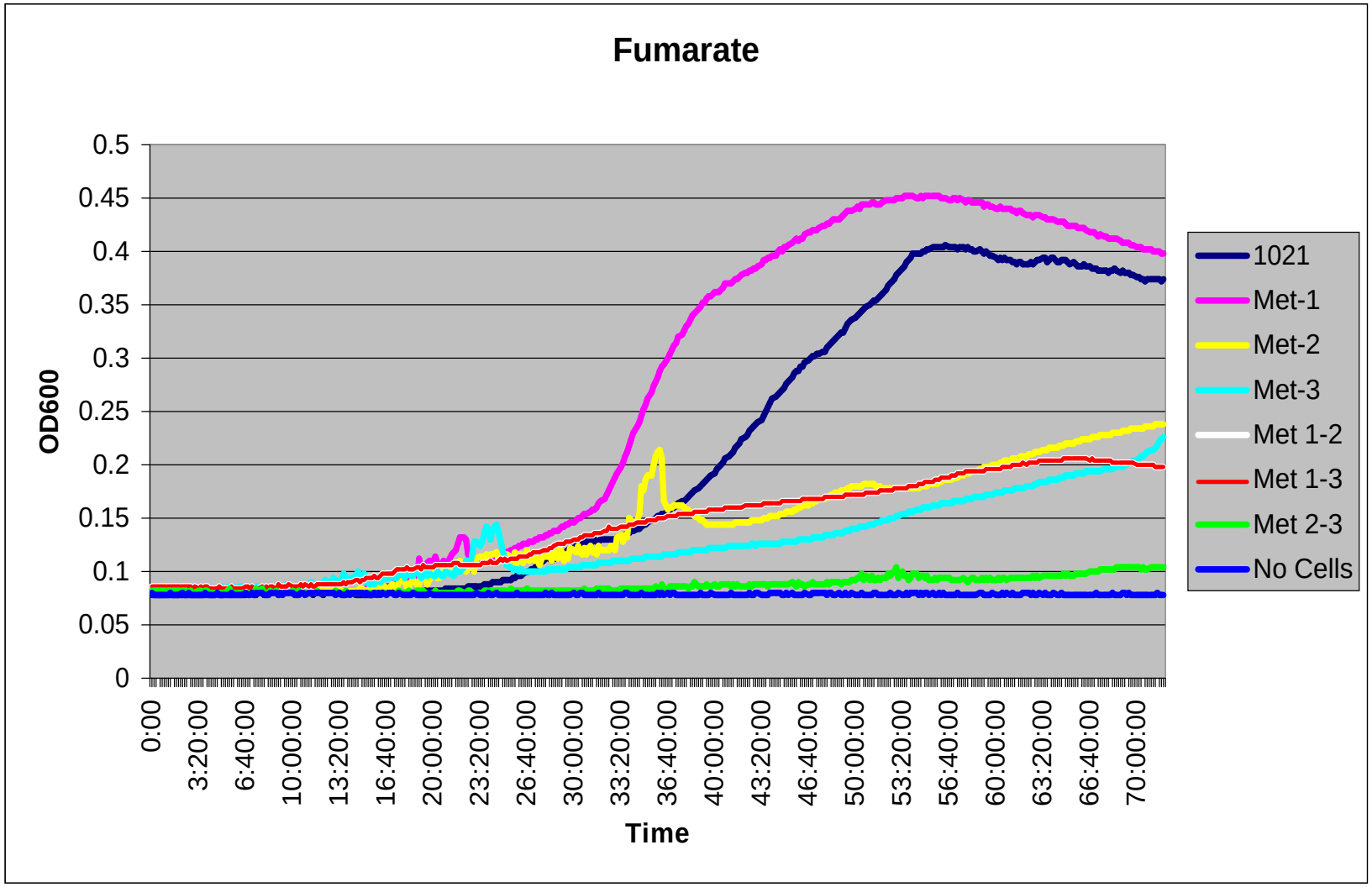

Figure 38. Growth Curve of *S. meliloti dctA* Methionine mutant strains in MinNH4 supplemented with 0.2% Fumarate

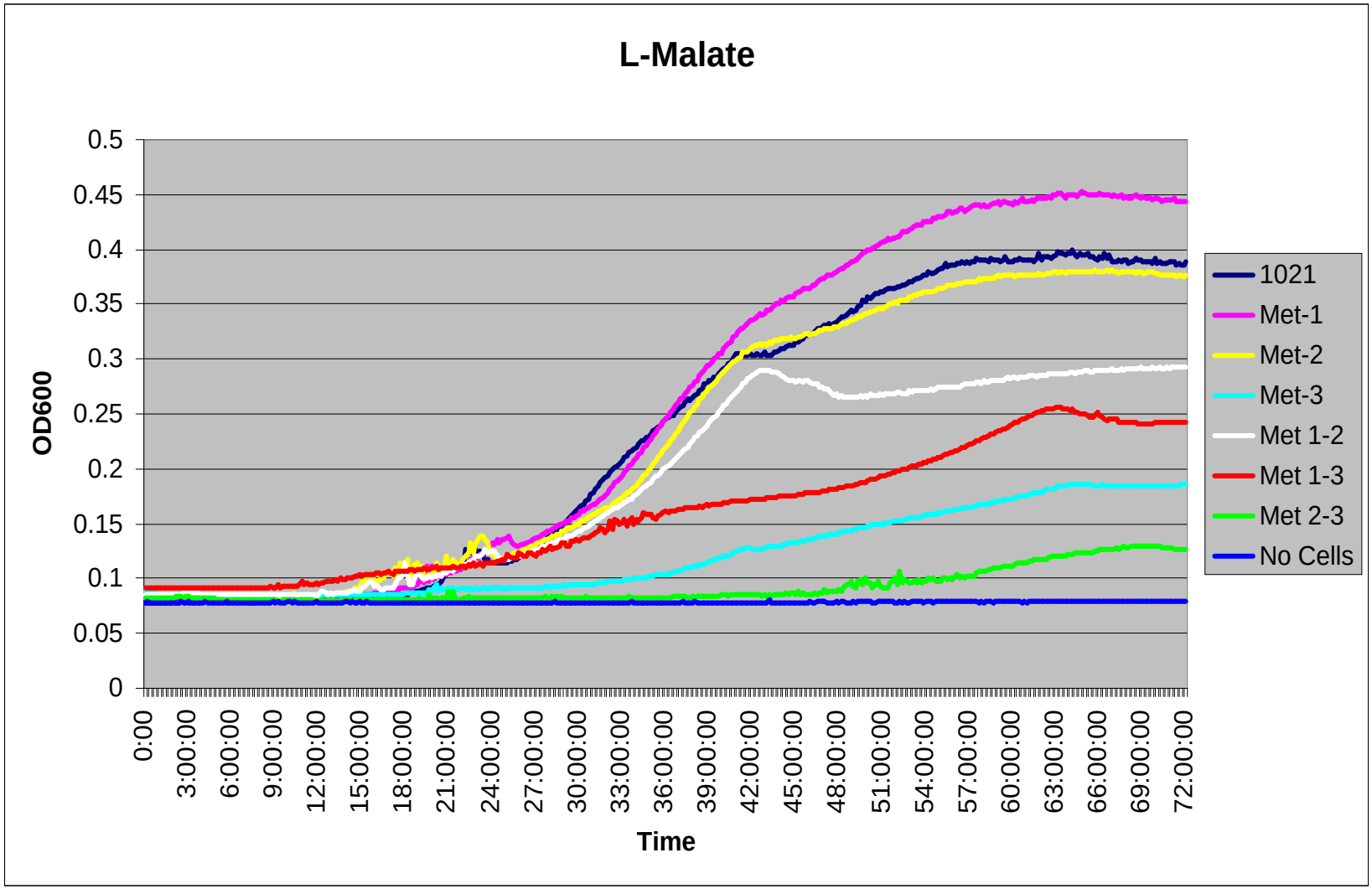

Figure 39. Growth Curve of *S. meliloti dctA* Methionine mutant strains in MinNH4 supplemented with 0.2% L-malate

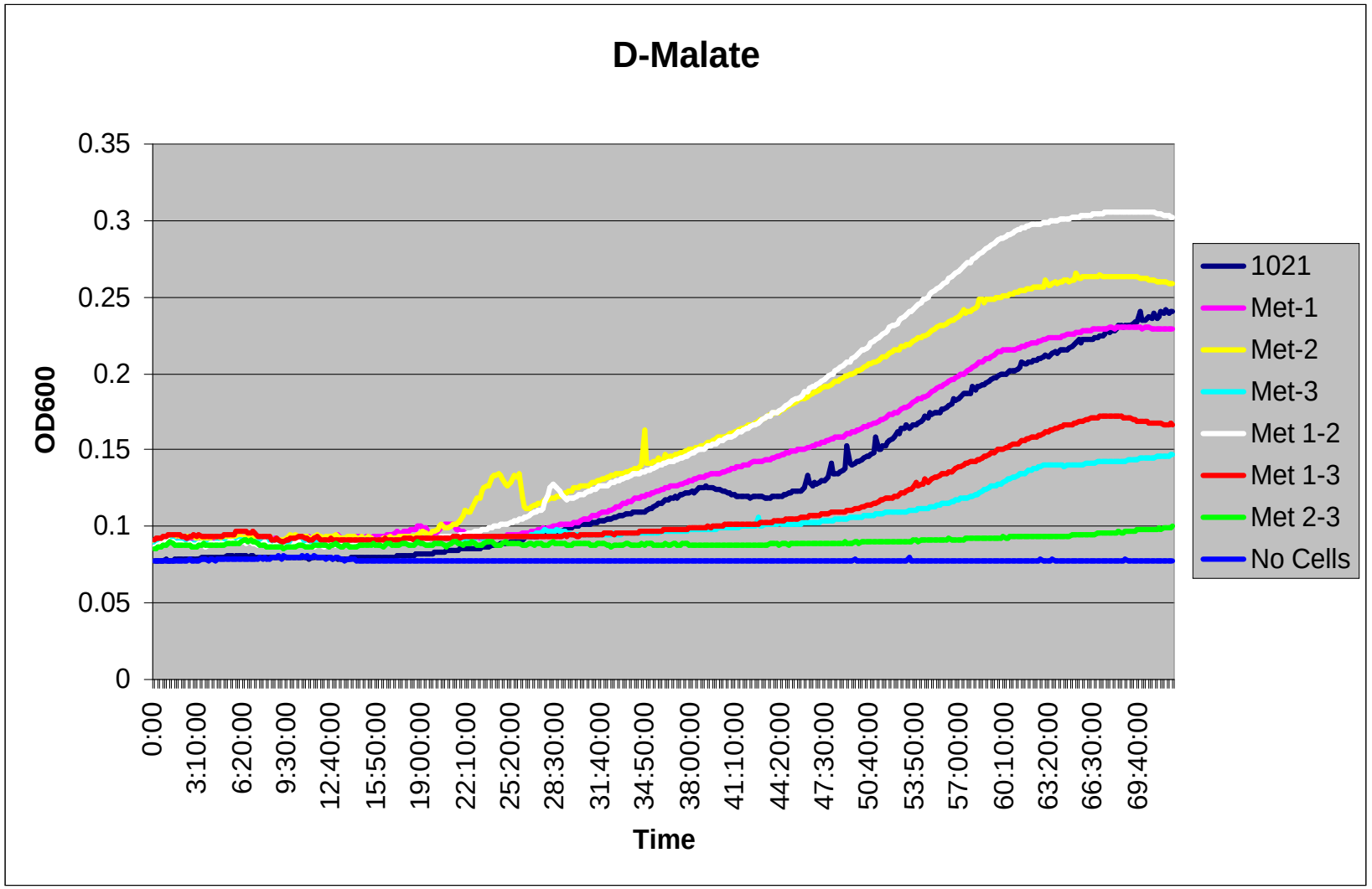

Figure 40. Growth Curve of *S. meliloti dctA* Methionine mutant strains in MinNH4 supplemented with 0.2% D-malate

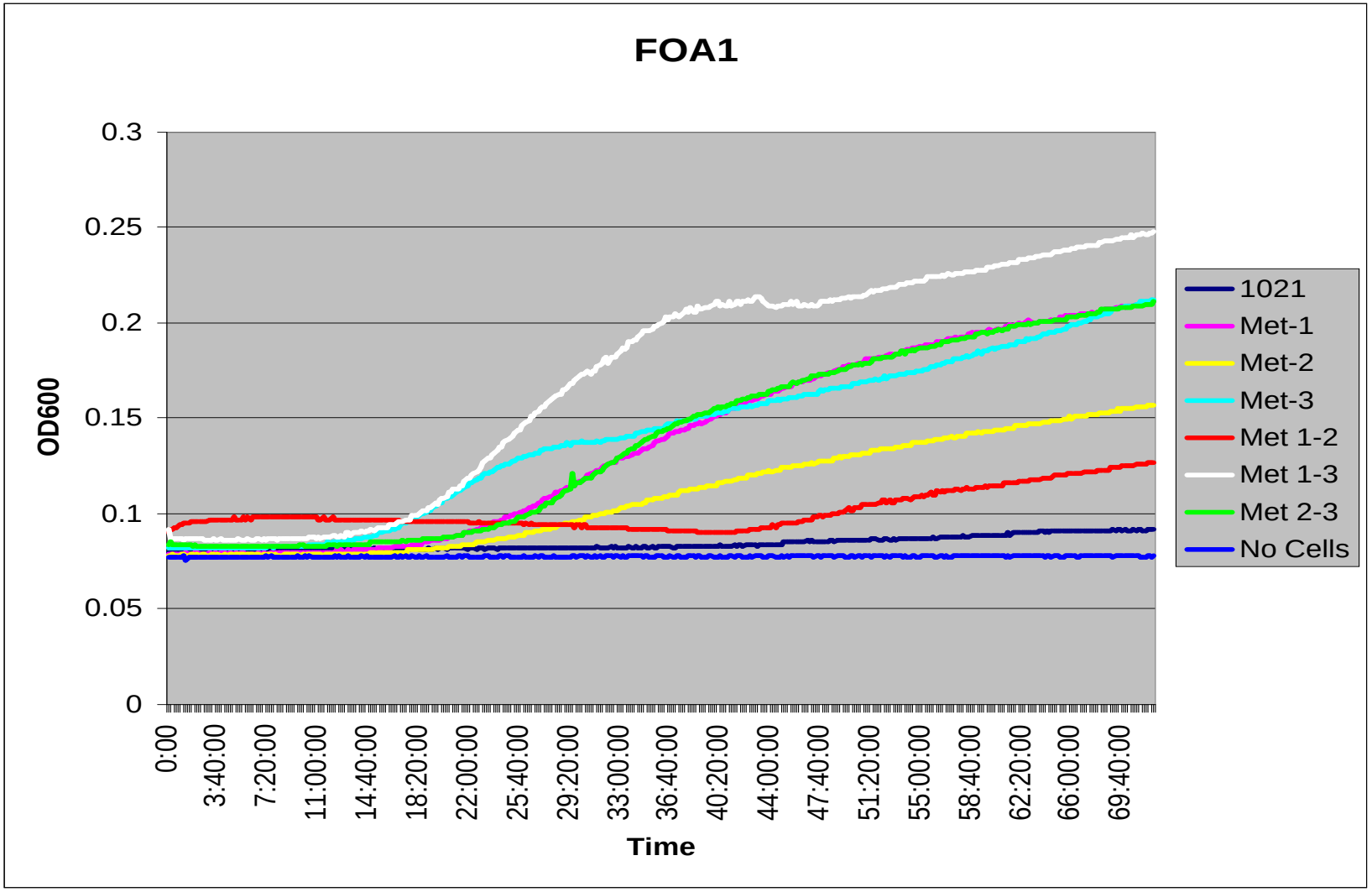

Figure 41. Growth Curve of *S. meliloti dctA* Methionine mutant strains in MMNH4 supplemented with 1µg/ml FOA

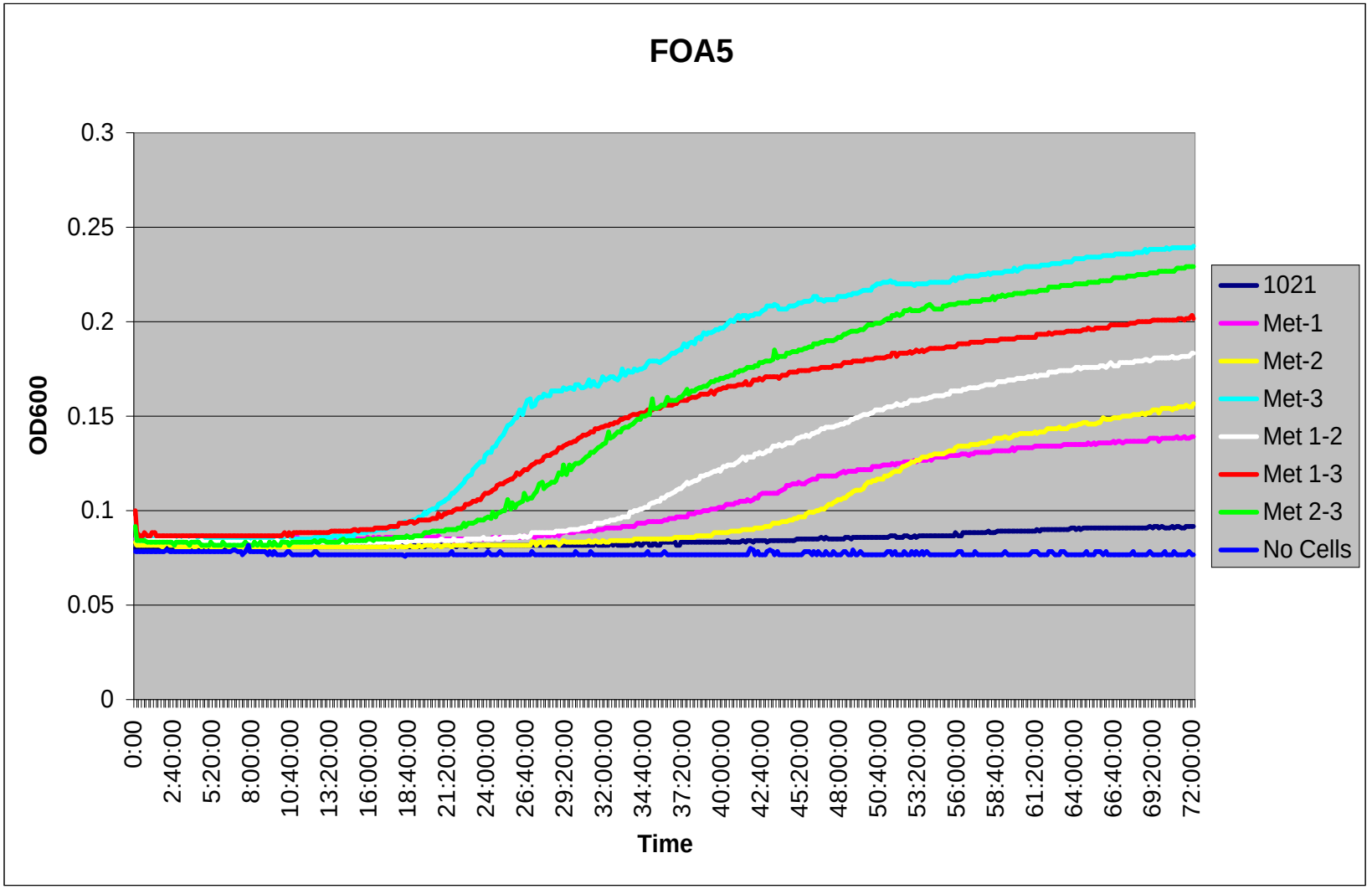

Figure 42. Growth Curve of *S. meliloti dctA* Methionine mutant strains in MMNH4 supplemented with 5µg/ml FOA

Growth using succinate as the sole carbon source, shown in Figure 37, clearly demonstrates this phenomenon. Each strain lacking either the first or second methionine grows as well as wild-type SM1021. Each strain that lacks a copy of the third methionine grows poorly. This pattern is repeated on both L-malate and D-malate. Growth using fumarate was more ambiguous. As shown in Figure 38, Met-3 and Met 1-3 grew at an equivalent rate to Met-2. However, Met 2-3 did not grow at all on fumarate suggesting that perhaps Met-2 and Met-3 were equally important on this substrate.

Growth on FOA is shown in Figures 41 and 42. Strains lacking the third methionine grow well on FOA, suggesting that levels of transport by DctA are low enough to not prove toxic to the cells. Strains lacking the second methionine do not grow as well as strains lacking the third, indicating that they have more residual DctA function. Strains lacking the first methionine are still sensitive to FOA, suggesting that the first methionine does not play a significant role in the initiation of DctA translation

3.4.3.2 Transport Assays

Transport data were collected for each mutant at 100µM succinate and compared to data from wild-type Sm1021 and the *dctA* strain 1021-II. The data collected are shown in Figure 43. These data support the growth rate data by showing that having the third methionine intact contributed the most to transport rate. These data also show that integration of *dctA* into the chromosome of Sm1021-II through homologous recombination of the pK19*mob-dctA* derivative

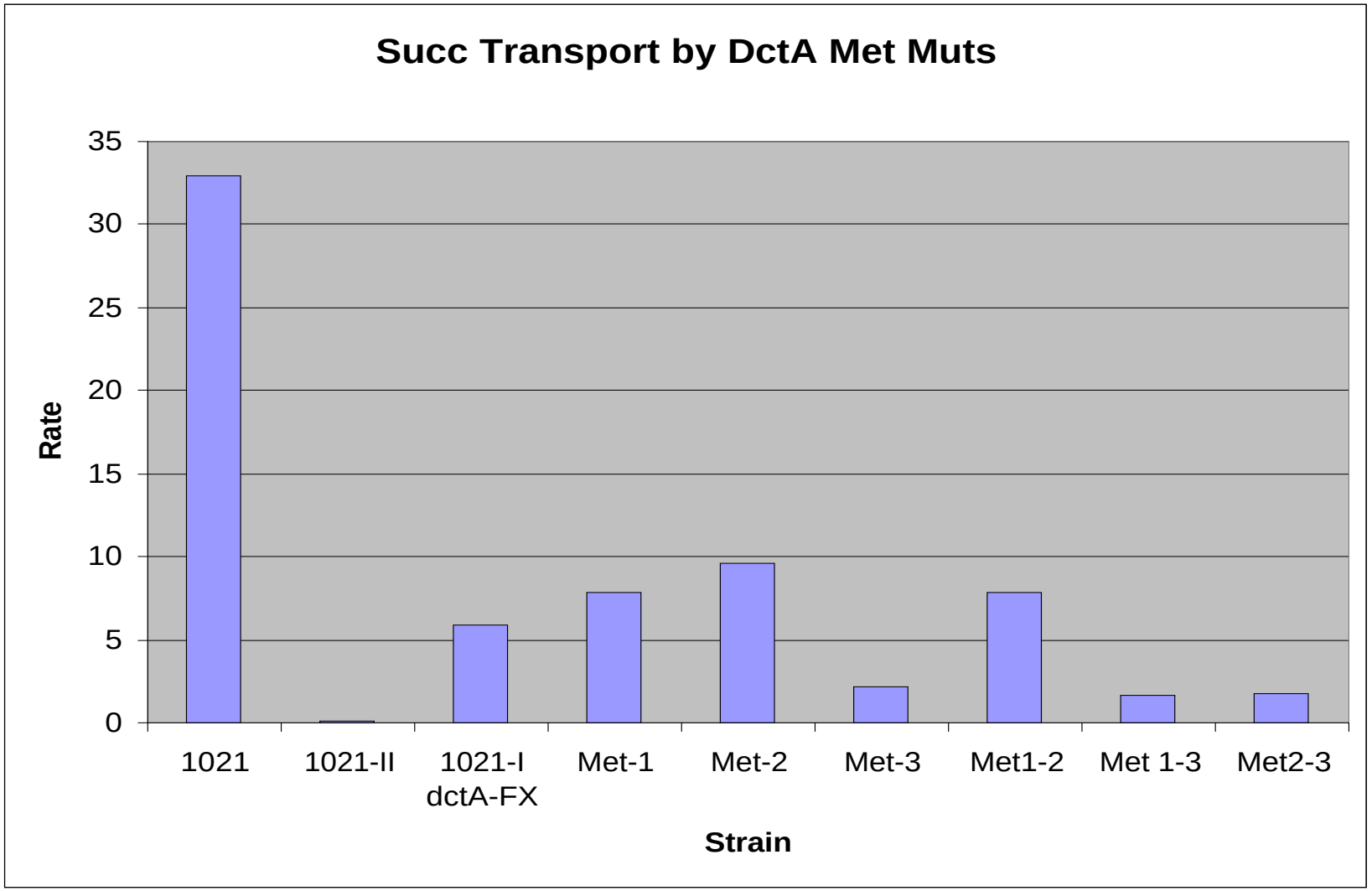

Figure 43. Succinate transport by methionine mutants of DctA

yields a strain with lower transport activity than wild-type Sm1021. This results in strain Sm1021-I *dctA*FX, which possesses two complete copies of the native *dctA* promoter, but only a single copy of the *dctA* gene (Figure 35). *dctA* is expressed from a σ^{54}-dependent promoter, (Figures 12 and 13) which requires the binding of two DctD molecules in order for transcription to initiate (38, 63, 69, 70, 102, 108, 109). In strains bearing two copies of the *dctA* promoter, only half of DctD binding events will result in transcriptional activation, resulting in a "diluting" of the effects of DctD. It is reasonable to expect that this effect could result in a reduction in DctA production if activated DctD is limiting.

Comparison of transport levels of [^{14}C]-succinate for the methionine mutants suggest that the third methionine is the main translational start codon for *dctA*. These data also suggest that the first methionine is not playing a role in transcriptional activation in the free-living state. This is in agreement with studies that have shown that under free-living conditions, *dctA* expression is driven from a σ^{54}-dependent promoter (38, 63, 68-70, 102, 107, 150). Met-1 lies within the spacer region of the RpoN binding site of the *dctA* promoter, and would not be expected to have any effect upon expression as it does not lie within the -12 -24 consensus sequence (34, 53). Primer extension studies (68) have shown that under free-living conditions, the transcriptional start site for *dctA* is 10 or 11 nucleotides downstream of the RpoN binding site, resulting in a transcript that would not include Met-1. It would be extremely informative to be able to analyze DctA levels in each of the mutant strains to confirm this hypothesis, but as discussed previously, it has not been possible to generate an effective anti-DctA antibody.

There is no data to show that under symbiotic conditions, the same *dctA* promoter is used, and it is possible that an alternative start codon might be preferred. Further studies looking at the symbiotic phenotypes of each of these mutants are currently underway, and will yield some interesting results regarding start codon usage for *dctA* under symbiotic conditions.

3.5 *Xenopus laevis* expression

My goal was to develop a transport assay using *Xenopus* oocytes. Using this protocol, it would have been possible to test many potential DctA substrates easily and rapidly without the need for radio-labeled substrates (87). Furthermore, its flexibility would permit the measurement of several different parameters within the course of a single experiment, for example; it would allow direct measurement of V_{max} and K_m and it would also facilitate investigation of the effects of ions on the activity of the transporter, and quantitative analysis of different DCAs as potential substrates or inhibitors of transport.

Developing an assay in *X. leavis* has many advantages relative to working in *S. meliloti* . First, it is currently not possible to directly measure ionic currents across the bacterial membrane owing to the extremely small size of the bacterial cell (1-2 µm) which, using current technology is too small to allow either patch-clamping or the insertion of electrodes on either side. *X. laevis* oocytes are much larger (approx. 1 mm in diameter), and have been used extensively in recent years as a reliable system for the heterologous expression of membrane-bound proteins,

including ion channels, membrane receptors and transport proteins (27, 66, 87, 129, 131, 132, 153)

The experiments currently used to measure DctA activity are limited in several respects, for example, they can only measure gross changes in transport activity in response to different conditions, whereas the sensitivity of the *Xenopus* system has been used extensively to detect very small changes in activity. The current assay does not allow us to look at the coupling of cations to substrate transport; again, *Xenopus* oocytes have been used extensively to study this phenomenon in other glutamate transporter systems (27). Furthermore, a single *Xenopus* oocyte can be used in multiple experiments to look at the effects of different substrates, ions etc. on transport. Using our current assay, each batch of cells can be studied under a single set of conditions, and each batch of cells must be prepared individually, a process which takes 3-4 days. These studies are very time-consuming and a maximum of six to twelve samples can realistically be analyzed at a time. For example, studying six mutant strains under two different concentrations of the same substrate takes an entire day.

Xenopus oocytes have been used successfully to express proteins from bacteria (159), yeast (19) and plants (12). Recent work has demonstrated that neuronal glutamate transporters can be successfully and reproducibly expressed and assayed in *Xenopus* (8, 12, 39) which would suggest that their bacterial counterparts might also be studied in this fashion.

The 3' and 5' UTRs of *Xenopus* β-globin have been demonstrated to enhance expression of heterologous proteins by several hundred fold (84, 130) and removal of the 3' UTR resulted in a

4-fold decrease in expression (*51*). *In vitro* transcription of the linearized construct using the commercially available mMessage mMachine kit from Ambion (Ambion Inc. Austin, TX) was used to generate an mRNA transcript of the *dctA* gene that contained the post-transcriptional modifications characteristic of a eukaryotic mRNA (2). This transcript was injected into specially prepared oocytes.

3.5.1 Cloning of *dctA*-His into pGEMHE

A high expression cloning vector, pGEM-HE, containing the 3' and 5' untranslated regions (UTR's) of the*X. leavis* β-globin gene, and the T7 polymerase promoter has been developed (61, 77), into which *dctA*-His (*dctA*-His was made by S. Yurgel) was inserted as a *Bam*HI/*Xma*I fragment. Insertion was confirmed by restriction analysis.

3.5.2 Western blots

Following injection of mRNA into the *X. laevis* oocytes, it was desirable to confirm translation of the transcript by western blot analysis. This was attempted using an Anti-His antibody (Sigma Cat. # H1029, Sigma-Aldrich Corp, St. Louis MO). Unfortunately, *X. laevis* has an endogenous 36.5kDa protein that contains an octa-histidine sequence. As a membrane protein, DctA tends to run faster in an SDS-PAGE gel than a soluble protein of the same size, so it was reasonable to expect that this endogenous protein was likely to cause a problem. As a result, *dctA* was cloned again using a FLAG epitope in place of the poly-histidine tag as it is known that *X. laevis*

oocytes do not contain proteins that cross-react with Anti-FLAG antibodies. To date however, the western blots in *X. laevis* have not been repeated to confirm translation of DctA.

3.5.3 Transport assays

Bulk transport assays were conducted using both [^{3}H]-orotate and [^{14}C]-succinate as substrates by exposing injected oocytes to a solution containing [^{14}C]-succinate for 15 min, washing them, and measuring total ^{14}C uptake following lysis in SDS. To date, I have detected no difference between injected and uninjected oocytes in the amount of ^{14}C substrates transported.

Chapter Four Conclusions and Future Directions

4.1 G114 Point Mutants

Four point mutants of G114 in DctA of *S. meliloti* were generated; G114A, G114D, G114F, and G114P. Analysis of the phenotypes of these point-mutants produced some interesting insights into the role that G114 may play in the overall tertiary and quarternary structure of DctA. Both G114A and G114P were active, albeit at a lower rate than wild-type, whilst G114D and G114F were not discernably different from the *dctA*$^{-}$ strain Sm1021-II. Perhaps surprisingly, G114P was the more active point mutant, with a Vmax almost three times higher than G114A. This result, whilst counterintuitive based upon our current understanding of soluble proteins, is in accordance with recent work published on polytopic membrane proteins (31, 56, 65). These studies argue that proline possesses a higher packing value in trans-membrane helices which allows it to stabilize interactions in much the same way as glycine can. In this type of stabilization, glycine is thought to facilitate inter-helical packing by allowing helices to approach more closely, and proline is now believed to be able to act in much the same way (56). The methyl side-chain of alanine might potentially be more bulky than the constrained ring of proline when packed into a membrane helix, resulting in a less active protein. These data, coupled with the complete conservation of G114, suggest that G114 is playing a significant structural role by facilitating helical packing of DctA, and that any disruption in this results in a reduction of activity.

This is an exciting result in its own right as the third transmembrane region of DctA has not previously been implicated in transport activity. It would be interesting to evaluate further the role(s) played by TMD3 in DctA transport activity. Mutagenesis of additional amino acids within TMD3 would provide additional insight into the importance of other residues within this region. For example, Figure 18 shows that residues A110, S107, F103, and Y102 are all highly conserved in all of the glutamate transporter family members that were evaluated during the design of this study and these residues are predicted to be on the same face of the helix.

Whilst site directed mutagenesis provides an efficient means of studying point mutations of specific amino acid residues, it might be interesting to use a more random method of generating mutants of TMD3 which could be selected for on the basis of growth characteristics. Multi-site mutagenesis would allow the targeting of up to 5 amino acid residues in a single experiment. These residues are predetermined, and a mixture of primers is synthesized, each encoding a single point mutation at one of the specified amino acids. This would provide an efficient means by which the effects of different amino acids at individual loci could be studied.

The secondary structure model depicting eight transmembrane helices suggests that DctA might form an oligomeric quaternary structure. This hypothesis is further corroborated by a recent study that used freeze fracture electron microscopy to study the structure of a human neuronal glutamate transporter (EAAT3) expressed in *X. laevis* oocytes (39). This study found evidence that the transporter was organized in a pentameric arrangement forming a membrane spanning channel. Based upon this information there are a number of studies that one can imagine providing valuable insight both structurally and functionally. The first would be to look at each

transmembrane region as a helical wheel in an attempt to identify potential regions of interaction. Based upon the information that this would provide, I believe performing an alanine scan of at least one transmembrane region would provide some interesting data giving both structure and function information.

It would also be interesting to study the effect of multiple *dctA* genotypes within the same strain. For example, expressing a G114 mutant *dctA* in wild-type 1021 under the control of different strength promoters to investigate any effect that hetero-multimers might have upon DctA functionality. This information might shed additional light upon the multimeric complex, three-dimensional structure formed by DctA *in vivo*.

As a follow-up to the G114 growth-assays, additional transport assays using different radio-labeled substrates would give a more complete picture of the transport capacities of these mutants. Looking at the ability of each strain to transport aspartate would allow confirmation of the growth assays. For example, if any of the strains truly do possess an increased capacity to transport aspartate, then it would be be interesting to investigate the effects of expressing them in strains compromised in any of the genes required for the amino-acid cycling pathways, especially the effects upon symbiotic phenotype. Also, transforming each strain with the maleate isomerase gene from *A. faecalis* would allow any strain that could transport maleate to actually utilize it as a substrate, this would in turn allow us to determine if any of the mutant strains could now transport maleate. Maleate transport would indicate a major change in the transport characteristics of DctA, as previous studies suggest that it is too structurally constrained to permit transport of the *cis*-carboxyl configuration of a dicarboxylic acid (160).

One component missing in this analysis is confirmation and quantitation of the amount of DctA present in each strain. This prevents me from making several arguments that depend upon knowing how much protein is present and thus what the significance of the Vmax rates of transport are relative to the ability of DctA to move substrates through the membrane. My inability to quantify DctA has not been for lack of trying; both the introduction of an epitope tag at the C-terminus of DctA and the attempt to make an anti-peptide antibody were focussed upon answering this question. Upon receipt of a purified, functional anti-DctA antibody, all of the western blots need to be repeated in order to determine approximate levels of protein expression, and to confirm transport to the membrane of each DctA. A functional anti-DctA antibody would also allow a more complete analysis of start codon usage in DctA by gel-shift analyses. It is possible that start codon usage is growth-condition dependent and that under different conditions, especially in symbiosis, a different start site is used.

4.2 Start Codon Mutants

Mutagenesis of the predicted start codons of DctA has demonstrated that it is the third methionine that is the most important under free-living conditions. Growth data suggests that the second methionine may be able to substitute for it when substrate levels are high, but analysis of transport activity at substrate concentrations approaching the Km of DctA reveals a reduction in activity levels. This is presumably due to a reduction in translation as a result of deletion of the third methionine. While it would be informative to look at DctA levels in these strains, it has not been possible due to the lack of an effective anti-DctA antibody.

To get a more complete picture of the effects of mutating individual start codons of *dctA*, it is necessary to collect additional transport data for each of the methionine mutant strains, to calculate Km and Vmax values for each. Furthermore, it would be interesting to assess the existence of additional transcriptional start signals for *dctA*, by deleting all three methionines and looking at both transport and growth abilities. It is possible that alternative mechanisms for expression and regulation might be used and this would shed some additional light on their existence.

4.3 *Xenopus laevis* assay development

The possibility of developing an accurate *in vitro* assay for DctA activity using the *X. laevis* system should not be abandoned yet. All of the bulk transport assays need to be repeated using the *dctA*-FLAG construct, and expression analyzed by western-blot. There are several commonly-used codons in *S. meliloti* DctA that are rare in *X. laevis*. Changing these codons to ones more familiar to *X. laevis* may help to improve expression levels.

Chapter Five References

1. **Amato, A., B. Barbour, M. Szatkowski, and D. Attwell.** 1994. Counter-transport of potassium by the glutamate uptake carrier in glial cells isolated from the tiger salamander retina. J Physiol **479 (Pt 3):**371-80.

2. **Ambion** 2002, posting date. mMessage mMachine manual. Ambion. [Online.]

3. **Arwas, R., McKay, J.A., Rowney, F.R.P., Dilworth, M.J. and Glenn, A.R.** 1985. Properties of organic acid utilization mutants of Rhizobium-leguminosarum strain v300. J. Gen. Microbiol. **131:**2059-2066.

4. **Association, I. F. I.** 21 Jan. 2004, posting date. Nitrogen, phosphate and potash statistics,1973-1973/74 to 2001-2001/02. IFADATA statistics online. International Fertilizer Industry Association. [Online.]

5. **Barbour, B., H. Brew, and D. Attwell.** 1988. Electrogenic glutamate uptake in glial cells is activated by intracellular potassium. Nature **335:**433-5.

6. **Barnett, M. J., V. Oke, and S. R. Long.** 2000. New genetic tools for use in the Rhizobiaceae and other bacteria. Biotechniques **29:**240-2, 244-5.

7. **Beijerink, M. W.** 1888. Die bacterien der Papilionaceen-Knollchen. Bot. Ztg. **46:**725-804.

8. **Bendahan, A., A. Armon, N. Madani, M. P. Kavanaugh, and B. I. Kanner.** 2000. Arginine 447 plays a pivotal role in substrate interactions in a neuronal glutamate transporter. J Biol Chem **275:**37436-42.

9. **Bohlool, B., Ladha, JK, Garrity, DP, and George, T.** 1992. Biological nitrogen fixation for sustainable agriculture: a perspective. Plant Soil **141:**1-11.

10. **Bolton, E., B. Higgisson, A. Harrington, and F. O'Gara.** 1986. Dicarboxylic acid transport in Rhizobium meliloti: isolation of mutants and cloning of dicarboxylic acid transport genes. Arch. Microbiol. **144:**142-46.

11. **Bolton, E., Higgisson, B., Harrington, A. and O'Gara F.** 1986. Dicarboxylate acid transport in Rhizobium meliloti: isolation of mutants and cloning of dicarboxylic acid transport genes. Arch. Microbiol. **144**.

12. **Boorer, K. J., B. G. Forde, R. A. Leigh, and A. J. Miller.** 1992. Functional expression of a plant plasma membrane transporter in Xenopus oocytes. FEBS Lett **302:**166-8.

13. **Bosworth, A., M. Williams, K. Albrecht, R. Kwiatkowski, J. Beynon, T. Hankinson, C. Ronson, F. Cannon, T. Wacek, and E. Triplett.** 1994. Alfalfa yield response to inoculation with recombinant strains of Rhizobium meliloti with an extra copy of dctABD and/or modified nifA expression. Appl Environ Microbiol **60:**3815-3832.

14. **Brandl, C. J., and C. M. Deber.** 1986. Hypothesis about the function of membrane-buried proline residues in transport proteins. Proc Natl Acad Sci U S A **83:**917-21.

15. **Brewin, N. J., and A. B. Legocki.** 1996. Biological nitrogen fixation for sustainable agriculture. Trends in Microbiology **4:**476-478.

16. **Buck, M., M. T. Gallegos, D. J. Studholme, Y. Guo, and J. D. Gralla.** 2000. The bacterial enhancer-dependent sigma(54) (sigma(N)) transcription factor. J Bacteriol **182:**4129-36.

17. **Burke, C. L., M. A. Lemmon, B. A. Coren, D. M. Engelman, and D. F. Stern.** 1997. Dimerization of the p185neu transmembrane domain is necessary but not sufficient for transformation. Oncogene **14:**687-96.

18. **Burns, R. C. a. R. W. F. H.** 1975. Nitrogen Fixation in Bacteria and Higher Plants. Springer-Verlag, New York.

19. **Calamita, G., W. R. Bishai, G. M. Preston, W. B. Guggino, and P. Agre.** 1995. Molecular cloning and characterization of AqpZ, a water channel from Escherichia coli. J Biol Chem **270:**29063-6.

20. **Castillo, D. d., S. H. L., and D. B. Layzell.** 1992. O2 regulation and O2 limitation of nitrogenase activity in root nodules of pea and lupin. Physiol. Plant **86:**5624-35.

21. **Catoira R, G. C., de Billy F, Penmetsa RV, Journet EP, Maillet F, Rosenberg C, Cook D, Gough C, Denarie J.** 2000. Four genes of Medicago truncatula controlling components of a nod factor transduction pathway. Plant Cell **12:**1647-1666.

22. **Chubert, R. G., and Brizzard, B.L.** 1996. Vectors for expression and secretion of FLAG epitope-tagged proteins in mammalian cells. Biotechniques **20:**136-141.

23. **Clark, S. R., I. J. Oresnik, and M. F. Hynes.** 2001. RpoN of Rhizobium leguminosarum bv. viciae strain VF39SM plays a central role in FnrN-dependent microaerobic regulation of genes involved in nitrogen fixation. Mol Gen Genet **264:**623-33.

24. **Cohn, J., Day, R.B., and Stacey, G.** 1998. Legume nodule organogenesis. Trends Plant Sci **3:**105-110.

25. **Conradt, M., and W. Stoffel.** 1995. Functional analysis of the high affinity, Na(+)-dependent glutamate transporter GLAST-1 by site-directed mutagenesis. J Biol Chem **270:**25207-12.

26. **Cosson, P., and J. S. Bonifacino.** 1992. Role of transmembrane domain interactions in the assembly of class II MHC molecules. Science **258:**659-62.

27. **Dascal, N.** 1987. The use of Xenopus oocytes for the study of ion channels. CRC Crit Rev Biochem **22:**317-87.

28. **Davidson, E. H.** 1976. In "Gene Activity in Early Development". E.H. Davidson, Ed. **Academic Press**.

29. **de Lorenzo, V., M. Herrero, U. Jakubzik, and K. N. Timmis.** 1990. Mini-Tn5 transposon derivatives for insertion mutagenesis, promoter probing, and chromosomal insertion of cloned DNA in gram-negative eubacteria. J Bacteriol **172:**6568-72.

30. **de Maagd, R. A., and B. Lugtenberg.** 1986. Fractionation of Rhizobium leguminosarum cells into outer membrane, cytoplasmic membrane, periplasmic, and cytoplasmic components. J Bacteriol **167:**1083-5.

31. **Deber, C. M., C. J. Brandl, R. B. Deber, L. C. Hsu, and X. K. Young.** 1986. Amino acid composition of the membrane and aqueous domains of integral membrane proteins. Arch Biochem Biophys **251:**68-76.

32. **Denarié J, D. F., Promé JC.** 1996. Rhizobium lipo-chitooligosaccharide nodulation factors: signaling molecules mediating recognition and morphogenesis. Annu Rev Biochem **65:**503-535.

33. **Development, B. o. S. a. T. f. I.** 1994. Biological Nitrogen Fixation Research Challenges - A Review of Research Grants Funded by the U.S. Agency for International Development. National Research Council.

34. **Dixon, R.** 1984. Tandem promoters determine regulation of the Klebsiella pneumoniae glutamine synthetase (glnA) gene. Nucleic Acids Res **12:**7811-30.

35. **Eilers, M., S. C. Shekar, T. Shieh, S. O. Smith, and P. J. Fleming.** 2000. Internal packing of helical membrane proteins. Proc Natl Acad Sci U S A **97:**5796-801.

36. **El Din, A. K. Y. G.** 1992. A succinate transport mutant of Bradyrhizobium japonicum forms ineffective nodules on soybean. Can. J. Microbiol **38:**230-234.

37. **Engelke, T., Jagadish, M.N., and Puhler, A.** 1987. Biochemical and genetical analysis of Rhizobium meliloti mutants defective in C4-dicarboxylate transport. J. Gen. Microbiol. **133:**3019-29.

38. **Engelke, T., D. Jording, D. Kapp, and A. Puhler.** 1989. Identification and sequence analysis of the Rhizobium meliloti dctA gene encoding the C4-dicarboxylate carrier. J Bacteriol **171:**5551-60.

39. **Eskandari, S., M. Kreman, M. P. Kavanaugh, E. M. Wright, and G. A. Zampighi.** 2000. Pentameric assembly of a neuronal glutamate transporter. Proc Natl Acad Sci U S A **97:**8641-6.

40. **Finan, T. M., I. Oresnik, and A. Bottacin.** 1988. Mutants of Rhizobium meliloti defective in succinate metabolism. J Bacteriol **170:**3396-403.

41. **Finan, T. M., J. M. Wood, and D. C. Jordan.** 1983. Symbiotic properties of C4-dicarboxylic acid transport mutants of Rhizobium leguminosarum. J. Bacteriol. **154:**1403-1413.

42. **Galibert, F., T. M. Finan, S. R. Long, A. Puhler, P. Abola, F. Ampe, F. Barloy-Hubler, M. J. Barnett, A. Becker, P. Boistard, G. Bothe, M. Boutry, L. Bowser, J. Buhrmester, E. Cadieu, D. Capela, P. Chain, A. Cowie, R. W. Davis, S. Dreano, N. A. Federspiel, R. F. Fisher, S. Gloux, T. Godrie, A. Goffeau, B. Golding, J. Gouzy, M. Gurjal, I. Hernandez-Lucas, A. Hong, L. Huizar, R. W. Hyman, T. Jones, D. Kahn, M. L. Kahn, S. Kalman, D. H. Keating, E. Kiss, C. Komp, V. Lelaure, D. Masuy, C. Palm, M. C. Peck, T. M. Pohl, D. Portetelle, B. Purnelle, U. Ramsperger, R. Surzycki, P. Thebault, M. Vandenbol, F. J. Vorholter, S. Weidner, D. H. Wells, K. Wong, K. C. Yeh, and J. Batut.** 2001. The composite genome of the legume symbiont Sinorhizobium meliloti. Science **293:**668-72.

43. **Galloway, J. N. a. E. B. C.** 2002. Nitrogen and the world. Ambio **31:**64-71.

44. **Giblin, L., Boesten, B., Turk, S., Hooykaas, P., and O'Gara, F.** 1995. Signal transduction in the *Rhizobium meliloti* dicarboxylic acid transport system. FEMS Microbiology Letters **126:**25-30.

45. **Gourdon, J. B., C. D. Lane, H. R. Woodland, and G. Marbaix.** 1971. Nature (London) **233**.

46. **Grunewald, M., A. Bendahan, and B. I. Kanner.** 1998. Biotinylation of single cysteine mutants of the glutamate transporter GLT-1 from rat brain reveals its unusual topology. Neuron **21:**623-32.

47. **Hegde, D. M.** 1998. Integrated nutrieht management effect on rice-wheat system productivity in subhumid ecosystem. Indian Journal of Agricultural Sciences **68:**144-148.

48. **Hellriegel, H., and Wilfarth, H.** 1888. Untersuchungen uber die Stickstoffnahrung der Gramineen und Leguminosen. Rubenzucker-Ind., Dtsh. Reichs.**:**234.

49. **Hentschel U, S. M., Hacker J.** 2000. Common molecular mechanisms of symbiosis and pathogenesi. Trends Microbiol **8:**226-231.

50. **Hornez J.-P., G. M. E. a. D. J.-C.** 1989. Succinate transport in Rhizobium meliloti: characteristics and impact in symbiosis. Cur. Microbiol. **19**.

51. **Huang, H. C., S. Y. He, D. W. Bauer, and A. Collmer.** 1992. The Pseudomonas syringae pv. syringae 61 hrpH product, an envelope protein required for elicitation of the hypersensitive response in plants. J Bacteriol **174:**6878-85.

52. **Humbeck, C. a. W., D.** 1989. Delayed nodule development in a succinate transport mutants of Bradyrhizobium japonicum. J. Plant Physiol. **134:**276-283.

53. **Hunt, T. P., and B. Magasanik.** 1985. Transcription of glnA by purified Escherichia coli components: core RNA polymerase and the products of glnF, glnG, and glnL. Proc Natl Acad Sci U S A **82:**8453-7.

54. **Immunology, P.**, posting date. AdjuLite Freunds Adjuvant Data Sheet. Pacific Immunology. [Online.]

55. **Institute, F.** 1989. Fertilizer Facts and Figures. Fertilizer Institute, Washington, DC.

56. **Javadpour, M. M., M. Eilers, M. Groesbeek, and S. O. Smith.** 1999. Helix packing in polytopic membrane proteins: role of glycine in transmembrane helix association. Biophys J **77:**1609-18.

57. **Jording, D., and A. Puhler.** 1993. The membrane topology of the Rhizobium meliloti C4-dicarboxylate permease (DctA) as derived from protein fusions with Escherichia coli K12 alkaline phosphatase (PhoA) and beta-galactosidase (LacZ). Mol Gen Genet **241:**106-14.

58. **Kanai, Y., and M. A. Hediger.** 1992. Primary structure and functional characterization of a high-affinity glutamate transporter. Nature **360:**467-71.

59. **Kanner, B. I., and I. Sharon.** 1978. Active transport of L-glutamate by membrane vesicles isolated from rat brain. Biochemistry **17:**3949-53.

60. **Kouchi, H., Fukai, K, Katagiri, H, Minamisawa, K, and Tajima, S.** 1988. Physiol. Plant **73:**327-334.

61. **Kreig, P. A., and D. A. Melton.** 1984. Functional messenger RNA's are produced by SP6 *in vitro* transcription of cloned cDNAs. Nucl. Acids Res. **12:**7057-7070.

62. **Kyte, J., and R. F. Doolittle.** 1982. A simple method for displaying the hydropathic character of a protein. J Mol Biol **157:**105-32.

63. **Labes, M., and T. M. Finan.** 1993. Negative regulation of sigma 54-dependent dctA expression by the transcriptional activator DctD. J Bacteriol **175:**2674-81.

64. **Lafontaine, P. J., LaFreniere, C. and Antoun, H.** 1989. Some propertied of carbohydrate and C4-dicarboxilic acid utilization negative mutants of Rhizobium leguminosarum biovar phaseoli strain P121. Plant Sci. **120:**195-201.

65. **Landolt-Marticorena, C., K. A. Williams, C. M. Deber, and R. A. Reithmeier.** 1993. Non-random distribution of amino acids in the transmembrane segments of human type I single span membrane proteins. J Mol Biol **229:**602-8.

66. **Lane, C. D.** 1983. The fate of genes, messengers, and proteins introduced into Xenopus oocytes. Curr Top Dev Biol **18:**89-116.

67. **Layzell, D.** 1998. Oxygen and the control of nodule metabolism and N2 fixation. In "Biological Nitrogen Fixation for the 21st Century" Elmerich, C et al, eds.**:**4435-440.

68. **Ledebur, H., B. Gu, J. Sojda, 3rd, and B. T. Nixon.** 1990. Rhizobium meliloti and Rhizobium leguminosarum dctD gene products bind to tandem sites in an activation sequence located upstream of sigma 54-dependent dctA promoters. J Bacteriol **172:**3888-97.

69. **Ledebur, H., and B. T. Nixon.** 1992. Tandem DctD-binding sites of the Rhizobium meliloti dctA upstream activating sequence are essential for optimal function despite a 50- to 100-fold difference in affinity for DctD. Mol Microbiol **6:**3479-92.

70. **Lee, J. H., and T. R. Hoover.** 1995. Protein crosslinking studies suggest that Rhizobium meliloti C4-dicarboxylic acid transport protein D, a sigma 54-dependent transcriptional activator, interacts with sigma 54 and the beta subunit of RNA polymerase. Proc Natl Acad Sci U S A **92:**9702-6.

71. **Lemmon, M. A., and D. M. Engelman.** 1994. Specificity and promiscuity in membrane helix interactions. FEBS Lett **346:**17-20.

72. **Lemmon, M. A., J. M. Flanagan, J. F. Hunt, B. D. Adair, B. J. Bormann, C. E. Dempsey, and D. M. Engelman.** 1992. Glycophorin A dimerization is driven by specific interactions between transmembrane alpha-helices. J Biol Chem **267:**7683-9.

73. **Lemmon, M. A., H. R. Treutlein, P. D. Adams, A. T. Brunger, and D. M. Engelman.** 1994. A dimerization motif for transmembrane alpha-helices. Nat Struct Biol **1:**157-63.

74. **LeVier K, P. R., Grippe VK, Roop RM, Walker GC.** 2000. Similar requirements of a plant symbiont and a mammalian pathogen for prolonged intracellular survival. Science **287:**2492-2493.

75. **Li, S. C., and C. M. Deber.** 1992. Glycine and beta-branched residues support and modulate peptide helicity in membrane environments. FEBS Lett **311:**217-20.

76. **Li, S. C., N. K. Goto, K. A. Williams, and C. M. Deber.** 1996. Alpha-helical, but not beta-sheet, propensity of proline is determined by peptide environment. Proc Natl Acad Sci U S A **93:**6676-81.

77. **Liman, E. R., J. Tytgat, and P. Hess.** 1992. Subunit stoichiometry of a mammalian K+ channel determined by construction of multimeric cDNAs. Neuron **9:**861-71.

78. **Lodwig, E. M., Hosie, A.H.F., Bourdes, A., Findlay, K., Allaway, D., Karunakaran, R., Downie, J.A., and Poole, P.S.** 2003. Amino-acid cycling drives nitrogen fixation in the legume-*Rhizobium* symbiosis. Nature **422:**722-726.

79. **Long, S., S. McCune, and G. C. Walker.** 1988. Symbiotic loci of Rhizobium meliloti identified by random TnphoA mutagenesis. J Bacteriol **170:**4257-65.

80. **Long, S. R.** 1996. Rhizobium symbiosis: Nod factors in perspective. Plant Cell **8:**1885-1898.

81. **MacKenzie, K. R., J. H. Prestegard, and D. M. Engelman.** 1997. A transmembrane helix dimer: structure and implications. Science **276:**131-3.

82. **Maskey, S. L., S. Bhattarai, M. B. Peoples, and D. F. Herridge.** 2001. On-farm measurements of nitrogen fixation by winter and summer legumes in the Hill and Terai regions of Nepal. Field Crops Research **70:**209-221.

83. **Matson, P., K. Lohse, and S.J. Hall.** 2002. The globalization of nitrogen: consequences for terrestrial ecosystems. Ambio **31:**113-119.

84. **Matsubara, H., E. R. Liman, P. Hess, and G. Koren.** 1991. Pretranslational mechanisms determine the type of potassium channels expressed in the rat skeletal and cardiac muscles. J Biol Chem **266:**13324-8.

85. **Merrick, M. J.** 1993. In a class of its own--the RNA polymerase sigma factor sigma 54 (sigma N). Mol Microbiol **10:**903-9.

86. **Michiels, J., M. Moris, B. Dombrecht, C. Verreth, and J. Vanderleyden.** 1998. Differential regulation of Rhizobium etli rpoN2 gene expression during symbiosis and free-living growth. J Bacteriol **180:**3620-8.

87. **Miller, A. J., and J. J. Zhou.** 2000. Xenopus oocytes as an expression system for plant transporters. Biochim Biophys Acta **1465:**343-58.

88. **Mimotopes** May 14th 2004 2004, posting date. Antipeptide Antibodies. Mimotopes Pty Ltd. [Online.]

89. **Minnick MF, M. S., McAllister SJ.** 1996. Cell entry and the pathogenesis of Bartonella infections. Trends Microbiol **4:**343-347.

90. **Nakashima, H., K. Nishikawa, and T. Ooi.** 1986. The folding type of a protein is relevant to the amino acid composition. J Biochem (Tokyo) **99:**153-62.

91. **O'Neil, K. T., and W. F. DeGrado.** 1990. A thermodynamic scale for the helix-forming tendencies of the commonly occurring amino acids. Science **250:**646-51.

92. **Parent, L., S. Supplisson, D. D. Loo, and E. M. Wright.** 1992. Electrogenic properties of the cloned Na+/glucose cotransporter: I. Voltage-clamp studies. J Membr Biol **125:**49-62.

93. **Park, S.** 2002. Structural studies on *Sinorhizobium meliloti* DctD related to ATP binding and activation. Ph.D. The Pennsylvania State University.

94. **Peoples, M. B., Bowaman, A.M., Gault, R.R., Herridge, D.F., McCallum, M.H., McCormick, K.M., Norton, R.M., Rochester, J.J., Scammel, G.J., Schwenke, G.D.** 2001. Factors regulating the contributions of fixed nitrogen by pasture and crop legumes to different farming systems of eastern Australia. Plant Soil**:**29-41.

95. **Peoples, M. B., Giller, K.E., Herridge, D.F., and Vessey, J.K.** 2001. Presented at the 13th International Congress of Nitrogen Fixation, Hamilton, Ontario, Canada.

96. **Peoples, M. B. a. C., E.T.** 1992. Biological nitrogen fixation: investments, expectation and actual contributions to agriculture. Plant Soil**:**13-39.

97. **Phillips, D.** 1980. Annual Review of Plant Physiology **11:**29-49.

98. **Pines, G., N. C. Danbolt, M. Bjoras, Y. Zhang, A. Bendahan, L. Eide, H. Koepsell, J. Storm-Mathisen, E. Seeberg, and B. I. Kanner.** 1992. Cloning and expression of a rat brain L-glutamate transporter. Nature **360:**464-7.

99. **Polinsky, A., M. Goodman, K. A. Williams, and C. M. Deber.** 1992. Minimum energy conformations of proline-containing helices. Biopolymers **32:**399-406.

100. **Poole, P., and D. Allaway.** 2000. Carbon and nitrogen metabolism in Rhizobium. Adv Microb Physiol **43:**117-63.

101. **Rabalais, N. N.** 2002. Nitrogen in aquatic ecosystems. Ambio **31:**102-112.

102. **Rastogi, V., Labes, M., Finan, T., and Watson, R.** 1992. Overexpresion of the *dctA* gene in *Rhizobium meliloti:* effect on transport of C4 dicarboxylates and symbiotic nitrogen fixation. Canadian Journal of Microbiology **38:**555-562.

103. **Rees, D. C., and J. B. Howard.** 2000. Nitrogenase: standing at the crossroads. Curr Opin Chem Biol **4:**559-66.

104. **Reid, C. J., and P. S. Poole.** 1998. Roles of DctA and DctB in signal detection by the dicarboxylic acid transport system of Rhizobium leguminosarum. J Bacteriol **180:**2660-9.

105. **Richards, F. M.** 1974. The interpretation of protein structures: total volume, group volume distributions and packing density. J Mol Biol **82:**1-14.

106. **Roberts, G.** 2003, posting date. Nitrogen fixation, Plant Biochemistry. [Online.]

107. **Ronson, C. W., P. M. Astwood, B. T. Nixon, and F. M. Ausubel.** 1987. Deduced products of C4-dicarboxylate transport regulatory genes of Rhizobium leguminosarum are homologous to nitrogen regulatory gene products. Nucleic Acids Res **15:**7921-34.

108. **Ronson, C. W., P. Lyttleton, and J. G. Robertson.** 1981. C4-dicarboxylate transport mutants of Rhizobium trifolii form ineffective nodules on Trifolium repens. Proc. Natl. Acad. Sci. USA **78:**4284-4288.

109. **Ronson, C. W., B. T. Nixon, L. M. Albright, and F. M. Ausubel.** 1987. Rhizobium meliloti ntrA (rpoN) gene is required for diverse metabolic functions. J Bacteriol **169:**2424-31.

110. **Saidijam, M., G. Psakis, J. L. Clough, J. Meuller, S. Suzuki, C. J. Hoyle, S. L. Palmer, S. M. Morrison, M. K. Pos, R. C. Essenberg, M. C. Maiden, A. Abu-bakr, S. G. Baumberg, A. A. Neyfakh, J. K. Griffith, M. J. Stark, A. Ward, J. O'Reilly, N. G. Rutherford, M. K. Phillips-Jones, and P. J. Henderson.** 2003. Collection and characterisation of bacterial membrane proteins. FEBS Lett **555:**170-5.

111. **Salminen, S. O., and J. G. Streeter.** 1987. Involvement of glutamate in the respiratory metabolism of Bradyrhizobium japonicum bacteroids. J Bacteriol **169:**495-9.

112. **Sambrook J, R. D.** 2001. Molecular Cloning: a laboratory manual., 3rd ed. Cold Spring Harbor Laboratory, Cold Spring Harbor, NY.

113. **Schafer, A., A. Tauch, W. Jager, J. Kalinowski, G. Thierbach, and A. Puhler.** 1994. Small mobilizable multi-purpose cloning vectors derived from the Escherichia coli plasmids pK18 and pK19: selection of defined deletions in the chromosome of Corynebacterium glutamicum. Gene **145:**69-73.

114. **Schultze, M., and Kondorosi, A.** 1998. Regulation of symbiotic root nodule development. Annu. Rev. Genet **32:**33-57.

115. **Service, U. N. A. S.** 2002, posting date. 2002 Census of Agriculture. United States Department of Agriculture. [Online.]

116. **Simon R, P. U., Puhler A.** 1983. A broad range host mobilization system for *in vivo* genetic engineering: transposon mutagenesis in gram negative bacteria. Biotehnology **1:**784-791.

117. **Slotboom, D. J., W. N. Konings, and J. S. Lolkema.** 1999. Structural features of the glutamate transporter family. Microbiol Mol Biol Rev **63:**293-307.

118. **Slotboom, D. J., W. N. Konings, and J. S. Lolkema.** 2001. The structure of glutamate transporters shows channel-like features. FEBS Lett **492:**183-6.

119. **Slotboom, D. J., J. S. Lolkema, and W. N. Konings.** 1996. Membrane topology of the C-terminal half of the neuronal, glial, and bacterial glutamate transporter family. J Biol Chem **271:**31317-21.

120. **Smith, S. O., and B. J. Bormann.** 1995. Determination of helix-helix interactions in membranes by rotational resonance NMR. Proc Natl Acad Sci U S A **92:**488-91.

121. **Somerville, J., and Kahn ML.** 1983. Cloning of the glutamine synthetase I gene from *Rhizobium meliloti* . J. Bacteriol. **156:**168-176.

122. **Sternberg, M. J., and W. J. Gullick.** 1989. Neu receptor dimerization. Nature **339:**587.

123. **Sternberg, M. J., and W. J. Gullick.** 1990. A sequence motif in the transmembrane region of growth factor receptors with tyrosine kinase activity mediates dimerization. Protein Eng **3:**245-8.

124. **Stigter, J., M. Schneider, and F. J. de Bruijn.** 1993. Azorhizobium caulinodans nitrogen fixation (nif/fix) gene regulation: mutagenesis of the nifA -24/-12 promoter element, characterization of a ntrA(rpoN) gene, and derivation of a model. Mol Plant Microbe Interact **6:**238-52.

125. **Storck, T., S. Schulte, K. Hofmann, and W. Stoffel.** 1992. Structure, expression, and functional analysis of a Na(+)-dependent glutamate/aspartate transporter from rat brain. Proc Natl Acad Sci U S A **89:**10955-9.

126. **Streeter, J. G.** 1991. Transport and Metabolism of Carbon and Nitrogen in Legume Nodules. Adv. Bot. Res. **18:**129-187.

127. **Strehlow, K. G., A. D. Robertson, and R. L. Baldwin.** 1991. Proline for alanine substitutions in the C-peptide helix of ribonuclease A. Biochemistry **30:**5810-4.

128. **Stryer, L.** 1995. Biochemistry, p. 192-199, Biochemistry, 4th ed, vol. 1. W.H. Freeman and Company, New York.

129. **Stuhmer, W.** 1998. Electrophysioloic recordings from Xenopus Oocytes. Methods in Enzymology **293:**280-300.

130. **Swanson, R., J. Marshall, J. S. Smith, J. B. Williams, M. B. Boyle, K. Folander, C. J. Luneau, J. Antanavage, C. Oliva, S. A. Buhrow, and et al.** 1990. Cloning and expression of cDNA and genomic clones encoding three delayed rectifier potassium channels in rat brain. Neuron **4:**929-39.

131. **Theodoulou, F. L., and A. J. Miller.** 1995. Xenopus oocytes as a heterologous expression system, p. 317-340. *In* H. Jones (ed.), Methods in molecular biology vol. 49: plant gene transfer and expression protocols, vol. 49. Humana Press, Totowa.

132. **Theodoulou, F. L., and A. J. Miller.** 1995. Xenopus oocytes as a heterologous expression system for plant proteins. Mol. Biotechnol. **3:**101-115.

133. **Tolner, B., B. Poolman, and W. N. Konings.** 1992. Characterization and functional expression in Escherichia coli of the sodium/proton/glutamate symport proteins of Bacillus stearothermophilus and Bacillus caldotenax. Mol Microbiol **6:**2845-56.

134. **Tolner, B., T. Ubbink-Kok, B. Poolman, and W. N. Konings.** 1995. Cation-selectivity of the L-glutamate transporters of Escherichia coli, Bacillus stearothermophilus and Bacillus caldotenax: dependence on the environment in which the proteins are expressed. Mol Microbiol **18:**123-33.

135. **Tolner, B., T. Ubbink-Kok, B. Poolman, and W. N. Konings.** 1995. Characterization of the proton/glutamate symport protein of Bacillus subtilis and its functional expression in Escherichia coli. J Bacteriol **177:**2863-9.

136. **Tuzimura, K. a. M., H.** 1960. **Respiration substrate of Rhizobium in the nodules**. **J. Biochem. 47:**391-397.

137. **Udvardi, M. K. D., D.** 1997. Metabolic transport across symbiotic membranes of legume nodules. Ann Rev Plant Physiology and Plant Molecular Biology **48:**493-523.

138. **Unkovich, M. J., and Pate, J.S.** 2000. An appraisal of recent field measurements of symbiotic N2 fixation by annual legumes. Field Crops Res.**:**211-228.

139. **US Bureau of the Census, R. W.** 1999. World Population Profile: 1998. US Government Printing Office.

140. **Vance, C., and Graham PH.** 1995. Nitrogen fixation in agriculture: applcation and perspective, p. 77-86. *In* N. A. P. I.A. Tikhonovich, V.I. Romanov, and W.E. Newton (ed.), Nitrogen Fixation: Fundamentals and Applications. Kluwer Academic Publishers, Dordrecht.

141. **Verma, D. P. S. H., Z.** 1996. Biogenesis of the peribacteroid membrane in root nodules. Trends in Microbiology **4:**364-365.

142. **Vogel, H.** 1992. Structure and dynamics of polypeptides and proteins in lipid membranes. Q Rev Biophys **25:**433-57.

143. **Wagner, J.** August 2002 1997, posting date. Addition of an epitope to a protein coding sequence: FLAG-tag. John Wagner. [Online.]

144. **Wahle, S., and W. Stoffel.** 1996. Membrane topology of the high-affinity L-glutamate transporter (GLAST-1) of the central nervous system. J Cell Biol **135:**1867-77.

145. **Wallin, E., T. Tsukihara, S. Yoshikawa, G. von Heijne, and A. Elofsson.** 1997. Architecture of helix bundle membrane proteins: an analysis of cytochrome c oxidase from bovine mitochondria. Protein Sci **6:**808-15.

146. **Ward, A., J. O'Reilly, N. G. Rutherford, S. M. Ferguson, C. K. Hoyle, S. L. Palmer, J. L. Clough, H. Venter, H. Xie, G. J. Litherland, G. E. Martin, J. M. Wood, P. E. Roberts, M. A. Groves, W. J. Liang, A. Steel, B. J. McKeown, and P. J. Henderson.** 1999. Expression of prokaryotic membrane transport proteins in Escherichia coli. Biochem Soc Trans **27:**893-9.

147. **Ward, A., O'Reilly, J., Rutherford, N.G., Ferguson, S.M., Hoyle, C.K., Palmer, S.l., Clough, J.L., Venter, H., Xie, H., Litherland, G.J., Martin, G.E.M., Wood, J.M., Roberts, P.E., Groves, M.A.T., Liang, W.-j., Steel, A., McKeown, B.J., and Henderson, P.J.F.** 1999. Expression of prokaryotic membrane transport proteins in *Escherichia coli* . Biochemical Society Transactions **27:**893-899.

148. **Ward, A., Sanderson, N.M., O'Reilly, J., Rutherford, N.G., Poolman, B., and Henderson, J.F.P.** 2000. The amplified expression, identification, purification, assay and properties of histidine-tagged bacterial membrane proteins., p. 141-166. *In* S. A. Baldwin (ed.), Membrane Transport - a practical approach. Blackwell's Press, Oxford, UK.

149. **Ward, A., Sanderson, N.M., O'Reilly, J., Rutherford, N.G., Poolman, B., and Henderson, P.J.F.** 2000. The amplified expression, identification, purification, assay, and properties of hexahistidine-tagged bacterial membrane transport proteins, p. 141-166. *In* S. A. Baldwin (ed.), Membrane Transport - a practical approach. Blackwell's Press, Oxford.

150. **Watson, R. J.** 1990. Analysis of the C4-dicarboxylate transport genes of Rhizobium meliloti: nucleotide sequence and deduced products of dctA, dctB, and dctD. Mol Plant Microbe Interact **3:**174-81.

151. **Watson, R. J., Y. K. Chan, R. Wheatcroft, A. F. Yang, and S. H. Han.** 1988. Rhizobium meliloti genes required for C4-dicarboxylate transport and symbiotic nitrogen fixation are located on a megaplasmid. J Bacteriol **170:**927-34.

152. **Watson, R. J., Chan, Y.K., Wheatcroft, R., Yang, A.F. and Han, S.H. (1988) . J. Bacteriol. 170, 927-934.** 1988. Rhizobium meliloti genes required for C4-dicarboxylate transport and symbiotic nitrogen fixation are located on a megaplasmid. J Bacteriol **170:**927-934.

153. **Weber, W.** 1999. Ion currents of Xenopus laevis oocytes: state of the art. Biochim Biophys Acta **1421:**213-33.

154. **Werner, D.** 1992. Physiology of nitrogen-fixing legume nodules: Compartments and functions. In "Symbiotic Nitrogen Fixation", G.Stacey, et al. eds**:**pp 399-430.

155. **Yang, F. a. L., LP.** 1998. Cytostructure, Lipopolysaccharides, and cell proteins analysis from *Rhizobium fredii* . Botanical Bulletin of Academia Sinica **39:**261-267.

156. **Yanisch-Perron, C., Vieira J, and Messing J.** 1985. Improved M13 phage cloning vectors and host strains: nucleotide sequence of the M13mp18 and pUC19 vectors. Gene **33:**103-119.

157. **Yarosh, O. K., T. C. Charles, and T. M. Finan.** 1989. Analysis of C4-dicarboxylate transport genes in Rhizobium meliloti. Mol Microbiol **3:**813-23.

158. **Yoshimura, K., A. Batiza, M. Schroeder, P. Blount, and C. Kung.** 1999. Hydrophilicity of a single residue within MscL correlates with increased channel mechanosensitivity. Biophys J **77:**1960-72.

159. **Yu, L., K. J. Blumer, N. Davidson, H. A. Lester, and J. Thorner.** 1989. Functional expression of the yeast alpha-factor receptor in Xenopus oocytes. J Biol Chem **264:**20847-50.

160. **Yurgel, S., M. W. Mortimer, K. N. Rogers, and M. L. Kahn.** 2000. New substrates for the dicarboxylate transport system of Sinorhizobium meliloti. J Bacteriol **182:**4216-21.

161. **Yurgel, S. a. K., M.L.** 2004. Mutants of *Sinorhizobium meliloti* DctA with a partial ability to transport dicarboxylates. J Bacteriol **submitted**.

162. **Zerangue, N., and M. P. Kavanaugh.** 1996. Flux coupling in a neuronal glutamate transporter. Nature **383:**634-7.

Chapter Six Appendices

6.1 Media, Solutions and Reagents:

6.1.1 Bacterial Growth Media:

6.1.1.1 Luria Bertani (LB)

10g Tryptone

5g Yeast extract

5g NaCl

(15g Agar)

1l dH_2O

6.1.1.2 Minimal Mannitol Medium with NH_4 ($MMNH_4$)

10g Mannitol

0.5g NH_4Cl

(15g Agar)

970ml dH_2O

This is autoclaved, cooled to 55ºC, and the following are added:

1ml Biotin (0.2mg/ml in 100% ethanol)

1ml Thiamine (2mg/ml)

10ml Minimal Mannitol Salts I

10ml Minimal Mannitol Salts II

6.1.1.2.1 Minimal Mannitol Salts I

100g K_2HPO_4

100g KH_2PO_4

25g Na_2SO_4

1l dH_2O

6.1.1.2.2 Minimal Mannitol Salts II

1g $FeCl_3.6H_2O$

1 drop concentrated HCl

10g $CaCl_2.2H_2O$

25g $MgCl_2.6H_2O$

1l dH_2O

6.1.1.3 M9 for *Rhizobium*

7g Na_2HPO_4

3g KH_2PO_4

1g NH_4Cl

1g NaCl

(15g Agar)

This is autoclaved, cooled to 55ºC, and the following are added:

1ml $MgSO_4$

0.1ml 1M $CaCl_2$

6.1.1.4 TY

5g Tryptone

5g Yeast extract

0.5g $CaCl_2$

1l dH_2O

6.1.1.5 NZY^+

10g NZ amine (casein hydrolysate)

5g Yeast extract

5g NaCl

1l dH_2O

Adjust pH to 7.5 with NaOH

This is autoclaved, cooled to 55ºC, and the following are added:

12.5ml 1M $MgCl_2$

12.5ml 1M $MgSO_4$

20ml of 20% (w/v) glucose

6.1.2 Antibiotic Concentrations:

All antibiotic concentrations listed here are for solid media. Typically these concentrations were halved for growth in liquid culture.

6.1.2.1 Antibiotic concentrations for *E. coli*

Tetracycline: 10µg/ml

Kanamycin: 40µg/ml

Ampicillin: 50µg/ml

6.1.2.2 Antibiotic concentrations for *S. meliloti*

Streptomycin: 200µg/ml

Neomycin: 200µg/ml

Tetracycline: 10µg/ml

6.2 Molecular Biology Reagents

6.2.1 6X loading buffer for agarose gel electrophoresis

0.25% (w/v) bromophenol blue

0.25% (w/v) xylene cyanol FF

40% (w/v) sucrose in H_2O

6.2.2 Typical PCR Reaction

Segment	Cycles	Temp	Time
1	25	94°C 55°C 68°C	1min 1min 6min
2	1	68°C	6min
3	1	4°C	For Ever

6.2.3 Typical Mutagenesis PCR Reaction

Segment	Cycles	Temp	Time
1	1	95°C	
2	16	95°C 55°C 68°C	30 sec 30 sec 5.5 mins

6.3 Protein Analysis

6.3.1 SDS-PAGE Gel Solutions

6.3.1.1 SDS-Loading Buffer

5ml Glycerol

2.5ml β-Mercaptoethanol

15ml 10% SDS

25ml Upper Buffer

2.5ml dH_2O

Add Bromophenol Blue to color

6.3.1.2 SDS-PAGE Running Buffer

6.3.1.2.1 4X Stock Solution:

12g Tris-Base

57.6g Glycine

1l dH_2O

pH 8.3 with HCl

6.3.1.2.2 1X Working Solution:

250ml 4X Stock solution

10ml 10% SDS

740ml dH_2O

6.3.1.3 SDS-PAGE EDTA gel (12% acrylamide):

	Resolver	Stack
H2O	6.6	4.1
30% Acrylamide	8	1
Tris Buffer*	5	0.75
10% SDS	0.2	0.06
0.5M EDTA	0.004	0.002

* Resolver: 1.5M Tris-HCl, pH 8.8

* Stack: 1M Tris-HCl, pH 6.0

Immediately before pouring, add:

10% APS	0.2	0.06
TEMED	0.008	0.006

6.3.1.4 Coomassie Brilliant Blue Stain:

0.25g Coomassie Brilliant Blue R250

45ml dH_2O

45ml Methanol

10ml Glacial Acetic Acid

Filter through a Whatman #1 filter to remove sediment

6.3.1.5 Destain:

880ml dH_2O

70ml Methanol

50ml Glacial Acetic Acid

6.3.2 Western Blot Solutions:

6.3.2.1 Western transfer buffer

6.3.2.1.1 25X Stock:

450ml dH_2O

120mM Tris Base

960mM Glycine

dH_2O to 500ml

6.3.2.1.2 1X Working Solution:

40ml 25X stock

200ml EtOH

760ml dH_2O

6.3.2.2 TBS:

6.3.2.2.1 10X Stock:

200mM Tris

5M NaCl

pH 7.5

6.3.2.2.2 1X Working Solution :

100ml 10X TBS stock

900ml dH_2O

6.3.2.3 TTBS

990ml 1X TBS

10ml Tween-20

6.3.2.4 Blocking Buffer:

2.5g Western Family non-fat dried milk

50ml 1X TBS

6.3.2.5 Antibody Buffer:

1g Western Family non-fat dried milk

50ml TTBS

6.3.3 Membrane Isolation Buffers

6.3.3.1 *E. coli:*

6.3.3.1.1 0.2M Tris-HCl pH 8.0:

0.2M Tris-HCl

pH 8.0

6.3.3.1.2 Sucrose Buffer:

1M Sucrose

1mM EDTA

0.2M Tris-HCl pH8.0

6.3.3.1.3 Membrane Resuspension Buffer:

0.1M Sodium phosphate

pH 7.2

1mM 2-mercaptoethanol

6.3.3.1.4 Tris-EDTA Buffer:

20mM Tris-HCl

pH 7.5

0.5mM EDTA

6.3.3.2 *S. meliloti :*

6.3.3.2.1 Resuspension Buffer

50mM Tris-HCl

pH 8.5

20% (w/v) Sucrose

0.2mM Dithiotreitol

6.4 *Xenopus laevis* Reagents

6.4.1 Formaldehyde Agarose Gel Electrophoresis

6.4.1.1 10X MOPS Buffer:

800ml RNase-free dH_2O

20ml RNase-free 0.5M EDTA, pH 8.0

41.8g MOPS

Bring volume to 1l with RNase-free dH_2O

16ml RNase-free 3M Sodium Acetate

pH 7.0 with NaOH

6.4.1.2 1.2% Formaldehyde-Agarose gel:

2.52g Agarose

180ml RNase-free dH_2O

21ml 10X MOPS Buffer

6.3ml 37% Formaldehyde

6.4.1.3 RNA Loading Buffer:

0.5% (w/v) Bromophenol Blue

1mM EDTA, pH8.0

50% (v/v) Glycerol

6.4.2 OR2 Solution:

82.5mM NaCl

2.5mM KCl

1mM MgCl

5mM Hepes

pH 7.6 with NaOH

6.4.3 ND96 Buffer:

96mM NaCl

2mM KCl

1.8mM $CaCl_2$

1mM $MgSO_4$

5mM HEPES

pH to 7.6 with NaOH

2.5mM Na-pyruvate

100U/ml Gentamycin

Filter sterilize

6.4.4 Standard Tris-Free Buffer

0.2M HEPES

0.15M NaCl

5mM EDTA

pH 7.0

6.4.5 Oocyte Lysis Buffer

0.5% Triton-X 100 in standard tris-free buffer

1 Complete Protease Inhibitor Tablet (Roche Diagnostics Corporation, Indianapolis, IN)

6.5 Plant Growth Solutions:

6.5.1 Plant Nutrient Solution

1l dH_2O

2mM $CaSO_4.2H_2O$

Autoclave, then add the following stock solutions:

2ml 0.5M K_2SO_4

0.5ml 1M KH_2PO_4

0.75ml 1M K_2HPO_4

0.5ml 1M $MgSO_4.7H_2O$

0.05ml 50mM $CoCl_2.6H_2O$

0.5ml 40mM $FeCl_3$

0.5ml M6 micro nutrients

6.5.1.1 M6 Micro Nutrients

10ml dH_2O

37.3mg KCl

15.5mg H_3BO_3

0.34mg $MnSO_4.2H_2O$

0.57mg $ZnSO_4.2H_2O$

0.125mg $CuSO_4.5H_2O$

0.103mg $NaMoO_4.2H_2O$

Filter-sterilize